

# UC Davis

## UC Davis Electronic Theses and Dissertations

### Title

Histone H3.3K27M Regulates the Chromatin Landscape in Diffuse Intrinsic Pontine Glioma

### Permalink

<https://escholarship.org/uc/item/1225j365>

### Author

Lewis, Nichole Ashley

### Publication Date

2021

Peer reviewed|Thesis/dissertation

Histone H3.3K27M Regulates the Chromatin Landscape in Diffuse Intrinsic Pontine Glioma

By

NICHOLE ASHLEY LEWIS  
DISSERTATION

Submitted in partial satisfaction of the requirements for the degree of

DOCTOR OF PHILOSOPHY

in

Biochemistry, Molecular, Cellular, and Developmental Biology

in the

OFFICE OF GRADUATE STUDIES

of the

UNIVERSITY OF CALIFORNIA

DAVIS

Approved:

---

Paul S. Knoepfler, Chair

---

Laura N. Borodinsky

---

Janine M. LaSalle

---

David Pleasure

---

David J. Segal

Committee in Charge

2022

## Table of Contents

Title Page.....	i
Abstract.....	iii
Acknowledgements.....	iv
Chapter 1: Introduction The epigenetic impact of the histone H3.3 K27M mutation.....	1
Chapter 2: Histone H3.3K27M promotes unique chromatin accessible regions in developmentally relevant genes in DIPG tumors.....	29
Chapter 3: Conclusions and Future Directions.....	77

## Abstract

Diffuse intrinsic pontine glioma (DIPG) is a fatal pediatric brain tumor with the average survival being only a year. To date the only treatment is radiotherapy, but it is not very effective leaving a need to better understand DIPG biology to develop more effective treatment methods. About 80% of DIPGs have a point mutation in one allele of *H3F3A*, one of two genes that codes for histone variant H3.3, resulting in lysine 27 being mutated to methionine. The H3.3K27M mutation is thought to be one of the first mutations to take place in DIPG tumorigenesis and results in the global depletion of the repressive mark H3K27me<sub>3</sub> and an increase in the activating mark H3K27ac. In order to further investigate the effects of H3.3K27M and its subsequent abrogation on normal histone post-translational modifications (PTMs) patterns, we used CRISPR-Cas9 to revert H3.3K27M back to wild-type H3.3 in two patient DIPG cell lines. Here I used ATAC-seq in these isogenic cell lines to study the unique chromatin structure and function at work in DIPG tumors, including specifically what features are due to the H3.3K27M mutation as opposed to other mutations DIPGs are known to have. H3.3K27M results in increased chromatin accessibility surrounding genes that regulate neurogenesis and neuronal development, processes that have been found to be key in DIPG tumor formation and maintenance. The binding sites of several transcription factors including NOTCH signaling factor *ASCL1* are enriched in unique open chromatin regions in K27M cells. This provides further support for drug treatments targeting NOTCH signaling and *ASCL1*. Overall, these studies indicate that both wildtype and mutant H3.3 are key regulators of chromatin dynamics and that K27M likely drives aberrant transcription in DIPG in part through altered chromatin structure.

## **Acknowledgements**

I could not have done this without the support of my family. To my mom Becky, who was always there through all the ups and downs of grad school and pushed me to never give up: this degree is as much for you as it is for me; we did it. To my brothers, Ty and Cameron, and my sister Samantha, thank you all so much for all the encouragement, support, love, and “You’re going to be a doctor like Ross from Friends” jokes along the way. I couldn’t have done this without your humor, encouragement, and inspiration. To Gianna and the twins, all three of you have inspired and motivated me so much in the last year and a half of my PhD program. I can’t wait to teach you all the science I have learned and do at home science experiments with you. Thank you to my adorable and sassy calico cat Rey, she always managed to make me laugh and provide the best snuggles after a long day in lab when experiments just did not want to cooperate. And last, but certainly by no means least, my husband Ivan. You have been there from day one of this crazy journey. From all-nighters to get through classes, letting me practice my qualifying exam with you, and meal prepping for me when I was just too overwhelmed and needed extra time to work. But most importantly, thank you for always supporting me and reminding me why I wanted this degree in moments when I couldn’t remember myself. Thank you for always believing in me.

I have been fortunate to have many academic mentors throughout my education and early stages of my career. First and foremost, Dr. Ken Kaplan who first let me enter a lab. Thank you for being my first mentor, guiding me through grad school applications, and giving me my first research project and presentation opportunity. Dr. Dan Starr, for giving me my first in-depth lessons about cells, helping to confirm I made the right the choice in majoring in Cell Biology, and later giving me my first teaching assistance position allowing me to see how much I truly loved teaching. Dr. Teresa Dillinger and Dr. Ellen Hartigan-O’Connor, for accepting me into the Professors For The Future program allowing me to learn about and solidify my goal of pursuing an education focused career after graduation. I would also like to thank Dr. Mona Monfared for telling me about SABER and giving me my first guest lecture opportunity, and Dr. Connie

Champagne for allowing me to solo lead my first ever undergraduate journal club classes. All of these experiences and opportunities have truly shaped my future career and I cannot thank you all enough.

I would not be receiving this degree if not for my mentor, Dr. Paul Knoepfler. His letters of support and science communication knowledge allowed me to explore communication fellowships and trainings that have proved to be important for my future career. I am very thankful for the opportunities I was given to present my work and improve my public speaking skills in addition to both the dry- and wet-lab skills I acquired throughout the course of my degree. I owe an immense amount of thanks to all my committee members, Dr. Dave Pleasure, Dr. Dave Segal, Dr. Janine LaSalle, and Dr. Laura Borodinsky. Thank you all for your support and guidance throughout this whole process and getting my dissertation work to its finished product. All your perspectives on how to approach research were incredibly helpful in shaping this project and I am very fortunate to have learned from all of you along the way. And Dr. Kermit Carraway for being my first rotation lab mentor and giving thoughtful, helpful advice whenever it was needed.

And to my friends, both in and out of the lab. To my labmates, there is no way I could have done this without you. Thank you all for your help with experiments, troubleshooting, and preparing for presentations. I have grown so much as a scientist over the past five and half years and it's in no small part thanks to each of you. I'm so fortunate to consider my coworkers dear friends. And to my friends outside of the lab and academia, thank you for always being there for me, cheering me on, and loving me even if I didn't always have time to text back or hangout. Your understanding and support kept me going and I cannot wait to celebrate this huge accomplishment with every single one of you.

And finally, thank you God for being there every day and guiding my life. It is by Your strength that I am finishing my education and starting a new chapter in life.

They say it takes a village. Everyone mentioned here is part of my village. From the bottom of my heart, thank you all.

# CHAPTER 1

## Introduction

### The epigenetic impact of the histone H3.3 K27M mutation

Nichole A. Lewis<sup>1, 2, 3</sup> and Paul S. Knoepfler<sup>1, 2, 3\*</sup>

*A manuscript version of this chapter is in preparation for submission soon to a journal.*

<sup>1</sup>Department of Cell Biology and Human Anatomy & <sup>2</sup>Genome Center, University of California Davis School of Medicine; <sup>3</sup>Institute of Pediatric Regenerative Medicine, Shriners Hospital For Children Northern California, Sacramento, CA 95817 \*corresponding author,

knoepfler@ucdavis.edu

## **Abstract**

Histone variant H3.3 is well-established as having an important role in development, including specifically at bivalent genes. In recent years it has also been positioned as a defining characteristic of two types of pediatric brain tumors: diffuse intrinsic pontine glioma (DIPG), which possess the H3.3 K27M mutation, and glioblastoma (GBM) which can have either the G34R or G34V mutations in H3.3. All three mutations influence histone marks resulting in changes to gene expression. These marks as well as the downstream processes whose expression they affect are the subjects of numerous potential drug therapies. This review focuses on the developmental impact of histone H3.3 mutations pointing to a potential cell of origin for these tumors and the epigenetic effects of these mutations. Furthermore, we discuss the recent advancements made in drug treatments and the potential therapies that target the mutant H3.3-associated epigenetic perturbations and their downstream pathways.

## **Introduction**

Pediatric brain tumors are one of the main contributors to childhood cancer diagnoses and deaths. Among the most aggressive of these tumors are diffuse intrinsic pontine glioma (DIPG) with an estimated median survival of less than a year. They are located in the ventral pons of the brainstem (Mackay et al., 2017; Warren, 2012). The poor prognosis of DIPGs is largely due to its invasiveness and the fact that the ventral pons is an inoperable region leaving radiation to be the main treatment method for these patients (Jones and Baker, 2014; Warren, 2012).

However, over the course of the last 8 years, significant progress has been made in uncovering the molecular mechanisms involved in DIPG tumor formation and progression. Specifically, the identification of the two mutually exclusive point mutations in the histone variant H3.3 resulting either in changing lysine 27 to methionine (H3.3K27M) or glycine 34 to arginine or valine (H3.3G34R/V) (Khuong-Quang et al., 2012; Schwartzentruber et al., 2012; Wu et al., 2012) has sparked new insights. H3.3K27M has been found to occur in approximately 70-80% of DIPG

and is specific to the pediatric age group while H3.3G34R/V is present in approximately 13-15% of glioblastomas (GBMs) and typically occurs in young adults (Bjerke et al., 2013; Khuong-Quang et al., 2012; Mackay et al., 2017; Schwartzenuber et al., 2012; Wu et al., 2012). Although these mutations are regarded as driver mutations, they cannot cause tumor formation on their own. Cells with histone H3 mutations are found to have one or more of the following alterations: loss of *TP53*, activation of *PDGFRA*, amplification of *MYCN*, upregulation of *MYC*, and mutations in *FGFR1* and *ATRX/DAXX* (Bjerke et al., 2013; Funato et al., 2014; Jones et al., 2013; Khuong-Quang et al., 2012; Lewis et al., 2013; Mackay et al., 2017; Pathania et al., 2017; Saratsis et al., 2014; Schwartzenuber et al., 2012; Sturm et al., 2012). The H3.3 coding mutations most often occur in the H3F3A gene and patients are heterozygous (Yuen and Knoepfler, 2013). Since the H3F3B gene encodes an identical H3.3 protein, DIPG patients have three wildtype H3.3 coding alleles and one mutant, but the mutant appears to have a dominant negative effect and can interfere with the modification of nearby wildtype histones (Yuen and Knoepfler, 2013).

Both the K27M and G34R/V mutations occur in the N-terminal histone tail of H3.3, a region of the protein that is heavily modified by post-translational modifications (PTMs). Lysine 27 plays an important role in gene regulation as it can be either methylated or acetylated leading to gene repression or activation, respectively. The H3.3K27M mutation causes a global reduction in H3K27me3 levels by interfering with the binding and enzymatic activity of PRC2, the protein responsible for adding K27me2 and K27me3 to histone H3 although the exact mechanism is still an open question (Bender et al., 2013; Chan et al., 2013; Fang et al., 2018; Lee et al., 2019; Lewis et al., 2013; Stafford et al., 2018). Conversely, levels of H3K27ac, a mark that is associated with active transcription, enhancers, and super-enhancers, have been shown to increase in H3.3K27M DIPG cells (K.-Y. Chen et al., 2020; Creighton et al., 2010; Funato et al., 2014; Hnisz et al., 2013; Krug et al., 2019; Larson et al., 2019; Lewis et al., 2013; Lovén et al., 2013; Nagaraja et al., 2017; Whyte et al., 2013). This signifies that changes in the levels of these two K27 marks impact gene expression, which in turn is a key contributor to tumorigenesis. The epigenetic effects

of the H3.3G34R/V mutation have been less extensively studied but there is emerging evidence that G34R/V impacts the methylation status and distribution of H3K36me3, which depending on the context can either activate or repress transcription, and H3K9me3, a well-established mark of heterochromatin and repressed gene expression (Becker et al., 2016; Bjerke et al., 2013; Lewis et al., 2013; Voon et al., 2018; Wagner and Carpenter, 2012).

In addition to the advances made in understanding the epigenetic mechanisms of DIPG, there has been progress testing different drugs in mice and cell line models. Many of the drug treatments being explored exploit the alterations to the epigenetic landscape in DIPG caused by the H3.3K27M mutation. Promising drug targets include BET bromodomain proteins, NOTCH signaling pathway, histone deacetylase (HDAC), cyclin-dependent kinases (CDK), and PRC2 or PRC2 components (K.-Y. Chen et al., 2020; Grasso et al., 2015; Lin et al., 2019; Mohammad et al., 2017; Nagaraja et al., 2017; Piunti et al., 2017; Wiese et al., 2020). Given that the standard treatment for these tumors is limited to radiation therapy the development, testing, validation, and approval of chemotherapy options are of high importance in order to improve patient outcomes and survival. This review will be focused on the epigenetic changes that occur as a result of the K27M and G34R/V mutations, the proposed mechanisms by which these mutations are thought to disrupt the epigenomic landscape, and the status of proposed drug treatments including those that have entered clinical trials.

### **A developmentally intermediate cell type is likely the cell of origin for DIPGs**

Identifying the cell of origin of DIPGs is important for better understanding the development-related mechanisms driving the disease as well as determining what genetic alterations initiate abnormal proliferation and, ultimately, cellular transformation. Currently, there are two likely candidates for the DIPG cell of origin: neural precursor cells (NPC) and oligodendrocyte precursor cells (OPC). In normal, healthy brainstem tissue the NPC markers Vimentin and Nestin are co-expressed. In addition, Nestin positive cells have an expression

pattern that coincides with DIPG occurrence. Nestin is first expressed during infancy, then decreases around 2 years old, before re-emerging again around 6 years old. This pattern has been shown to coincide with the ages that many patients are diagnosed with DIPG (Monje et al., 2011; Schwartzenuber et al., 2012; Sturm et al., 2012). Additionally, this initial study by Monje et al. (2011) determined that human DIPG cells grown in culture express several NPC markers including Nestin, Vimentin, and GFAP as well as CD133, a stem cell-related cell surface marker that is used to identify tumor-initiating cells in the brain. Together these observations make NPCs a cell type of high interest as the potential cell of origin of DIPG.

Funato et al. (2014) built off of this work by testing what effect known DIPG mutations H3.3K27M, H3.3G34R/V, constitutively active *PDGFRA*, and loss of function of *TP53* have on NPC proliferation and transformation (Fontebasso et al., 2014; Khuong-Quang et al., 2012; Nikbakht et al., 2016; Sturm et al., 2012). H3.3K27M on its own resulted in increased proliferation but did not induce tumor formation, which is consistent with other reports (Larson et al., 2019; Pathania et al., 2017). It is also important to note that this increase in proliferation in NPCs with mutant histone expression alone is specific to H3.3K27M and is not observed with wild-type H3.3 or H3.3G34R/V (Funato et al., 2014). This contributes to a growing body of evidence suggesting that H3.3K27M and H3.3G34R/V have different cells of origin due to tumors with these mutations arising in different regions and times of brain development (Pathania et al., 2017; Sturm et al., 2012).

Addition of *TP53* loss of function and *PDGFRA* amplification alongside H3.3K27M have more mixed results in NPCs. In the context of postnatal mouse brainstem NPCs, H3.3K27M mutation and loss of p53 results in increased cell proliferation and result in the formation of ectopic cell clusters but not tumorigenesis (Lewis et al., 2013; Pathania et al., 2017). *PDGFRA* amplification along with H3.3K27M mutation and p53 loss of function increased proliferation in postnatal NPCs, and these cells developed into tumors following injection into the pons region (Funato et al., 2014). However, these tumors were slow-growing and regarded as low-grade

glioma, whereas DIPGs obtained from patients are by definition high-grade cancers (Funato et al., 2014; Louis et al., 2016). These data suggest that while NPCs may still be the cell of origin, the early initiation steps of tumorigenesis likely take place during development in utero and not postnatally.

Other groups have turned to mouse models that induce these mutations during embryonic development to test if a specific developmental window is the key to triggering tumorigenesis (Larson et al., 2019; Pathania et al., 2017). In this context, loss of p53 together with H3.3K27M mutation in NPCs resulted in tumorigenesis, accelerated tumor growth, and decreased survival compared to loss of p53 alone and loss of p53 with wild-type H3.3 expression (Larson et al., 2019; Pathania et al., 2017). Amplification of *PDGFRA* together with knock-down of the histone chaperone *ATRX* (loss of *ATRX* has also been associated with DIPG and GBM) served to decrease tumor latency and increase penetrance in H3.3K27M p53 loss of function mice (Goldberg et al., 2010; Lewis et al., 2010; Pathania et al., 2017; Schwartzentruber et al., 2012). Together, these results further support the idea that embryonic NPCs are a strong candidate for the cell of origin, and at minimum H3.3K27M mutation and loss of p53 are required to induce DIPG formation.

When DIPGs are grown in culture as neurospheres, a subset of those cells has been found to express the OPC marker OLIG2 (Monje et al., 2011). This is consistent with the finding that about half of Nestin positive cells in healthy ventral pontine cell populations express OLIG2 indicating that OPCs may also be a cell lineage of interest (Monje et al., 2011). A survey of normal brain tissue from postnatal day 1 to 18 years old affirms that there is a peak of OLIG2 and proliferation marker Ki67 expressing cells from 0-1 months old in the pons region, which makes a significant contribution to the observed growth of the pons until approximately 5 years old (Tate et al., 2015). Furthermore, single-cell RNAseq and super-enhancer analysis of H3.3K27M DIPG tumor samples indicated increased gene expression and enrichment of the super-enhancer mark H3K27ac at genes corresponding to OPCs and oligodendrocyte lineage differentiating cells such

as *PDGFRA*, *CSPG4*, *MBP*, and *OLIG1/2*, to name a few (Filbin et al., 2018; Nagaraja et al., 2017). In addition, OPCs are the most abundant cell type among H3K27M malignant cells (Filbin et al., 2018; Nagaraja et al., 2019, 2017). Further investigation into OPCs harboring the H3.3K27M mutation revealed this cell type, similar to H3.3K27M DIPGs, is enriched for expression of PRC2 target genes, which are repressed in more differentiated cell types (Filbin et al., 2018; Nagaraja et al., 2019). When compared directly to NPCs possessing the H3.3K27M mutation, notably H3.3K27M OPC enhancer profiles more closely match those of DIPG than NPCs (Nagaraja et al., 2019).

Recently, an induced pluripotent stem cell (iPSC) model has shed light on how and when in development and cell lineage specification DIPG tumor initiation occurs. H3.3K27M over-expression and *TP53* knock-down were induced in iNSCs (induced neural stem cells) and iOPCs (induced oligodendrocyte progenitor cells) and injected into the brainstem of mice (Haag et al., 2021). Surprisingly, malignant tumors were only detected in mice that were injected with iNSCs and not iOPCs despite previous reports that DIPG tumors contain OPCs and H3.3K27M conferring a growth advantage in iOPCs in the present study (Filbin et al., 2018; Haag et al., 2021; Monje et al., 2011; Nagaraja et al., 2019, 2017). Interestingly, further investigation into the gene expression pattern of iNSCs with H3.3K27M and shTP53 revealed that many genes associated with the OPC lineage are upregulated in these iNSC tumors (Haag et al., 2021). These genes are largely found in developmental bivalent domains that contain heterotypic nucleosomes (H3.3K27M and wild-type H3.3) and demonstrate decreased H3K27me3 following H3.3K27M expression indicating that H3.3K27M expression in NSCs results in the dysregulation of developmental programs and the premature activation of OPC programs while the ultimately NSC cell identity allows the cells to retain stem-like characteristics leading to continued self-renewal and proliferation and ultimately tumor formation (Banaszynski et al., 2013; Goldberg et al., 2010; Haag et al., 2021). This phenomenon could serve as an explanation for why distinguishing between NSC/NPC and OPC as the cell of origin for DIPG has been a hurdle in the field; because

characteristics of both cell types are present and this is triggered by the disruption of normal development.

Altogether these findings suggest that rather than NPCs being the point of full transformation they instead are likely the cell type where the H3.3K27M mutation first arises. It is possible that only after partially differentiating into OPCs, gaining a more active chromatin landscape, and expressing genes ultimately upregulated in DIPG (such as *PDGFRA*, and PRC2 target genes) as well as acquiring more mutations that these H3.3K27M-bearing OPCs continue to proliferate and self-renew leading to full transformation to give rise to the DIPG tumor (Filbin et al., 2018; Nagaraja et al., 2019; Tate et al., 2015). A similar developmental path has been found for adult glioma, making the existence of an at least somewhat similar mechanism in pediatric brain tumors plausible (Liu et al., 2011). An additional possibility is that the findings pointing to both NPCs and OPCs as potential DIPG cells of origin are both in a sense correct and that an intermediate cell type is the most common cell of origin.

Further investigation into how exactly H3.3 mutant DIPGs arise including the developmental time-points that various mutations occur and how they affect development and lineage specification will be key to uncovering the exact cell of origin and transformation. Similar studies on G34 mutant gliomas will also be crucial. Such knowledge could prove useful for early detection of these tumor cells, subsequent early treatment, and improved survival for these young patients.

### **H3.3G34R/V results in histone mark and transcriptomic changes that are unique from H3.3K27M**

In addition to the H3.3K27M mutation, H3.3 is in some cases mutated at glycine 34 (G34) to either arginine or valine, often denoted as H3.3G34R/V. These two mutations in *H3F3A* are mutually exclusive and the G34R/V mutation only occurs in *H3F3A* whereas the K27M mutation is found in both *H3F3A* and more rarely in *HIST1H3B* (H3.1) (Nagaraja et al., 2017;

Schwartzentruber et al., 2012; Sturm et al., 2012; Wu et al., 2012). H3.3G34R/V tumors are typically found in the cerebral hemispheres (H3.3K27M tumors are generally found throughout the midline and pons regions), and most often manifest in adolescents and young adults. They have relatively somewhat longer survival than H3.3K27M tumors (Bjerke et al., 2013; Mackay et al., 2017; Schwartzentruber et al., 2012), but also a very poor prognosis. H3.3K27M and H3.3G34R/V have significantly different gene expression profiles while H3.3G34R and H3.3G34V have very similar gene expression patterns and include increased expression of genes related to cell adhesion, cell membrane, phosphoprotein, and glycoproteins (Bjerke et al., 2013; K.-Y. Chen et al., 2020; Funato et al., 2014; Paugh et al., 2010; Schwartzentruber et al., 2012). However, when human astrocyte (HA) and H3.3 wild-type high-grade glioma (HGG) cell lines undergo gene-editing using CRISPR to introduce either the H3.3K27M or H3.3G34R mutations into H3F3A, expression of many of the same genes related to neurogenesis, differentiation, developmental proteins, and the NOTCH signaling pathway are induced in each case suggesting that these two mutations may act through more similar mechanisms than previously thought (K.-Y. Chen et al., 2020). Altogether this indicates that H3.3K27M and H3.3G34R/V mutations often cause unique glioma tumors compared to each other and H3.3 wild-type tumors, that each glioma type forms at different stages of development, and they may have different cells of origin (Bjerke et al., 2013; Mackay et al., 2017; Schwartzentruber et al., 2012).

H3.3G34R/V tumors also have loss of function mutations in *TP53* and the H3.3 chaperones *ATRX-DAXX* that deposit H3.3 at heterochromatin and telomeres. *ATRX-DAXX* are thought to be linked to alternative lengthening of telomeres (ALT) in glioma (Goldberg et al., 2010; Lewis et al., 2010; Schwartzentruber et al., 2012; Sturm et al., 2012). Many of the differentially expressed genes in H3.3G34R/V tumor cells are related to distinct regions of brain development, developmentally regulated transcription factors, and cell fate determining factors (Bjerke et al., 2013; K.-Y. Chen et al., 2020). Among these differentially expressed factors is *MYCN* which regulates brain development in normal, healthy tissue but gain-of-function mutations or

overexpression in neural stem cells results in the formation of a variety of neural tumors (Bjerke et al., 2013; Knoepfler et al., 2002; Swartling et al., 2012). Identification of *MYCN* overexpression in H3.3G34R/V gliomas provides insight for possible treatments of these otherwise difficult-to-treat tumors by targeting proteins that normally help stabilize *MYCN* such as CHK1 and AURKA (Bjerke et al., 2013; Cole et al., 2011; Otto et al., 2009).

A recent study utilized CRISPR-Cas9 to edit endogenous *H3F3A* to generate HA and HGG cells with the H3.3G34 or H3.3K27M mutations to determine what cellular and molecular changes in GBM are specific to H3.3G34R and if any are shared with H3.3K27M (K.-Y. Chen et al., 2020). Several changes were observed between wild-type H3.3 cells and their edited H3.3G34R counterparts including increased growth and proliferation in HA-H3.3G34R cells and changes in chromatin marks at NOTCH signaling pathway promoters (K.-Y. Chen et al., 2020). H3.3 was increased at the promoters of neurogenesis and NOTCH signaling genes in HA- and HGG-H3.3G4R/K27M cells compared to wild-type along with decreased levels of H3K27me<sub>3</sub>, H3K27ac, and H3K36me<sub>3</sub> at these same promoters (K.-Y. Chen et al., 2020). Consequently, increased expression at both the transcript and protein level of NOTCH signaling and neurogenesis genes was seen in HA- and HGG-H3.3G4R/K27M cells demonstrating that NOTCH and neurogenesis pathways are shared key mechanisms in DIPG and GBM (K.-Y. Chen et al., 2020). This is further supported by the finding that combining standard irradiation with DAPT, a  $\gamma$ -secretase inhibitor that inhibits NOTCH signaling, significantly decreased cell viability of HA-H3.3K27M and HGG-H3.3G34R in culture in comparison to wild-type cells demonstrating that this combination therapy could be an effective treatment for both DIPG and GBM harboring either H3.3K27M or H3.3G34R mutations (K.-Y. Chen et al., 2020).

Despite these insights, the mechanisms by which the H3.3G34R/V mutations stimulate tumor formation and changes to gene expression are still mostly open questions. Glycine 34 itself is not a site for post-translational modifications (PTMs) but it is only two residues away from H3K36, which can either be methylated or acetylated. Different studies report that H3K36me<sub>3</sub>

levels are either increased, decreased, or unchanged in GBM patient samples (Bjerke et al., 2013; K.-Y. Chen et al., 2020; Fontebasso et al., 2014; Jain et al., 2020; Lewis et al., 2013; Schwartzenruber et al., 2012; Voon et al., 2018). There are two main theories for how H3K36me3 levels are affected by G34 mutations: H3.3G34R/V either prevents methylation by the methyltransferase SETD2 or blocks demethylases KDM4 A/B/C (Jain et al., 2020; Lewis et al., 2013; Voon et al., 2018). It is worth noting that these theories are not mutually exclusive, both methyltransferase and demethylase dynamics could be affected by G34 mutations in the same cell, but one mechanism may be more affected than the other in a given cell line or patient (Jain et al., 2020; Voon et al., 2018). G34 mutations do not result in global decreases in H3K36me3 but do cause H3K36me3 to be depleted from nucleosomes that contain the H3.3G34 mutant thus supporting their hypothesis that G34 mutations inhibit SETD2 activity (Lewis et al., 2013). These H3.3G34 mutant nucleosomes with decreased H3K36me3 are improved substrates for the methyltransferase PRC2 and result in increased levels of H3K27me2/3 (the mark that PRC2 deposits) on the same nucleosome containing the H3.3G34 mutation suggesting a *cis*-acting mechanism (Jain et al., 2020). This leads to a spreading and increase of the H3K27me2/3 repressive mark while simultaneously decreasing the activating marks H3K27ac and H3K36me3 at a subset of enhancers and active genes resulting in decreased gene expression leading to tumorigenesis in these cells.

Conversely, it has been found that H3K36me3 levels can be unchanged or slightly increased in H3.3G34R/V GBM due to a decrease in KDM4 A/B/C demethylase activity (Bjerke et al., 2013; Schwartzenruber et al., 2012; Voon et al., 2018). This slight increase in H3K36me3 does not uniformly occur throughout the genome and instead is concentrated to specific gene regions and genes, including *MYCN*, resulting in increases in gene expression at these specific regions because H3K36me3 is a transcription activating mark (Bjerke et al., 2013; Voon et al., 2018; Wagner and Carpenter, 2012). KDM4 family of demethylases bind preferentially to H3.3G34R compared to wild-type H3.3 and H3.3G34R not only binds to KDM4 but also

inactivates and sequesters it suggesting that H3.3G34R is a *trans*-acting mutation in this situation (Voon et al., 2018).

While the two theories explained here ultimately would have generally opposite effects on H3K36me3 levels and distribution within different regions of the genome, protein structure analysis work demonstrates in both cases that inactivation of the respective enzymes is likely due to hindrance caused by the small glycine group at residue 34 being replaced by the considerably larger arginine or valine and that these larger residues significantly reduce enzymatic activity of SETD2 and KDM 4 A/B/C (Chen et al., 2006; Couture et al., 2007; Jain et al., 2020; Voon et al., 2018; Yang et al., 2016). While H3G34 is not directly modified, it may play an important role in maintaining H3K36 modifications and the mutations found in GBM disrupt key epigenetic writers, which then substantially change gene expression either through H3K36me3 levels or through the spread of H3K27me3 via PRC2. These differences in mechanisms could be due to variation between patient samples or another biological change that has not yet been found. In future studies it will be important to determine under what circumstances SETD2 is inhibited versus KDM4 is inhibited (or both). It will also be important to know if this enzyme inhibition varies across patients or if an active cellular mechanism balances increases and decreases in H3K36me3 at specific locations to drive tumorigenesis. H3.3G34R/V gliomas are not nearly as extensively studied as H3.3K27M and further investigation into epigenetic mechanisms at play, gene expression changes, and drug sensitivities are proceeding to improve our understanding and treatment for this subset of high-grade childhood glioma.

### **H3.3K27M increases H3K27ac levels leading to increased expression of super-enhancer related genes**

Lysine 27 on histone H3 is a heavily modified residue and can either be acetylated or methylated, generally resulting in gene activation or repression, respectively. Therefore, it would be expected that the H3.3K27M mutation in DIPG would have an effect on H3K27ac levels.

Multiple studies have reported global increases in H3K27ac levels accompanied by increases in gene expression and, in some cases, increase chromatin accessibility in H3.3K27M DIPG samples (K.-Y. Chen et al., 2020; Krug et al., 2019; Larson et al., 2019; Lewis et al., 2013; Nagaraja et al., 2019; Wang et al., 2021). Interestingly, the increase in H3K27ac is found on heterotypic nucleosomes, those that contain an H3.3 mutant (either K27M or G34R) and H3.3 wild-type (Lewis et al., 2013; Piunti et al., 2017; Wang et al., 2021; Wiese et al., 2020). This increase in H3K27ac coincides with a sharp decrease in H3K27me3 leading to very low to no detectable H3K27me3, aberrant gene expression, and hyperacetylation in the same genomic locations as H3.3K27M-H3K27ac nucleosomes due to H3.3K27M negatively impacting PRC2 activity (Krug et al., 2019; Lewis et al., 2013; Piunti et al., 2017; Wiese et al., 2020). Increases in H3K27ac appear to be H3K27M dependent with knock-down, knock-out, and gene-editing K27M to wild-type each reduce H3K27ac (K.-Y. Chen et al., 2020; Krug et al., 2019; Silveira et al., 2019). Similarly, mouse H3.3K27M knock-in and CRISPR-Cas9 gene editing wild-type *H3F3A* to *H3F3A-K27M* models result in increased H3K27ac levels indicating that H3.3 mutation status has a direct effect on H3K27ac levels (K.-Y. Chen et al., 2020; Larson et al., 2019). There is evidence suggesting that changes in H3K27ac are reflective of changes to the amount of H3K27ac at these sites and not a complete loss of H3K27ac sites, in the case of removing H3.3K27M mutation, or gain of *de novo* sites, when H3.3K27M mutation is present (Krug et al., 2019).

Importantly, H3K27ac is a mark associated with enhancers and super-enhancers. Super-enhancers are similar to enhancers in that both are *cis*-regulatory regions but super-enhancers can be thousands of base pairs long (compared to enhancers which are typically hundreds of base pairs), have high levels of Mediator complex and transcription factors important for establishing and maintaining cell identity such as Oct4, Sox2, Nanog, Klf4, and Essrb, and high levels of H3K27ac (Whyte et al., 2013). Genes regulated by super-enhancers tend to be very highly transcribed and related to cell identity and/or oncogenesis making them prime regions of

study in DIPG and potential drug targets (Hnisz et al., 2013; Lovén et al., 2013; Whyte et al., 2013).

Super-enhancers specific to H3.3K27M DIPG tumors have high levels of H3K27ac and are linked to highly transcribed genes involved in neurogenesis, axon guidance, proliferation, Rho GTPase signaling, development, and signal transduction of several pathways including NOTCH signaling, Hedgehog, and PDGF signaling, all of which have been shown to play key roles in DIPG tumorigenesis and maintenance (C. C. L. Chen et al., 2020; K.-Y. Chen et al., 2020; Krug et al., 2019; Larson et al., 2019; Monje et al., 2011; Nagaraja et al., 2019, 2017; Pathania et al., 2017; Paugh et al., 2013; Taylor et al., 2015; Wang et al., 2021; Wiese et al., 2020). CRISPR-Cas9 gene editing models show that the high levels of H3K27ac at super-enhancers and subsequent gene activation are dependent on the H3.3K27M mutation. After gene-editing of *H3F3A-K27M* (either knockout or reversion to wild-type) there is a reduction of H3K27ac and an increase in H3K27me3 at super-enhancers leading to decreases in gene expression of many oncogenic and Notch signaling pathways (K.-Y. Chen et al., 2020; Krug et al., 2019). Altogether these data indicate that H3K27ac and super-enhancer are potential candidates for therapeutic targets. In fact, to date there has been some success in using histone deacetylase (HDAC) inhibitors, CDK7 inhibitors, Notch signaling inhibitors, and bromodomain and extra-terminal (BET) domain inhibitors to treat these tumors in cell culture and mouse xenograft models (K.-Y. Chen et al., 2020; Grasso et al., 2015; Nagaraja et al., 2017; Piunti et al., 2017; Wang et al., 2021; Wiese et al., 2020).

Enhancers and super-enhancers are not the only genomic regions that display an increase in H3K27ac and subsequent increases in gene expression in H3.3K27M DIPG. H3K27ac levels have also been shown to be elevated in repetitive elements, specifically at endogenous retrovirus (ERVs) sequences, resulting in activation of these otherwise silenced regions (Krug et al., 2019). The activation of ERVs results in viral mimicry, a phenomenon wherein double-stranded RNA expression is induced leading to activation of immune response pathways (Chiappinelli et al.,

2015; Roulois et al., 2015). This is a clear demonstration of increased global H3K27ac levels resulting in aberrant gene expression and presents another potential therapeutic strategy. There is evidence in DIPG that combining DNA demethylating drugs and HDAC inhibitors further increase ERV expression resulting in decreased cell viability in H3.3K27M cells (Krug et al., 2019). Enhancers, super-enhancers, repeat elements, and the interplay between H3K27ac and H3K27me3 levels play a key role in regulating gene expression in pathways that are targetable with known drug treatments. Further characterization of these genomic regions and histone marks will be important to better understand the epigenetic intricacies of DIPG as well as determine potential drug treatments that specifically target mutant H3.3 DIPG cells while not harming healthy tissues, something that the current radiation alone treatment plan lacks.

### **HDAC inhibitor mono- and combination therapies are promising treatments for DIPG**

One of the largest obstacles facing the DIPG field is developing drug therapies that can cross the blood brain barrier and specifically target tumor tissue and not healthy brain tissue. In recent years, huge strides have been made in uncovering vulnerabilities in these tumors and one drug has even advanced to clinical trials specifically for DIPG. Perhaps one of the most extensively investigated drug treatments for DIPG is the histone deacetylase inhibitor (HDACi) panobinostat. Panobinostat is currently FDA approved for treating multiple myeloma and has been in phase I clinical trials for a variety of adult cancers, including brain (NCT01324635) (Grasso et al., 2015; Hennika et al., 2017). Following a large drug-screening study it was found that DIPG tumor cells are sensitive to panobinostat resulting in decreased cell viability and reduction of proliferation genes (Grasso et al., 2015; Hennika et al., 2017). Panobinostat increases H3K27ac levels which then restores H3K27me3 levels because acetylation of other residues on the histone tail blocks PRC2 interaction with H3K27M (Brown et al., 2014; Grasso et al., 2015). This allows PRC2 to interact with and methylate the K27 on the wild-type H3 histone on a heterotypic nucleosome resulting in the rescue of normal gene expression profiles (Brown

et al., 2014; Grasso et al., 2015). *In vivo* mouse studies yield mixed results with some indicating that panobinostat significantly decreases tumor cell growth and increases survival but others have struggled to replicate this citing toxicity issues and no improvements to survival (Grasso et al., 2015; Hennika et al., 2017; Krug et al., 2019; Lin et al., 2019; Meel et al., 2020). This could be due to differences in drug delivery systems which is worth investigating further given the difficulty of identifying drugs that can cross the blood-brain barrier (Grasso et al., 2015; Hennika et al., 2017; Sandberg et al., 2002).

Despite being one of the few drugs for treating DIPG to advance to clinical trials (NCT02717455), panobinostat is not without complications that need to be carefully considered (Cooney et al., 2018). For one, the detrimental effect on cell viability and proliferation is observed in H3.3K27M, H3.3G34R, and wild-type H3.3 cells which on the one hand alleviates the need to sequence patient tumors prior to administration but could also be the underlying cause for cytotoxicity observed in xenograft studies and negative side-effects observed in current clinical trials (K.-Y. Chen et al., 2020; Grasso et al., 2015; Hennika et al., 2017; Vitanza et al., 2021). Additionally, it has been well documented that H3.3K27M DIPG cells develop resistance to panobinostat upon long-term exposure or follow-up treatment indicating that combination therapeutic approaches will be key to effectively using panobinostat in the clinic (Grasso et al., 2015; Nagaraja et al., 2017).

Many different cellular processes have been targeted in combination with panobinostat in order to address drug resistance including proteasomes, epithelial to mesenchymal transition (EMT), CDK signaling, and BET proteins (Grasso et al., 2015; Krug et al., 2019; Lin et al., 2019; Meel et al., 2020; Nagaraja et al., 2017). A high-throughput drug screening study revealed that the proteasome inhibitor marizomib had a high degree of synergy with panobinostat and could cross the blood-brain barrier (Lin et al., 2019). Just as with panobinostat alone, marizomib and panobinostat together resulted in decreased cell proliferation and increased apoptosis in all glioma samples, regardless of H3 status, and this effect was greater than either drug alone (Lin

et al., 2019). Patient-derived xenograft mouse experiments with combination therapy resulted in a 20% increase in survival which, while arguably marginal, is still an improvement over current treatment options and predicted patient outcomes (Lin et al., 2019). Current data suggests that the combination therapy largely affects metabolism and cellular respiration by triggering oxidative stress and downregulating oxidative phosphorylation genes, increasing levels of ubiquitinated proteins, and upregulating genes related to the unfolded protein response (Lin et al., 2019). This demonstrates that metabolic processes are compromised in DIPGs and are therefore vulnerable to compounds that target metabolic pathways showcasing another approach that should be investigated further.

A common characteristic of cancer, including DIPG, is the activation of mesenchymal genes through the epithelial to mesenchymal transition (EMT) and has been shown to occur when H3.3K27M is introduced into mouse NSCs making it a target worth investigating (Larson et al., 2019; Meel et al., 2020; Puget et al., 2012). Specifically, the receptor tyrosine kinase *AXL* is highly expressed in DIPG which is dependent on the presence of H3.3K27M and is a known initiator of EMT in adult glioma making it a prime drug target (Meel et al., 2020; Paugh et al., 2011; Silveira et al., 2019; Vajkoczy et al., 2006). Inhibiting *AXL* alone with BGB324 resulted in decreased viability and a significant decrease in the expression of mesenchymal-associated genes, an effect that was even more pronounced when combined with panobinostat (Meel et al., 2020). The combination therapy led to further gene expression changes that were not observed with either drug alone including a decrease in stem cell markers and an increase in neuronal differentiation genes (Meel et al., 2020). The synergy of the two drugs was maintained in *in vivo* xenograft studies where a modest increase in survival was observed but it is important to note that this result was only seen when the convection-enhanced delivery (CED) system was used providing further evidence that this method is likely crucial to delivering the necessary concentrations of drugs to the brain (Meel et al., 2020; Sandberg et al., 2002). Importantly, the synergist effects were specific to H3K27M DIPG cells and were not observed in wild-type H3 glioblastoma thus

making this particular regimen most promising for H3K27M tumors and potentially easing side-effects because surrounding wild-type H3 cells will be minimally affected if at all (Meel et al., 2020).

While this was not included in the *in vivo* studies, the group also tested BGB324 and panobinostat together with radiation and found that this resulted in triple synergy *in vitro* with DIPG neurospheres being the most sensitive to this treatment regimen and no regrowth was observed after treatment ended (Meel et al., 2020). This finding is especially important given that the only approved treatment method to date for DIPG is radiation therapy which by itself does not abolish the tumors. Future studies replicating the benefits of combining HDACi and EMT inhibition as well as HDACi, EMT inhibition, and radiotherapy could be critical next steps to developing an effective treatment regimen and improving the survival outcomes for these young patients.

In addition to alterations in histone mark levels and distribution, transcription dysregulation is another main characteristic of DIPG making it a prime candidate to target in combination with H3K27ac. The two primary ways of doing this are by targeting BET proteins and CDKs that regulate RNA Pol II i.e. BRD4 via JQ1 (Nagaraja et al., 2017; Piunti et al., 2017; Taylor et al., 2015; Wiese et al., 2020) and CDK7 via THZ1 (Nagaraja et al., 2017). Combining panobinostat with JQ1 or THZ1 both resulted in reduced cell viability and proliferation and increased apoptosis to a greater degree than any of the three drugs alone (Nagaraja et al., 2017). The issue of drug resistance was also specifically tested and DIPG that developed resistance to panobinostat were also resistant to JQ1 but were sensitive to THZ1 (Nagaraja et al., 2017). Upon investigation, it seems that cells may become resistant to JQ1 following panobinostat treatment because the two drugs downregulate many of the same genes that are related to nervous system development instead of targeting different families of genes such as *ASCL1* (Nagaraja et al., 2017). THZ1 and panobinostat however do target different gene sets with THZ1 largely downregulating genes related to transcription and gene regulation likely explaining why these two drugs have synergy and sensitivity to THZ1 is maintained even after panobinostat treatment (Nagaraja et al., 2017).

Many of the genes that were repressed by the three drugs were also those associated with super-enhancers with H3K27ac specifically being reduced following panobinostat treatment further reinforcing that super-enhancers are elements to assess and test further for pathways that are important to DIPG biology and be modulated with chemotherapies (Nagaraja et al., 2017; Wiese et al., 2020). All three drugs target core processes central to DIPG biology and therefore make promising combination therapies, CDK targeting drugs more so than BET inhibitors, once CDK and BET inhibitor compounds that can cross the blood brain barrier are developed (Nagaraja et al., 2017).

## **Overview**

High-throughput sequencing has allowed the field to identify key, unifying mutations in DIPG tumors including H3.K27M. While it is clear that H3.3K27M plays a key role in DIPG disease biology and has recently been shown to play a crucial role in tumor maintenance, there are still many unanswered questions regarding its effect on gene expression, the chromatin landscape, and downstream pathways that can serve as drug targets.

In Chapter 2, the role of H3.3K27M in chromatin dynamics is discussed. Isogenic H3.3 wild-type cell lines were made using the CRISPR-Cas9 gene-editing system and matched to parental, unedited H3.3K27M DIPG patient cell lines. Distinct differences in accessible gene groups were found between with impacts on gene expression, namely regarding neuronal development and cell adhesion. The differences in accessible chromatin and genes expression were found to potentially also be due to differences in transcription factor binding sites and we identify some transcription factors of interest for future study.

Chapter 3 discusses future directions for studies that should be conducted on H3.3K27M DIPG tumors, summarizes our chromatin dynamics study, and concludes with proposed drug targets based on regions and genes of interest we found to be accessible and upregulated.

## References

Banaszynski, L.A., Wen, D., Dewell, S., Whitcomb, S.J., Lin, M., Diaz, N., Elsässer, S.J., Chappier, A., Goldberg, A.D., Canaani, E., Rafii, S., Zheng, D., Allis, C.D., 2013. Hira-Dependent Histone H3.3 Deposition Facilitates PRC2 Recruitment at Developmental Loci in ES Cells. *Cell* 155, 107–120. <https://doi.org/10.1016/j.cell.2013.08.061>

Becker, J.S., Nicetto, D., Zaret, K.S., 2016. H3K9me3-Dependent Heterochromatin: Barrier to Cell Fate Changes. *Trends in Genetics* 32, 29–41. <https://doi.org/10.1016/j.tig.2015.11.001>

Bender, S., Tang, Y., Lindroth, A.M., Hovestadt, V., Jones, D.T.W., Kool, M., Zapatka, M., Northcott, P.A., Sturm, D., Wang, W., Radlwimmer, B., Højfeldt, J.W., Truffaux, N., Castel, D., Schubert, S., Ryzhova, M., Şeker-Cin, H., Gronych, J., Johann, P.D., Stark, S., Meyer, J., Milde, T., Schuhmann, M., Ebinger, M., Monoranu, C.-M., Ponnuswami, A., Chen, S., Jones, C., Witt, O., Collins, V.P., von Deimling, A., Jabado, N., Puget, S., Grill, J., Helin, K., Korshunov, A., Lichter, P., Monje, M., Plass, C., Cho, Y.-J., Pfister, S.M., 2013. Reduced H3K27me3 and DNA Hypomethylation Are Major Drivers of Gene Expression in K27M Mutant Pediatric High-Grade Gliomas. *Cancer Cell* 24, 660–672. <https://doi.org/10.1016/j.ccr.2013.10.006>

Bjerke, L., Mackay, A., Nandhabalan, M., Burford, A., Jury, A., Popov, S., Bax, D.A., Carvalho, D., Taylor, K.R., Vinci, M., Bajrami, I., McGonnell, I.M., Lord, C.J., Reis, R.M., Hargrave, D., Ashworth, A., Workman, P., Jones, C., 2013. Histone H3.3 Mutations Drive Pediatric Glioblastoma through Upregulation of MYCN. *Cancer Discovery* 3, 512–519. <https://doi.org/10.1158/2159-8290.CD-12-0426>

Brown, Z.Z., Müller, M.M., Jain, S.U., Allis, C.D., Lewis, P.W., Muir, T.W., 2014. Strategy for “Detoxification” of a Cancer-Derived Histone Mutant Based on Mapping Its Interaction with the Methyltransferase PRC2. *J. Am. Chem. Soc.* 136, 13498–13501. <https://doi.org/10.1021/ja5060934>

Chan, K.-M., Fang, D., Gan, H., Hashizume, R., Yu, C., Schroeder, M., Gupta, N., Mueller, S., James, C.D., Jenkins, R., Sarkaria, J., Zhang, Z., 2013. The histone H3.3K27M mutation in pediatric glioma reprograms H3K27 methylation and gene expression. *Genes & Development* 27, 985–990. <https://doi.org/10.1101/gad.217778.113>

Chen, C.C.L., Deshmukh, S., Jessa, S., Hadjadj, D., Lisi, V., Andrade, A.F., Faury, D., Jawhar, W., Dali, R., Suzuki, H., Pathania, M., A, D., Dubois, F., Woodward, E., Hébert, S., Coutelier, M., Karamchandani, J., Albrecht, S., Brandner, S., De Jay, N., Gayden, T., Bajic, A., Harutyunyan, A.S., Marchione, D.M., Mikael, L.G., Juretic, N., Zeinieh, M., Russo, C., Maestro, N., Bassenden, A.V., Hauser, P., Virga, J., Bogнар, L., Klekner, A., Zapotocky, M., Vicha, A., Krskova, L., Vanova, K., Zamecnik, J., Sumerauer, D., Ekert, P.G., Ziegler, D.S., Ellezam, B., Filbin, M.G., Blanchette, M., Hansford, J.R., Khuong-Quang, D.-A., Berghuis, A.M., Weil, A.G., Garcia, B.A., Garzia, L., Mack, S.C., Beroukhir, R., Ligon, K.L., Taylor, M.D., Bandopadhyay, P., Kramm, C., Pfister, S.M., Korshunov, A., Sturm, D., Jones, D.T.W., Salomoni, P., Kleinman, C.L., Jabado, N., 2020. Histone H3.3G34-Mutant Interneuron Progenitors Co-opt PDGFRA for Gliomagenesis. *Cell* 183, 1617-1633.e22. <https://doi.org/10.1016/j.cell.2020.11.012>

Chen, K.-Y., Bush, K., Klein, R.H., Cervantes, V., Lewis, N., Naqvi, A., Carcaboso, A.M., Lechpammer, M., Knoepfler, P.S., 2020. Reciprocal H3.3 gene editing identifies K27M and G34R mechanisms in pediatric glioma including NOTCH signaling. *Commun Biol* 3, 363. <https://doi.org/10.1038/s42003-020-1076-0>

Chen, Z., Zang, J., Whetstine, J., Hong, X., Davrazou, F., Kutateladze, T.G., Simpson, M., Mao, Q., Pan, C.-H., Dai, S., Hagman, J., Hansen, K., Shi, Y., Zhang, G., 2006. Structural Insights into Histone Demethylation by JMJD2 Family Members. *Cell* 125, 691–702. <https://doi.org/10.1016/j.cell.2006.04.024>

Chiappinelli, K.B., Strissel, P.L., Desrichard, A., Li, H., Henke, C., Akman, B., Hein, A., Rote, N.S., Cope, L.M., Snyder, A., Makarov, V., Buhu, S., Slamon, D.J., Wolchok, J.D., Pardoll, D.M., Beckmann, M.W., Zahnow, C.A., Merghoub, T., Chan, T.A., Baylin, S.B., Strick, R., 2015. Inhibiting DNA Methylation Causes an Interferon Response in Cancer via dsRNA Including Endogenous Retroviruses. *Cell* 162, 974–986. <https://doi.org/10.1016/j.cell.2015.07.011>

Cole, K.A., Huggins, J., Laquaglia, M., Hulderman, C.E., Russell, M.R., Bosse, K., Diskin, S.J., Attiyeh, E.F., Sennett, R., Norris, G., Laudenslager, M., Wood, A.C., Mayes, P.A., Jagannathan, J., Winter, C., Mosse, Y.P., Maris, J.M., 2011. RNAi screen of the protein kinome identifies checkpoint kinase 1 (CHK1) as a therapeutic target in neuroblastoma. *PNAS* 108, 3336–3341. <https://doi.org/10.1073/pnas.1012351108>

Cooney, T., Onar-Thomas, A., Huang, J., Lulla, R., Fangusaro, J., Kramer, K., Baxter, P., Fouladi, M., Dunkel, I.J., Warren, K.E., Monje, M., 2018. DIPG-22. A PHASE 1 TRIAL OF THE HISTONE DEACETYLASE INHIBITOR PANOBINOSTAT IN PEDIATRIC PATIENTS WITH RECURRENT OR REFRACTORY DIFFUSE INTRINSIC PONTINE GLIOMA: A PEDIATRIC BRAIN TUMOR CONSORTIUM (PBTC) STUDY. *Neuro-Oncology* 20, i53–i53. <https://doi.org/10.1093/neuonc/noy059.115>

Couture, J.-F., Collazo, E., Ortiz-Tello, P.A., Brunzelle, J.S., Trievel, R.C., 2007. Specificity and mechanism of JMJD2A, a trimethyllysine-specific histone demethylase. *Nature Structural & Molecular Biology* 14, 689–695. <https://doi.org/10.1038/nsmb1273>

Creyghton, M.P., Cheng, A.W., Welstead, G.G., Kooistra, T., Carey, B.W., Steine, E.J., Hanna, J., Lodato, M.A., Frampton, G.M., Sharp, P.A., Boyer, L.A., Young, R.A., Jaenisch, R., 2010. Histone H3K27ac separates active from poised enhancers and predicts developmental state. *Proceedings of the National Academy of Sciences* 107, 21931–21936. <https://doi.org/10.1073/pnas.1016071107>

Fang, D., Gan, H., Cheng, L., Lee, J.-H., Zhou, H., Sarkaria, J.N., Daniels, D.J., Zhang, Z., 2018. H3.3K27M mutant proteins reprogram epigenome by sequestering the PRC2 complex to poised enhancers. *eLife* 7, e36696. <https://doi.org/10.7554/eLife.36696>

Filbin, M.G., Tirosh, I., Hovestadt, V., Shaw, M.L., Escalante, L.E., Mathewson, N.D., Neftel, C., Frank, N., Pelton, K., Hebert, C.M., Haberler, C., Yizhak, K., Gojo, J., Egervari, K., Mount, C., van Galen, P., Bonal, D.M., Nguyen, Q.-D., Beck, A., Sinai, C., Czech, T., Dorfer, C., Goumnerova, L., Lavarino, C., Carcaboso, A.M., Mora, J., Mylvaganam, R., Luo, C.C., Peyrl, A., Popović, M., Azizi, A., Batchelor, T.T., Frosch, M.P., Martinez-Lage, M., Kieran, M.W., Bandopadhyay, P., Beroukhi, R., Fritsch, G., Getz, G., Rozenblatt-Rosen, O., Wucherpennig, K.W., Louis, D.N., Monje, M., Slavc, I., Ligon, K.L., Golub, T.R., Regev, A., Bernstein, B.E., Suvà, M.L., 2018. Developmental and oncogenic programs in H3K27M gliomas dissected by single-cell RNA-seq. *Science* 360, 331–335. <https://doi.org/10.1126/science.aao4750>

Fontebasso, A.M., Gayden, T., Nikbakht, H., Neirinck, M., Papillon-Cavanagh, S., Majewski, J., Jabado, N., 2014. Epigenetic dysregulation: a novel pathway of oncogenesis in pediatric brain tumors. *Acta Neuropathol* 13.

Funato, K., Major, T., Lewis, P.W., Allis, C.D., Tabar, V., 2014. Use of human embryonic stem cells to model pediatric gliomas with H3.3K27M histone mutation. *Science* 346, 1529–1533. <https://doi.org/10.1126/science.1253799>

Goldberg, A.D., Banaszynski, L.A., Noh, K.-M., Lewis, P.W., Elsaesser, S.J., Stadler, S., Dewell, S., Law, M., Guo, X., Li, X., Wen, D., Chappier, A., DeKaveler, R.C., Miller, J.C., Lee, Y.-L., Boydston, E.A., Holmes, M.C., Gregory, P.D., Grealley, J.M., Rafii, S., Yang, C., Scambler, P.J., Garrick, D., Gibbons, R.J., Higgs, D.R., Cristea, I.M., Urnov, F.D., Zheng, D., Allis, C.D., 2010. Distinct Factors Control Histone Variant H3.3 Localization at Specific Genomic Regions. *Cell* 140, 678–691. <https://doi.org/10.1016/j.cell.2010.01.003>

Grasso, C.S., Tang, Y., Truffaux, N., Berlow, N.E., Liu, L., Debily, M.-A., Quist, M.J., Davis, L.E., Huang, E.C., Woo, P.J., Ponnuswami, A., Chen, S., Johung, T.B., Sun, W., Kogiso, M., Du, Y., Qi, L., Huang, Y., Hütt-Cabezas, M., Warren, K.E., Le Dret, L., Meltzer, P.S., Mao, H., Quezado, M., van Vuurden, D.G., Abraham, J., Fouladi, M., Svalina, M.N., Wang, N., Hawkins, C., Nazarian, J., Alonso, M.M., Raabe, E.H., Hulleman, E., Spellman, P.T., Li, X.-N., Keller, C., Pal, R., Grill, J., Monje, M., 2015. Functionally defined therapeutic targets in diffuse intrinsic pontine glioma. *Nat Med* 21, 555–559. <https://doi.org/10.1038/nm.3855>

Haag, D., Mack, N., Benites Goncalves da Silva, P., Statz, B., Clark, J., Tanabe, K., Sharma, T., Jäger, N., Jones, D.T.W., Kawauchi, D., Wernig, M., Pfister, S.M., 2021. H3.3-K27M drives neural stem cell-specific gliomagenesis in a human iPSC-derived model. *Cancer Cell* 39, 407–422.e13. <https://doi.org/10.1016/j.ccell.2021.01.005>

Hennika, T., Hu, G., Olaciregui, N.G., Barton, K.L., Ehteda, A., Chitranjan, A., Chang, C., Gifford, A.J., Tsoli, M., Ziegler, D.S., Carcaboso, A.M., Becher, O.J., 2017. Pre-Clinical Study of Panobinostat in Xenograft and Genetically Engineered Murine Diffuse Intrinsic Pontine Glioma Models. *PLOS ONE* 12, e0169485. <https://doi.org/10.1371/journal.pone.0169485>

Hnisz, D., Abraham, B.J., Lee, T.I., Lau, A., Saint-André, V., Sigova, A.A., Hoke, H.A., Young, R.A., 2013. Super-Enhancers in the Control of Cell Identity and Disease. *Cell* 155, 934–947. <https://doi.org/10.1016/j.cell.2013.09.053>

Jain, S.U., Khazaei, S., Marchione, D.M., Lundgren, S.M., Wang, X., Weinberg, D.N., Deshmukh, S., Juretic, N., Lu, C., Allis, C.D., Garcia, B.A., Jabado, N., Lewis, P.W., 2020. Histone H3.3 G34 mutations promote aberrant PRC2 activity and drive tumor progression. *PNAS*. <https://doi.org/10.1073/pnas.2006076117>

Jones, C., Baker, S.J., 2014. Unique genetic and epigenetic mechanisms driving paediatric diffuse high-grade glioma. *Nat Rev Cancer* 14, 651–661. <https://doi.org/10.1038/nrc3811>

Jones, D.T., Hutter, B., Jäger, N., Korshunov, A., Kool, M., Warnatz, H.-J., Zichner, T., Lambert, S.R., Ryzhova, M., Quang, D.A.K., Fontebasso, A.M., Stütz, A.M., Hutter, S., Zuckermann, M., Sturm, D., Gronych, J., Lasitschka, B., Schmidt, S., Şeker-Cin, H., Witt, H., Sultan, M., Ralsner, M., Northcott, P.A., Hovestadt, V., Bender, S., Pfaff, E., Stark, S., Faury, D., Schwartzentruber, J., Majewski, J., Weber, U.D., Zapatka, M., Raeder, B., Schlesner, M., Worth, C.L., Bartholomae, C.C., von Kalle, C., Imbusch, C.D., Radomski, S., Lawerenz, C., van Sluis, P.,

Koster, J., Volckmann, R., Versteeg, R., Lehrach, H., Monoranu, C., Winkler, B., Unterberg, A., Herold-Mende, C., Milde, T., Kulozik, A.E., Ebinger, M., Schuhmann, M.U., Cho, Y.-J., Pomeroy, S.L., von Deimling, A., Witt, O., Taylor, M.D., Wolf, S., Karajannis, M.A., Eberhart, C.G., Scheurlen, W., Hasselblatt, M., Ligon, K.L., Kieran, M.W., Korbel, J.O., Yaspo, M.-L., Brors, B., Felsberg, J., Reifemberger, G., Collins, V.P., Jabado, N., Eils, R., Lichter, P., 2013. Recurrent somatic alterations of FGFR1 and NTRK2 in pilocytic astrocytoma. *Nat Genet* 45, 927–932. <https://doi.org/10.1038/ng.2682>

Khuong-Quang, D.-A., Buczkowicz, P., Rakopoulos, P., Liu, X.-Y., Fontebasso, A.M., Bouffet, E., Bartels, U., Albrecht, S., Schwartzentruber, J., Letourneau, L., Bourgey, M., Bourque, G., Montpetit, A., Bourret, G., Lepage, P., Fleming, A., Lichter, P., Kool, M., von Deimling, A., Sturm, D., Korshunov, A., Faury, D., Jones, D.T., Majewski, J., Pfister, S.M., Jabado, N., Hawkins, C., 2012. K27M mutation in histone H3.3 defines clinically and biologically distinct subgroups of pediatric diffuse intrinsic pontine gliomas. *Acta Neuropathol* 124, 439–447. <https://doi.org/10.1007/s00401-012-0998-0>

Knoepfler, P.S., Cheng, P.F., Eisenman, R.N., 2002. N-myc is essential during neurogenesis for the rapid expansion of progenitor cell populations and the inhibition of neuronal differentiation. *Genes Dev.* 16, 2699–2712. <https://doi.org/10.1101/gad.1021202>

Krug, B., De Jay, N., Harutyunyan, A.S., Deshmukh, S., Marchione, D.M., Guilhamon, P., Bertrand, K.C., Mikael, L.G., McConechy, M.K., Chen, C.C.L., Khazaei, S., Koncar, R.F., Agnihotri, S., Faury, D., Ellezam, B., Weil, A.G., Ursini-Siegel, J., De Carvalho, D.D., Dirks, P.B., Lewis, P.W., Salomoni, P., Lupien, M., Arrowsmith, C., Lasko, P.F., Garcia, B.A., Kleinman, C.L., Jabado, N., Mack, S.C., 2019. Pervasive H3K27 Acetylation Leads to ERV Expression and a Therapeutic Vulnerability in H3K27M Gliomas. *Cancer Cell* 35, 782-797.e8. <https://doi.org/10.1016/j.ccell.2019.04.004>

Larson, J.D., Kasper, L.H., Paugh, B.S., Jin, H., Wu, G., Kwon, C.-H., Fan, Y., Shaw, T.I., Silveira, A.B., Qu, C., Xu, R., Zhu, X., Zhang, Junyuan, Russell, H.R., Peters, J.L., Finkelstein, D., Xu, B., Lin, T., Tinkle, C.L., Patay, Z., Onar-Thomas, A., Pounds, S.B., McKinnon, P.J., Ellison, D.W., Zhang, Jinghui, Baker, S.J., 2019. Histone H3.3 K27M Accelerates Spontaneous Brainstem Glioma and Drives Restricted Changes in Bivalent Gene Expression. *Cancer Cell* 35, 140-155.e7. <https://doi.org/10.1016/j.ccell.2018.11.015>

Lee, C.-H., Yu, J.-R., Granat, J., Saldaña-Meyer, R., Andrade, J., LeRoy, G., Jin, Y., Lund, P., Stafford, J.M., Garcia, B.A., Ueberheide, B., Reinberg, D., 2019. Automethylation of PRC2 promotes H3K27 methylation and is impaired in H3K27M pediatric glioma. *Genes Dev.* 33, 1428–1440. <https://doi.org/10.1101/gad.328773.119>

Lewis, P.W., Elsaesser, S.J., Noh, K.-M., Stadler, S.C., Allis, C.D., 2010. Daxx is an H3.3-specific histone chaperone and cooperates with ATRX in replication-independent chromatin assembly at telomeres. *PNAS* 107, 14075–14080. <https://doi.org/10.1073/pnas.1008850107>

Lewis, P.W., Muller, M.M., Koletsky, M.S., Cordero, F., Lin, S., Banaszynski, L.A., Garcia, B.A., Muir, T.W., Becher, O.J., Allis, C.D., 2013. Inhibition of PRC2 Activity by a Gain-of-Function H3 Mutation Found in Pediatric Glioblastoma. *Science* 340, 857–861. <https://doi.org/10.1126/science.1232245>

Lin, G.L., Wilson, K.M., Ceribelli, M., Stanton, B.Z., Woo, P.J., Kreimer, S., Qin, E.Y., Zhang, X., Lennon, J., Nagaraja, S., Morris, P.J., Quezada, M., Gillespie, S.M., Duveau, D.Y., Michalowski,

A.M., Shinn, P., Guha, R., Ferrer, M., Klumpp-Thomas, C., Michael, S., McKnight, C., Minhas, P., Itkin, Z., Raabe, E.H., Chen, L., Ghanem, R., Geraghty, A.C., Ni, L., Andreasson, K.I., Vitanza, N.A., Warren, K.E., Thomas, C.J., Monje, M., 2019. Therapeutic strategies for diffuse midline glioma from high-throughput combination drug screening. *Sci. Transl. Med.* 11, eaaw0064. <https://doi.org/10.1126/scitranslmed.aaw0064>

Liu, C., Sage, J.C., Miller, M.R., Verhaak, R.G.W., Hippenmeyer, S., Vogel, H., Foreman, O., Bronson, R.T., Nishiyama, A., Luo, L., Zong, H., 2011. Mosaic Analysis with Double Markers Reveals Tumor Cell of Origin in Glioma. *Cell* 146, 209–221. <https://doi.org/10.1016/j.cell.2011.06.014>

Louis, D.N., Perry, A., Reifenberger, G., von Deimling, A., Figarella-Branger, D., Cavenee, W.K., Ohgaki, H., Wiestler, O.D., Kleihues, P., Ellison, D.W., 2016. The 2016 World Health Organization Classification of Tumors of the Central Nervous System: a summary. *Acta Neuropathol* 131, 803–820. <https://doi.org/10.1007/s00401-016-1545-1>

Lovén, J., Hoke, H.A., Lin, C.Y., Lau, A., Orlando, D.A., Vakoc, C.R., Bradner, J.E., Lee, T.I., Young, R.A., 2013. Selective Inhibition of Tumor Oncogenes by Disruption of Super-Enhancers. *Cell* 153, 320–334. <https://doi.org/10.1016/j.cell.2013.03.036>

Mackay, A., Burford, A., Carvalho, D., Izquierdo, E., Fazal-Salom, J., Taylor, K.R., Bjerke, L., Clarke, M., Vinci, M., Nandhabalan, M., Temelso, S., Popov, S., Molinari, V., Raman, P., Waanders, A.J., Han, H.J., Gupta, S., Marshall, L., Zacharoulis, S., Vaidya, S., Mandeville, H.C., Bridges, L.R., Martin, A.J., Al-Sarraj, S., Chandler, C., Ng, H.-K., Li, X., Mu, K., Trabelsi, S., Brahim, D.H.-B., Kisljakov, A.N., Konovalov, D.M., Moore, A.S., Carcaboso, A.M., Sunol, M., de Torres, C., Cruz, O., Mora, J., Shats, L.I., Stavale, J.N., Bidinotto, L.T., Reis, R.M., Entz-Werle, N., Farrell, M., Cryan, J., Crimmins, D., Caird, J., Pears, J., Monje, M., Debily, M.-A., Castel, D., Grill, J., Hawkins, C., Nikbakht, H., Jabado, N., Baker, S.J., Pfister, S.M., Jones, D.T.W., Fouladi, M., von Bueren, A.O., Baudis, M., Resnick, A., Jones, C., 2017. Integrated Molecular Meta-Analysis of 1,000 Pediatric High-Grade and Diffuse Intrinsic Pontine Glioma. *Cancer Cell* 32, 520-537.e5. <https://doi.org/10.1016/j.ccell.2017.08.017>

Meel, M.H., Gooijer, M.C. de, Metselaar, D.S., Sewing, A.C.P., Zwaan, K., Waranecki, P., Breur, M., Buil, L.C.M., Lagerweij, T., Wedekind, L.E., Twisk, J.W.R., Koster, J., Hashizume, R., Raabe, E.H., Carcaboso, A.M., Bugiani, M., Phoenix, T.N., Tellingén, O. van, Vuurden, D.G. van, Kaspers, G.J.L., Hulleman, E., 2020. Combined Therapy of AXL and HDAC Inhibition Reverses Mesenchymal Transition in Diffuse Intrinsic Pontine Glioma. *Clin Cancer Res* 26, 3319–3332. <https://doi.org/10.1158/1078-0432.CCR-19-3538>

Mohammad, F., Weissmann, S., Leblanc, B., Pandey, D.P., Højfeldt, J.W., Comet, I., Zheng, C., Johansen, J.V., Rapin, N., Porse, B.T., Tvardovskiy, A., Jensen, O.N., Olaciregui, N.G., Lavarino, C., Suñol, M., de Torres, C., Mora, J., Carcaboso, A.M., Helin, K., 2017. EZH2 is a potential therapeutic target for H3K27M-mutant pediatric gliomas. *Nat Med* 23, 483–492. <https://doi.org/10.1038/nm.4293>

Monje, M., Mitra, S.S., Freret, M.E., Raveh, T.B., Kim, J., Masek, M., Attema, J.L., Li, G., Haddix, T., Edwards, M.S.B., Fisher, P.G., Weissman, I.L., Rowitch, D.H., Vogel, H., Wong, A.J., Beachy, P.A., 2011. Hedgehog-responsive candidate cell of origin for diffuse intrinsic pontine glioma. *Proceedings of the National Academy of Sciences* 108, 4453–4458. <https://doi.org/10.1073/pnas.1101657108>

Nagaraja, S., Quezada, M.A., Gillespie, S.M., Arzt, M., Lennon, J.J., Woo, P.J., Hovestadt, V., Kambhampati, M., Filbin, M.G., Suva, M.L., Nazarian, J., Monje, M., 2019. Histone Variant and Cell Context Determine H3K27M Reprogramming of the Enhancer Landscape and Oncogenic State. *Molecular Cell* 76, 965-980.e12. <https://doi.org/10.1016/j.molcel.2019.08.030>

Nagaraja, S., Vitanza, N.A., Woo, P.J., Taylor, K.R., Liu, F., Zhang, L., Li, M., Meng, W., Ponnuswami, A., Sun, W., Ma, J., Hulleman, E., Swigut, T., Wysocka, J., Tang, Y., Monje, M., 2017. Transcriptional Dependencies in Diffuse Intrinsic Pontine Glioma. *Cancer Cell* 31, 635-652.e6. <https://doi.org/10.1016/j.ccell.2017.03.011>

Nikbakht, H., Panditharatna, E., Mikael, L.G., Li, R., Gayden, T., Osmond, M., Ho, C.-Y., Kambhampati, M., Hwang, E.I., Faury, D., Siu, A., Papillon-Cavanagh, S., Bechet, D., Ligon, K.L., Ellezam, B., Ingram, W.J., Stinson, C., Moore, A.S., Warren, K.E., Karamchandani, J., Packer, R.J., Jabado, N., Majewski, J., Nazarian, J., 2016. Spatial and temporal homogeneity of driver mutations in diffuse intrinsic pontine glioma. *Nat Commun* 7, 11185. <https://doi.org/10.1038/ncomms11185>

Otto, T., Horn, S., Brockmann, M., Eilers, U., Schüttrumpf, L., Popov, N., Kenney, A.M., Schulte, J.H., Beijersbergen, R., Christiansen, H., Berwanger, B., Eilers, M., 2009. Stabilization of N-Myc Is a Critical Function of Aurora A in Human Neuroblastoma. *Cancer Cell* 15, 67-78. <https://doi.org/10.1016/j.ccr.2008.12.005>

Pathania, M., De Jay, N., Maestro, N., Harutyunyan, A.S., Nitarska, J., Pahlavan, P., Henderson, S., Mikael, L.G., Richard-Londt, A., Zhang, Y., Costa, J.R., Hébert, S., Khazaei, S., Ibrahim, N.S., Herrero, J., Riccio, A., Albrecht, S., Ketteler, R., Brandner, S., Kleinman, C.L., Jabado, N., Salomoni, P., 2017. H3.3K27M Cooperates with Trp53 Loss and PDGFRA Gain in Mouse Embryonic Neural Progenitor Cells to Induce Invasive High-Grade Gliomas. *Cancer Cell* 32, 684-700.e9. <https://doi.org/10.1016/j.ccell.2017.09.014>

Paugh, B.S., Broniscer, A., Qu, C., Miller, C.P., Zhang, J., Tatevossian, R.G., Olson, J.M., Geyer, J.R., Chi, S.N., Silva, N.S. da, Onar-Thomas, A., Baker, J.N., Gajjar, A., Ellison, D.W., Baker, S.J., 2011. Genome-Wide Analyses Identify Recurrent Amplifications of Receptor Tyrosine Kinases and Cell-Cycle Regulatory Genes in Diffuse Intrinsic Pontine Glioma. *Journal of Clinical Oncology*. <https://doi.org/10.1200/JCO.2011.35.5677>

Paugh, B.S., Qu, C., Jones, C., Liu, Z., Adamowicz-Brice, M., Zhang, J., Bax, D.A., Coyle, B., Barrow, J., Hargrave, D., Lowe, J., Gajjar, A., Zhao, W., Broniscer, A., Ellison, D.W., Grundy, R.G., Baker, S.J., 2010. Integrated Molecular Genetic Profiling of Pediatric High-Grade Gliomas Reveals Key Differences With the Adult Disease. *JCO* 28, 3061-3068. <https://doi.org/10.1200/JCO.2009.26.7252>

Paugh, B.S., Zhu, X., Qu, C., Endersby, R., Diaz, A.K., Zhang, Junyuan, Bax, D.A., Carvalho, D., Reis, R.M., Onar-Thomas, A., Broniscer, A., Wetmore, C., Zhang, Jinghui, Jones, C., Ellison, D.W., Baker, S.J., 2013. Novel Oncogenic PDGFRA Mutations in Pediatric High-Grade Gliomas. *Cancer Res* 73, 6219-6229. <https://doi.org/10.1158/0008-5472.CAN-13-1491>

Piunti, A., Hashizume, R., Morgan, M.A., Bartom, E.T., Horbinski, C.M., Marshall, S.A., Rendleman, E.J., Ma, Q., Takahashi, Y., Woodfin, A.R., Misharin, A.V., Abshiru, N.A., Lulla, R.R., Saratsis, A.M., Kelleher, N.L., James, C.D., Shilatfard, A., 2017. Therapeutic targeting of polycomb and BET bromodomain proteins in diffuse intrinsic pontine gliomas. *Nat Med* 23, 493-500. <https://doi.org/10.1038/nm.4296>

Puget, S., Philippe, C., Bax, D.A., Job, B., Varlet, P., Junier, M.-P., Andreiuolo, F., Carvalho, D., Reis, R., Guerrini-Rousseau, L., Roujeau, T., Dessen, P., Richon, C., Lazar, V., Teuff, G.L., Sainte-Rose, C., Georger, B., Vassal, G., Jones, C., Grill, J., 2012. Mesenchymal Transition and PDGFRA Amplification/Mutation Are Key Distinct Oncogenic Events in Pediatric Diffuse Intrinsic Pontine Gliomas. *PLOS ONE* 7, e30313. <https://doi.org/10.1371/journal.pone.0030313>

Roulois, D., Loo Yau, H., Singhania, R., Wang, Y., Danesh, A., Shen, S.Y., Han, H., Liang, G., Jones, P.A., Pugh, T.J., O'Brien, C., De Carvalho, D.D., 2015. DNA-Demethylating Agents Target Colorectal Cancer Cells by Inducing Viral Mimicry by Endogenous Transcripts. *Cell* 162, 961–973. <https://doi.org/10.1016/j.cell.2015.07.056>

Sandberg, D.I., Edgar, M.A., Souweidane, M.M., 2002. Convection-enhanced delivery into the rat brainstem. *Journal of Neurosurgery* 96, 885–891. <https://doi.org/10.3171/jns.2002.96.5.0885>

Saratsis, A.M., Kambhampati, M., Snyder, K., Yadavilli, S., Devaney, J.M., Harmon, B., Hall, J., Raabe, E.H., An, P., Weingart, M., Rood, B.R., Magge, S.N., MacDonald, T.J., Packer, R.J., Nazarian, J., 2014. Comparative multidimensional molecular analyses of pediatric diffuse intrinsic pontine glioma reveals distinct molecular subtypes. *Acta Neuropathol* 127, 881–895. <https://doi.org/10.1007/s00401-013-1218-2>

Schwartzentruber, J., Korshunov, A., Liu, X.-Y., Jones, D.T.W., Pfaff, E., Jacob, K., Sturm, D., Fontebasso, A.M., Quang, D.-A.K., Tönjes, M., Hovestadt, V., Albrecht, S., Kool, M., Nantel, A., Konermann, C., Lindroth, A., Jäger, N., Rausch, T., Ryzhova, M., Korbel, J.O., Hielscher, T., Hauser, P., Garami, M., Klekner, A., Bogner, L., Ebinger, M., Schuhmann, M.U., Scheurlen, W., Pekrun, A., Frühwald, M.C., Roggendorf, W., Kramm, C., Dürken, M., Atkinson, J., Lepage, P., Montpetit, A., Zakrzewska, M., Zakrzewski, K., Liberski, P.P., Dong, Z., Siegel, P., Kulozik, A.E., Zapatka, M., Guha, A., Malkin, D., Felsberg, J., Reifenberger, G., von Deimling, A., Ichimura, K., Collins, V.P., Witt, H., Milde, T., Witt, O., Zhang, C., Castelo-Branco, P., Lichter, P., Faury, D., Tabori, U., Plass, C., Majewski, J., Pfister, S.M., Jabado, N., 2012. Driver mutations in histone H3.3 and chromatin remodelling genes in paediatric glioblastoma. *Nature* 482, 226–231. <https://doi.org/10.1038/nature10833>

Silveira, A.B., Kasper, L.H., Fan, Y., Jin, H., Wu, G., Shaw, T.I., Zhu, X., Larson, J.D., Easton, J., Shao, Y., Yergeau, D.A., Rosencrance, C., Boggs, K., Rusch, M.C., Ding, L., Zhang, Junyuan, Finkelstein, D., Noyes, R.M., Russell, B.L., Xu, B., Broniscer, A., Wetmore, C., Pounds, S.B., Ellison, D.W., Zhang, Jinghui, Baker, S.J., 2019. H3.3 K27M depletion increases differentiation and extends latency of diffuse intrinsic pontine glioma growth in vivo. *Acta Neuropathol* 137, 637–655. <https://doi.org/10.1007/s00401-019-01975-4>

Stafford, J.M., Lee, C.-H., Voigt, P., Descostes, N., Saldaña-Meyer, R., Yu, J.-R., Leroy, G., Oksuz, O., Chapman, J.R., Suarez, F., Modrek, A.S., Bayin, N.S., Placantonakis, D.G., Karajannis, M.A., Snuderl, M., Ueberheide, B., Reinberg, D., 2018. Multiple modes of PRC2 inhibition elicit global chromatin alterations in H3K27M pediatric glioma. *Science Advances* 4, eaau5935. <https://doi.org/10.1126/sciadv.aau5935>

Sturm, D., Witt, H., Hovestadt, V., Khuong-Quang, D.-A., Jones, D.T.W., Konermann, C., Pfaff, E., Tönjes, M., Sill, M., Bender, S., Kool, M., Zapatka, M., Becker, N., Zucknick, M., Hielscher, T., Liu, X.-Y., Fontebasso, A.M., Ryzhova, M., Albrecht, S., Jacob, K., Wolter, M., Ebinger, M., Schuhmann, M.U., van Meter, T., Frühwald, M.C., Hauch, H., Pekrun, A., Radlwimmer, B., Niehues, T., von Komorowski, G., Dürken, M., Kulozik, A.E., Madden, J., Donson, A., Foreman,

N.K., Drissi, R., Fouladi, M., Scheurle, W., von Deimling, A., Monoranu, C., Roggendorf, W., Herold-Mende, C., Unterberg, A., Kramm, C.M., Felsberg, J., Hartmann, C., Wiestler, B., Wick, W., Milde, T., Witt, O., Lindroth, A.M., Schwartzentruber, J., Faury, D., Fleming, A., Zakrzewska, M., Liberski, P.P., Zakrzewski, K., Hauser, P., Garami, M., Klekner, A., Bogner, L., Morrissy, S., Cavalli, F., Taylor, M.D., van Sluis, P., Koster, J., Versteeg, R., Volckmann, R., Mikkelsen, T., Aldape, K., Reifenberger, G., Collins, V.P., Majewski, J., Korshunov, A., Lichter, P., Plass, C., Jabado, N., Pfister, S.M., 2012. Hotspot Mutations in H3F3A and IDH1 Define Distinct Epigenetic and Biological Subgroups of Glioblastoma. *Cancer Cell* 22, 425–437. <https://doi.org/10.1016/j.ccr.2012.08.024>

Swartling, F.J., Savov, V., Persson, A.I., Chen, J., Hackett, C.S., Northcott, P.A., Grimmer, M.R., Lau, J., Chesler, L., Perry, A., Phillips, J.J., Taylor, M.D., Weiss, W.A., 2012. Distinct Neural Stem Cell Populations Give Rise to Disparate Brain Tumors in Response to N-MYC. *Cancer Cell* 21, 601–613. <https://doi.org/10.1016/j.ccr.2012.04.012>

Tate, M.C., Lindquist, R.A., Nguyen, T., Sanai, N., Barkovich, A.J., Huang, E.J., Rowitch, D.H., Alvarez-Buylla, A., 2015. Postnatal growth of the human pons: A morphometric and immunohistochemical analysis. *Journal of Comparative Neurology* 523, 449–462. <https://doi.org/10.1002/cne.23690>

Taylor, I.C., Hütt-Cabezas, M., Brandt, W.D., Kambhampati, M., Nazarian, J., Chang, H.T., Warren, K.E., Eberhart, C.G., Raabe, E.H., 2015. Disrupting NOTCH Slows Diffuse Intrinsic Pontine Glioma Growth, Enhances Radiation Sensitivity, and Shows Combinatorial Efficacy With Bromodomain Inhibition. *Journal of Neuropathology & Experimental Neurology* 74, 778–790. <https://doi.org/10.1097/NEN.0000000000000216>

Vajkoczy, P., Knyazev, P., Kunkel, A., Capelle, H.-H., Behrndt, S., Tengg-Kobligk, H. von, Kiessling, F., Eichelsbacher, U., Essig, M., Read, T.-A., Erber, R., Ullrich, A., 2006. Dominant-negative inhibition of the Axl receptor tyrosine kinase suppresses brain tumor cell growth and invasion and prolongs survival. *PNAS* 103, 5799–5804. <https://doi.org/10.1073/pnas.0510923103>

Vitanza, N.A., Biery, M.C., Myers, C., Ferguson, E., Zheng, Y., Girard, E.J., Przystal, J.M., Park, G., Noll, A., Pakiam, F., Winter, C.A., Morris, S.M., Sarthy, J., Cole, B.L., Leary, S.E.S., Crane, C., Lieberman, N.A.P., Mueller, S., Nazarian, J., Gottardo, R., Brusniak, M.-Y., Mhyre, A.J., Olson, J.M., 2021. Optimal therapeutic targeting by HDAC inhibition in biopsy-derived treatment-naïve diffuse midline glioma models. *Neuro-Oncology* 23, 376–386. <https://doi.org/10.1093/neuonc/noaa249>

Voon, H.P.J., Udugama, M., Lin, W., Hii, L., Law, R.H.P., Steer, D.L., Das, P.P., Mann, J.R., Wong, L.H., 2018. Inhibition of a K9/K36 demethylase by an H3.3 point mutation found in paediatric glioblastoma. *Nat Commun* 9, 3142. <https://doi.org/10.1038/s41467-018-05607-5>

Wagner, E.J., Carpenter, P.B., 2012. Understanding the language of Lys36 methylation at histone H3. *Nat Rev Mol Cell Biol* 13, 115–126. <https://doi.org/10.1038/nrm3274>

Wang, J., Huang, T.Y.-T., Hou, Y., Bartom, E., Lu, X., Shilatfard, A., Yue, F., Saratsis, A., 2021. Epigenomic landscape and 3D genome structure in pediatric high-grade glioma. *Science Advances* 7, eabg4126. <https://doi.org/10.1126/sciadv.abg4126>

Warren, K.E., 2012. Diffuse intrinsic pontine glioma: poised for progress. *Frontiers in Oncology* 2, 1–9. <https://doi.org/10.3389/fonc.2012.00205>

Whyte, W.A., Orlando, D.A., Hnisz, D., Abraham, B.J., Lin, C.Y., Kagey, M.H., Rahl, P.B., Lee, T.I., Young, R.A., 2013. Master Transcription Factors and Mediator Establish Super-Enhancers at Key Cell Identity Genes. *Cell* 153, 307–319. <https://doi.org/10.1016/j.cell.2013.03.035>

Wiese, M., Hamdan, F.H., Kubiak, K., Diederichs, C., Gielen, G.H., Nussbaumer, G., Carcaboso, A.M., Hulleman, E., Johnsen, S.A., Kramm, C.M., 2020. Combined treatment with CBP and BET inhibitors reverses inadvertent activation of detrimental super enhancer programs in DIPG cells. *Cell Death Dis* 11, 673. <https://doi.org/10.1038/s41419-020-02800-7>

Wu, G., Broniscer, A., McEachron, T.A., Lu, C., Paugh, B.S., Beckfort, J., Qu, C., Ding, L., Huether, R., Parker, M., Zhang, Junyuan, Gajjar, A., Dyer, M.A., Mullighan, C.G., Gilbertson, R.J., Mardis, E.R., Wilson, R.K., Downing, J.R., Ellison, D.W., Zhang, Jinghui, Baker, S.J., 2012. Somatic histone H3 alterations in pediatric diffuse intrinsic pontine gliomas and non-brainstem glioblastomas. *Nat Genet* 44, 251–253. <https://doi.org/10.1038/ng.1102>

Yang, S., Zheng, X., Lu, C., Li, G.-M., Allis, C.D., Li, H., 2016. Molecular basis for oncohistone H3 recognition by SETD2 methyltransferase. *Genes Dev.* 30, 1611–1616. <https://doi.org/10.1101/gad.284323.116>

Yuen, B.T.K., Knoepfler, P.S., 2013. Histone H3.3 Mutations: A Variant Path to Cancer. *Cancer Cell* 24, 567–574. <https://doi.org/10.1016/j.ccr.2013.09.015>

## CHAPTER 2

### **Histone H3.3K27M promotes unique chromatin accessible regions in developmentally relevant genes in DIPG tumors**

Nichole A. Lewis<sup>1,2,3</sup>, Rachel Herndon Klein<sup>1,2,3</sup>, and Paul S. Knoepfler<sup>1,2,3\*</sup>

*A manuscript version of this chapter is in preparation for submission soon to a journal.*

I collected the samples for ATAC-seq, analyzed the data, conducted the qPCR, made the figures, and wrote the manuscript. RHK provided guidance and training for analyzing bioinformatics data and read, edited, and approved the manuscript. PSK conceived of the project, contributed to experiment design and data interpretation, and edited the manuscript.

<sup>1</sup>Department of Cell Biology and Human Anatomy & <sup>2</sup>Genome Center, University of California Davis School of Medicine; <sup>3</sup>Institute of Pediatric Regenerative Medicine, Shriners Hospital For Children Northern California, Sacramento, CA 95817 \*corresponding author,

knoepfler@ucdavis.edu

## **Abstract**

The H3.3K27M mutation is a defining characteristic of diffuse intrinsic pontine glioma (DIPG). This histone mutation is responsible for drastic alterations to histone H3 post-translational modification (PTMs) and subsequent aberrant gene expression. However, much less is known about the effect this mutation has on chromatin structure and function, specifically open versus closed chromatin regions. Recently, we developed isogenic CRISPR-edited cell lines that are wild-type for histone H3.3 that can be compared to their matched K27M lines. Here we show via ATAC-seq analysis that H3.3K27M glioma cells have unique open chromatin at gene regions corresponding to NOTCH, neurogenesis, and neuronal development pathways and correspond to genes that are overexpressed in H3.3K27M compared to isogenic wild-type cell line. Accessible enhancers and super-enhancers corresponding to increased gene expression in H3.3K27M cells were mapped to genes involved in neurogenesis and NOTCH signaling, further supporting our previous findings that these pathways are key to DIPG tumor maintenance. MOTIF analysis implicates specific factors as central to K27M signaling including ASCL1. Altogether our findings indicate that H3.3K27M causes chromatin to take on a more open configuration at key regulatory regions for NOTCH and neurogenesis genes, resulting in increased oncogenic gene expression, which is reversible upon editing K27M back to wild-type.

## **Introduction**

Diffuse intrinsic pontine gliomas (DIPG) are a leading cause of cancer-related deaths in children with survival typically being less than 2 years (Mackay et al., 2017). One of the defining features of DIPG is the presence of the histone tail mutation H3.3K27M, which is estimated to be in 80% of DIPG tumors (Khuong-Quang et al., 2012; Sturm et al., 2012; Yuen and Knoepfler, 2013). The K27M mutation greatly impacts epigenetic modifications including causing global decreases in the repressive mark H3K27me<sub>3</sub>, an increase in the activating mark H3K27ac, and a reduction in DNA methylation (Bender et al., 2013; Chan et al., 2013; Creighton et al., 2010;

Lewis et al., 2013). Current data suggests that H3.3K27M either sequesters, excludes, or enzymatically inactivates PRC2 thus preventing it from methylating wild-type H3 nucleosomes except at strong affinity sites that lack H3.3K27M deposition (Bender et al., 2013; Fang et al., 2018; Herz et al., 2014; Justin et al., 2016; Lee et al., 2019; Lewis et al., 2013; Mohammad et al., 2017; Piunti et al., 2017; Sarthy et al., 2020; Stafford et al., 2018). More recently, a fourth hypothesis was proposed that H3K27M prevents the spread of H3K27me3 from high-affinity PRC2 sites, specifically large unmethylated CpG islands related to lineage differentiation (Harutyunyan et al., 2019).

The exact mechanisms are still to be defined, but it is established that this disruption to epigenetic marks by H3.3K27M is essential for the maintenance of tumor properties (Chen et al., 2020; Harutyunyan et al., 2019). Several studies have been conducted investigating interventions to correct the disrupted epigenetic landscape with some showing possible clinical promise. Namely, small-molecule inhibitors of EZH2, the catalytic subunit of PRC2 responsible for the H3K27me3 mark, and the histone deacetylase inhibitor (HDACi) panobinostat have been heavily investigated with the latter advancing to clinical trials (Grasso et al., 2015; Hennika et al., 2017; Mohammad et al., 2017; Piunti et al., 2017). Further decreasing H3K27me3 initially appears counter-intuitive, but this approach reduced H3K27me3 at tumor-suppressor genes that are otherwise silenced in DIPG leading to reduced proliferation (Mohammad et al., 2017; Piunti et al., 2017). Similarly, further increasing histone H3 acetylation has the unexpected result of partially restoring H3K27me3 levels due to histone tail polyacetylation blocking PRC2, and H3K27M interactions leading to decreased proliferation and restoration of normal gene expression (Brown et al., 2014; Grasso et al., 2015). However, both strategies have pitfalls including patient-to-patient variability, development of resistance, and cytotoxicity (Grasso et al., 2015; Krug et al., 2019; Lin et al., 2019; Meel et al., 2020; Mohammad et al., 2017; Piunti et al., 2017). This complexity demonstrates the necessity to further understand the mechanism(s) at play in DIPG

that disrupt histone marks and the downstream effects on chromatin and gene expression to identify other potential drug targets.

Importantly, the DIPG H3.3K27M mutation, and subsequent chromatin mark changes, results in modifications to the transcriptome that are unique from H3.1K27M DIPG and H3-WT glioblastoma, including increased expression of genes related to neural development, neurogenesis, NOTCH signaling, and differentiation (Chen et al., 2020; Harutyunyan et al., 2019; Larson et al., 2019; Nagaraja et al., 2017; Sturm et al., 2012). Drug studies have demonstrated that inhibition of the NOTCH pathway leads to both reduced proliferation and viability in DIPG further supporting its importance to tumor maintenance and presenting a promising treatment method (Chen et al., 2020; Hurtado et al., 2019; Taylor et al., 2015). While the epigenetic effects of K27M have been extensively studied, relatively much less is known about the impacts on chromatin structure and function (Krug et al., 2019; Wang et al., 2021).

Here we build upon our previous work where we used CRISPR-Cas9 to gene edit the point mutation responsible for the H3.3K27M mutation in established DIPG lines to generate isogenic H3.3 wild-type cell lines (Chen et al., 2020). We assessed differential open chromatin regions (ATAC-seq) between the pairs of isogenic DIPG cell lines and found that in H3.3K27M DIPG cells genes regulating neurogenesis and neuronal processes were enriched in open chromatin regions, including their corresponding enhancers and super-enhancers. These genes also had increased expression in H3.3K27M DIPG compared to their matched control H3.3 wild-type gene-edited cell lines. Binding motifs for ASCL1, which we previously showed to be upregulated in H3.3K27M and important to tumorigenesis, and NEUROD1, a transcription factor known to be essential for neurogenesis, were enriched in H3.3K27M cells at genes related to neuronal processes and nervous system development. Based on these findings, we propose a model in which H3.3K27M nucleosome deposition results in a more euchromatic structure at super-enhancers and gene bodies of genes related to neurogenesis and NOTCH signaling,

exposing the binding site motifs for key transcription factors like ASCL1 and NEUROD1, resulting in increased expression of their target genes that contribute to tumorigenesis.

## Results

### Accessible chromatin regions in pediatric gliomas

To study how the oncohistone H3.3K27M affects chromatin dynamics and gene expression, we used Assay for Transposase-Accessible Chromatin using sequencing (ATAC-seq) (Buenrostro et al., 2015, 2013; Corces et al., 2017) on our previously described panel of isogenic DIPG cell lines that were gene-edited to have wild-type H3.3 using CRISPR-Cas9 (Buenrostro et al., 2013; Chen et al., 2020; Corces et al., 2017). Briefly, two H3.3K27M DIPG lines SU-DIPG-XIII and SU-DIPG-XVII (hereafter referred to as XIII and XVII, respectively, and also more generally as “parental” cells), and their CRISPR gene-edited counterparts (XIII-WT and XVII-WT) were used for this study.

We performed ATAC-seq using biological duplicates for each cell line and called peaks for each replicate. We then used the R package DiffBind to identify open chromatin peaks shared between replicates and that were differential between H3.3-WT and H3.3K27M cell lines. The XIII and XIII-WT cells had 4,522 and 12,860 unique peaks, respectively, and XVII and XVII-WT had 13,136 and 211 unique peaks, respectively (Supplementary Table 1). Distinct chromatin accessibility profiles were observed between H3.3-WT and H3.3K27M cells for each line, consistent with substantial changes in chromatin accessibility (Fig. 1a-d). Principal Component Analysis (PCA) analysis of the matched isogenic lines indicated high reproducibility between replicates and that H3.3-WT and H3.3K27M separate from each other (Fig. 1e-f). When both sets of matched isogenic lines were included in the DiffBind analysis, hierarchical clustering suggested that lines clustered by *H3F3A* mutation status (Supplementary Fig. 1a). However, PCA analysis suggested a slight bias for clustering based on the original cell line, with XVII and XVII-WT separating from XIII and XIII-WT (Supplementary Fig. 1b). This suggests that across DIPG cell

lines the presence of H3.3K27M results in significant differences in open chromatin regions compared to wild-type, however there are unique features in DIPG patient lines that are maintained regardless of *H3F3A* status. These findings point to other factors likely influencing open chromatin regions that are specific to each cell line and are worthy of future investigation.

We determined the proportion of open chromatin peaks that were in exons, introns, promoters (defined as between 2 kb upstream and 1 kb downstream of the TSS), and intergenic regions of the genome for each cell line. Interestingly, the percentage of peaks that mapped to the promoter regions decreased upon reversion of H3.3K27M to wild-type (Fig. 2a). Approximately 40% or more of the peaks across all lines (except XVII, which had a more even distribution across all genomic categories) were found in intergenic and intronic regions while the remaining 5-20% of peaks were found in promoters and exons (Fig. 2a and Supplementary Table 1). This analysis demonstrates that most of the accessible chromatin are located in regulatory regions.

### **Open chromatin regions are uniquely enriched for neuronal genes in K27M cells**

Within the ATAC-seq datasets we looked to see which functional groups of genes were enriched in the open chromatin peaks using gene ontology (GO) analysis of biological processes, cellular components, molecular function, and KEGG Pathways. Both parental lines (XIII and XVII) showed enrichment for nervous system development and homophilic cell adhesion terms in their respective open chromatin regions (Fig. 2b and d, blue graphs). Due to low peak numbers, no significant GO terms were identified for XVII-WT, but the XIII-WT open regions corresponded to GO terms related to cytoskeleton, actin binding, and focal adhesion (Fig. 2c, blue graph).

When the ATAC-seq data from all four lines were compared using DiffBind, some specific gene clusters were enriched in all H3.3K27M cell lines compared to wild-type H3.3 and vice versa. Parental lines XIII and XVII shared 464 peaks, mapping to 245 genes, while XIII-WT and XVII-WT shared 3,402 peaks and 1,378 genes (Supplementary Table 1). No significant GO terms for

the open chromatin genes shared between parental lines, despite sharing the key H3.3K27M mutation that is a defining feature of DIPG, suggesting that there is some degree of heterogeneity between patient tumors. The CRISPR gene-edited H3.3 wild-type cells, however, did have significant shared GO terms including cytoskeleton, cytosol, pathways in cancer, and actin binding, further supporting the hypothesis that H3K27M plays a key role in regulating chromatin accessibility at genes that contribute to cell morphology and tumor characteristics (Supplementary Fig. 2a).

To determine if the differentially open regions of chromatin in each cell line corresponded to genes that showed increased expression in the same cell types, we compared our ATAC-seq data with 3' Tag-seq gene expression data from our previous study (Chen et al., 2020). ATAC-seq peaks from DiffBind for each cell line were mapped to the genomic coordinates of genes that demonstrated increased expression via Tag-seq analysis. This intersection analysis determined that 1,881 and 5,627 statistically significant upregulated genes in XIII and XVII, respectively, mapped to open chromatin ATAC-seq peaks in the two parental cell lines (Supplementary Table 2). Conversely, 4,874 and 119 statistically significant upregulated genes in H3.3-WT cell lines corresponded to open chromatin ATAC-seq peaks in XIII-WT and XVII-WT, respectively (Supplementary Table 2). This analysis demonstrated that many genes with increased expression also reside in these accessible regions of chromatin, likely explaining in part why these genes are upregulated.

GO analysis was conducted on these overlapping gene lists to determine which gene families were enriched for open chromatin resulting in increased expression (Fig. 2b-d, red graphs). Parental lines (XIII and XVII) had open chromatin in numerous upregulated genes related to the nervous system such as to cell junction, axon guidance, postsynaptic density, neuron migration, nervous system development, neuronal cell body, and glutamatergic synapse to name a few (Fig. 2b and d, red graphs). The XIII-WT line had open regions corresponding to upregulated genes in terms related to adhesion, actin, and the extracellular matrix (Fig. 2c, red graphs). This

is consistent with our observation that XIII-WT cells undergo morphological changes and become more adherent even in suspension culturing conditions following the reversion of H3.3K27M to wild-type (Chen et al., 2020).

### **Enhancer analysis points to nervous system signaling and stem cell pathways**

Since H3.3K27M DIPG cells have a distinct active enhancer profile compared to normal pons tissue (Nagaraja et al., 2019), we compared the enhancer regions with open chromatin specific to our parental DIPG to the isogenic wild-type DIPG lines using the Genomic Regions Enrichment of Annotations Tool (GREAT) analysis (Fig. 3a) (McLean et al., 2010). Briefly, enhancers were defined as regions with H3K27ac, the peaks for which were obtained from a previous CHIP-seq dataset (Nagaraja et al., 2017) and were called using MACS2 default parameters (Feng et al., 2012; Zhang et al., 2008), excluding promoters as previously defined (Supplementary Table 3). Similar to GO analysis conducted on gene bodies and upregulated genes, parental H3.3K27M lines were enriched for enhancers linked to genes related to various signaling pathways and nervous system development including NOTCH signaling and myelination, both of which have previously been shown to play a role in pons development and be upregulated in DIPG tumors (Chen et al., 2020; Tate et al., 2015; Taylor et al., 2015). Additionally, neuronal stem cell population maintenance and oligodendrocyte differentiation-related enhancers were present in parental lines. These results support prior findings that key mutations, such as H3.3K27M, likely occur in neural precursor cells (NPCs)/neural stem cells (NSCs), but the cells continue to either partially differentiate into oligodendrocytes or at least gain key oligodendrocyte lineage characteristics and this disrupted development contributes to tumor formation (Filbin et al., 2018; Haag et al., 2021; Nagaraja et al., 2019; Tate et al., 2015). Visualization of ATAC-seq peaks for select genes of interest overlaid with the previously described H3K27ac CHIP-seq dataset revealed increased accessible chromatin peaks that

mirrored increased H3K27ac signal and known enhancer regions for genes known to be involved in NOTCH signaling and neuronal development (Fig. 3b).

Conversely, XIII-WT cells continued to show enrichment for processes important to cell adhesion and differentiation into a variety of cell types (Fig. 3a). Interestingly, the GO category negative regulation of MAPK cascade was also enriched in XIII-WT enhancers, which has been shown to be an important signaling pathway in DIPG tumors demonstrating that reverting the K27M mutation may be sufficient to somewhat reverse the activation of this pathway and contribute to a decrease in tumor-like characteristics in the isogenic line (Nagaraja et al., 2019, 2017). Together, these results suggest that oncohistones specifically contribute to chromatin accessibility at enhancers that are important to cell identity and key signaling pathways resulting in activation of processes linked to DIPG tumorigenesis.

### **Open chromatin regions are enriched for transcription factor binding sites related to neuronal lineage in K27M cells**

Given the distinct ATAC-seq profiles in gene bodies, enhancers, and super-enhancers, and transcriptomic differences between parental and wild-type cell lines, we decided to assess the potential transcription factors at play at the interface between gene expression and regulatory elements. We first scanned for motifs and mapped them to parental or wild-type ATAC-seq peak regions using MEME-FIMO and HOMER (Fig. 4a-b and Supplementary Fig. 3d-e). One notable finding was enrichment of the DNA binding motif for ASCL1, which we previously identified as upregulated in H3.3K27M DIPG cells and important for cancer-related cellular functions (Chen et al., 2020), in both XIII and XVII cells compared to their wild-type counterparts. Motifs for transcription factors known to play roles in stem cell potency, development, and differentiation into the neuronal lineage including *GBX1*, *GBX2*, *NEUROD1*, *OLIG2*, and *HOXA2* were also enriched in parental K27M cells (Fig. 4a and Supplementary Fig. 3d). In support of previous data, GO analysis of *ASCL1* and *NEUROD1* FIMO regions indicated that these motifs were found in

genes related to nervous system development, axon guidance, GTPase activity, cell junction, and postsynaptic density (Supplementary Fig. 3a-b). By contrast, XIII- and XVII-WT cells were enriched for a number of FOS::JUN family transcription factors motifs, which have previously been identified to either be enriched in wild-type H3K27 high-grade gliomas or shared across multiple glioma subtypes (Fig. 4b and Supplementary Fig. 3e) (Krug et al., 2019).

We also used HINT-ATAC (Li et al., 2019) to identify differential transcription factor footprints in open chromatin regions of parental and wild-type cell lines. This analysis also identified transcription factors related to NOTCH signaling, neurogenesis, development, and oncogenesis including *HEY1*, *PAX2*, and *HOXB9* in parental lines (Fig. 4c and e). While the MEME-FIMO and HINT-ATAC analyses did not identify shared specific factors, the factors that were identified did belong to shared common pathways further highlighting the importance of these pathways in DIPG disease biology. *FOSL1::JUN* was present in wild-type using both analysis methods as well as factors related to migration, cytoskeleton remodeling, and Sonic Hedgehog signaling including *LHX6*, *GLI2*, *CDX1*, *CDX2*, and *SNAI1* (Fig. 4d and f, Supplementary Fig. 3c). This is consistent with GO analysis of XIII-WT ATAC-seq peaks and open chromatin corresponding to increased gene expression (Fig. 2c). Transcription factor analysis further confirmed differences between parental and wild-type lines that are H3.3K27M dependent and likely driven by neuronal factors and NOTCH signaling.

### **Super-enhancer analysis points to actin nucleator *COBL* as a shared open region in DIPGs**

Super-enhancers are linked to oncogenesis in several tumor types, including DIPG, and we have previously demonstrated that H3.3K27M leads to loss of H3K27me3 at super-enhancers, resulting in increased expression of linked genes that likely lead to tumorigenesis (Chen et al., 2020; Lovén et al., 2013; Nagaraja et al., 2017). We found that XIII cells had 306 uniquely accessible super-enhancers with 107 of these linked to transcriptionally upregulated genes (Supplementary Table 4). Similarly, XVII cells had 294 accessible super-enhancers and 99 of

these were tied to upregulated genes (Supplementary Table 4). XIII-WT cells had uniquely accessible super-enhancers at 282 genes and only 52 of those corresponded to upregulated genes in that cell line (Supplementary Table 5). The XVII-WT cells only had one accessible super-enhancer that corresponded to upregulated genes in that cell line, likely due to the low number of unique peaks, and were not analyzed further (Supplementary Table 5). Additionally, visualization of ATAC-seq peaks for select super-enhancer regions of interest displayed differences in peak patterns between parental and wild-type cell lines providing further evidence that H3.3K27M deposition results in more open chromatin, especially at key regulatory regions such as super-enhancers (Fig. 5c).

Upregulated genes linked to super-enhancers in either parental line included some related to neurogenesis and NOTCH signaling including *NOTCH1*, *RAP1GAP*, *POU3F2*, and *NEUROD1* as well as genes important for stemness, differentiation, and development such as *SOX2*, *OLIG2*, and *PTCH1* (Fig. 5a-b and Supplementary Table 4). Further, XIII and XVII cells shared the following nine genes that were associated with accessible super-enhancers and displayed increased expression: *CELF2*, *COBL*, *DAB2IP*, *FAM222A*, *GAB2*, *LINC01158*, *SASH1*, *STK32B*, and *TSHZ1* (Fig 5a-c and Supplementary Table 4). From this list of common genes we decided to validate the gene expression of *COBL*, an actin nucleator responsible for neurite outgrowth and of particular importance to proper cerebellum formation (Ahuja et al., 2007; Haag et al., 2012), via RT-qPCR and also included *OLIG2* as a control due to its established importance in DIPG biology and having already been validated in our previous study (Chen et al., 2020; Filbin et al., 2018; Haag et al., 2021; Monje et al., 2011; Nagaraja et al., 2019, 2017; Tate et al., 2015; Wang et al., 2021). We were able to validate the general changes in gene expression by RT-qPCR (Fig. 5d). Taken together, these analyses suggest that the super-enhancers of neurodevelopmental genes become more open in H3.3K27M cells and this contributes to aberrant gene expression, whereas in H3.3 wild-type these regions become more closed resulting in a gene expression profile more typical of normal NPCs.

## Discussion

A substantial amount of progress has been made in understanding DIPG biology, arguably one of the most important discoveries being the prevalence of the mutations in histone H3 proteins. The subsequent changes to epigenetic marks and the transcriptome have been extensively studied, however, the mechanisms behind these changes remain an active area of study. In an effort to better understand the mechanisms behind these transcription changes, a few groups have investigated the chromatin landscape in H3.3K27M DIPG and H3.3K27M knockout DIPG cell lines (Krug et al., 2019; Wang et al., 2021). However, these studies did not primarily focus on chromatin accessibility leaving this an under-studied component of DIPG biology. We built upon this previous work using ATAC-seq and our isogenic CRISPR-Cas9 reverted to wild-type H3.3 and H3.3K27M DIPG lines. While there were consistencies between the two DIPG cell lines and the isogenic H3.3 wild-type lines, distinct differences still remained resulting in some degree of clustering based on patient origin rather than completely based on *H3F3A* status as was originally expected. It has been extensively documented that while histone H3 and IDH1 mutation status are the main identifiers for pediatric high grade-glioma (HGG) and DIPG subgroups, there are other secondary mutations within these subgroups that drive disease progression (Castel et al., 2018, 2015; Mackay et al., 2017; Nikbakht et al., 2016; Saratsis et al., 2014; Schwartzenruber et al., 2012; Sturm et al., 2012). Therefore, it is possible that these secondary mutations are involved in chromatin dynamics and could explain why we observe a degree of clustering based on cell line instead of solely based on H3.3 mutation status as expected.

To address if more accessible chromatin is in part responsible for increased gene expression, we integrated our ATAC-seq data with our previous 3' Tag-seq expression data (Chen et al., 2020). XIII and XVII open chromatin regions corresponding to increased gene expression were enriched for genes with GO terms related to neuronal development. The abundance of

nervous system-related terms reflects the developmental origins of these tumors (Funato et al., 2014; Monje et al., 2011; Nagaraja et al., 2019) and supports the hypothesis that the formation of these DIPG tumors is through the dysregulation of neuronal developmental programs (Funato et al., 2014; Haag et al., 2021; Harutyunyan et al., 2019; Mohammad et al., 2017; Pathania et al., 2017). Conversely, XIII-WT analysis of overexpressed genes with open chromatin regions revealed enrichment for morphology genes, including actin cytoskeleton and cell adhesion, with little to no enrichment for neuronal terms. Together these results suggest that the mutant H3.3K27M promotes open chromatin and subsequent increased expression of genes related to the nervous system and development, thus driving the progression of tumor formation. In contrast, wild-type H3.3 results in open chromatin and upregulation of cell adhesion genes that lead to decreased tumor-like morphology. This is consistent with changes to cell morphology we had previously observed as well as previous reports indicating that H3K27M DIPG cells express mesenchymal and oligodendroglial gene signatures and phenotypes (Castel et al., 2015; Chen et al., 2020; Haag et al., 2021; Meel et al., 2020; Puget et al., 2012).

A similar pattern was also observed following overlaying the regulatory enhancer and super-enhancer regions with open chromatin regions. XIII and XVII were enriched for enhancers and super-enhancers related to NOTCH signaling and nervous system development genes including, but not limited to, *ASCL1* and *NEUROD1*. *ASCL1* and *NEUROD1* are basic-helix-loop-helix (bHLH) transcription factors with known functions in neuronal cell fate and differentiation of glioblastoma stem cells (GSCs) and normal neuronal cells (Gao et al., 2009; Guichet et al., 2013; Park et al., 2017; Rajakulendran et al., 2019; Vierbuchen et al., 2010). Our group and others have shown that *ASCL1*, in connection to NOTCH and WNT signaling pathways, plays a key role in GBM and DIPG tumors and can act as a pioneer factor and bind to chromatin in order to promote a more open chromatin configuration at enhancers of neuronal genes (Chen et al., 2020; Park et al., 2017; Rajakulendran et al., 2019; Vue et al., 2020; Wang et al., 2021). *NEUROD1* has similar dynamics to *ASCL1* in medulloblastoma and has also been shown to be a pioneer factor in

embryonic stem cells (ESCs) binding to heterochromatic promoters and inactive enhancers resulting in increased H3K27ac levels and subsequent increased expression of neuronal development genes (Cheng et al., 2020; Pataskar et al., 2016). Motif analysis revealed that open chromatin regions in H3.3K27M cells are enriched for *ASCL1* and *NEUROD1* binding motifs. Those motifs are located in genes related to neuronal development including *COBL*, which is upregulated and has accessible enhancer and super-enhancer regions in H3.3K27M cells. *COBL* is a calcium and calmodulin-dependent actin nucleator in developing neurons, particularly in the cerebellum, that increases neurite formation and branching (Ahuja et al., 2007; Haag et al., 2012; Hou et al., 2015). Calcium and calmodulin GO terms are enriched in H3.3K27M DIPG open chromatin regions which potentially explains the previously mentioned morphology changes between our H3.3K27M and H3.3 wild-type cells.

Taken together, our data support a model wherein the H3.3K27M-H3K27ac heterotypic nucleosomes are incorporated into the genome specifically at enhancers and super-enhancers related to neuronal genes that in H3.3 wild-type cells are located in heterochromatic regions and contain H3K27me3 (Lewis et al., 2013; Piunti et al., 2017). H3.3K27M promotes the opening of chromatin at these neurodevelopmental enhancers and leads to the initial increase in expression of *ASCL1* and *NEUROD1*. These transcription factors are then recruited to their binding motifs at enhancers and super-enhancers to further increase chromatin accessibility and ultimately promote enhancer/super-enhancer interaction to aberrantly induce other neurogenesis and oncogenesis related genes, such as *COBL* (Fig. 6).

Our study confirmed the increase in open chromatin in the *OLIG2* enhancer region for both H3.3K27M DIPG lines compared to matched isogenic H3.3 wild-type lines (Wang et al., 2021), as well as open chromatin in the super-enhancer of *OLIG2* in line XIII and the promoter of line XVII. Similar to previous work, we found that approximately 50% of our ATAC-seq peaks in H3.3K27M lines had the activating mark H3K27ac (Krug et al., 2019). However, in our dataset we observed a sharp decrease in the percentage of open chromatin regions with H3K27ac in our

gene-edited H3.3 wild-type lines, approximately 10%, whereas previous work demonstrated an increase in the overlap of ATAC-seq and H3K27ac peaks in wild-type and K27M knockout lines (Krug et al., 2019). This could be because the previous dataset was collected from K27M knockout lines whereas our data was collected using edited H3.3 wild-type lines. In line with this, reversion to wild-type, along with increased H3K27me3 levels, resulted in 5 times more unique H3.3 ChIP-seq peaks in our wild-type lines compared to parental H3.3K27M which we concluded to mean that H3.3K27M alters normal H3.3 distribution in the genome (Chen et al., 2020). This increase in unique H3.3 peaks in our wild-type lines could explain the discrepancy in the proportion of open chromatin with H3K27ac because these “new” H3.3 sites may have other PTMs that are not H3K27ac which would be in agreement with previous reports that H3.3K27M results in increased H3K27ac in DIPG over normal tissue and knockout/reversion of K27M to wild-type reduces H3K27ac levels (Chen et al., 2020; Krug et al., 2019; Larson et al., 2019; Lewis et al., 2013; Nagaraja et al., 2019; Wang et al., 2021). Additionally, H3K27ac ChIP-seq has not yet been conducted on our isogenic H3.3 wild-type lines and a previous dataset (Nagaraja et al., 2017) was used to approximate where the H3K27ac mark would be located in the genome and therefore could be missing *de novo* H3K27ac sites in our wild-type lines. Future work would involve performing ChIP-seq for the H3K27ac mark as well as other important histone marks in our matched parental and wild-type lines to obtain a complete picture of what epigenetic changes are specifically caused by the K27M mutation as opposed to H3.3 itself. Additionally, analysis of chromatin dynamics following drug treatments, especially NOTCH inhibition given its promise as a drug target and our data supporting its importance in DIPG biology, could provide further insight into how drug treatments are affecting open versus closed chromatin and the subsequent changes to gene expression and downstream processes (Chen et al., 2020; Hurtado et al., 2019; Taylor et al., 2015).

## **Materials and Methods**

## **Cell Culture**

Patient-derived pediatric glioma cells were provided by Dr. Michelle Monje (SU-DIPG-XIII and SU-DIPG-XVII) and isogenic H3 wild-type cell lines were made by Dr. Kuang-Yui Chen as previously described (Chen et al., 2020). All cell lines were cultured in Tumor Stem Media as described in (Nagaraja et al., 2017). Briefly, the media contains DMEM/F12 1:1 (Invitrogen), Neurobasal-A (Invitrogen), 10 mM HEPES (Invitrogen), 1 × MEM sodium pyruvate (Invitrogen), human basic fibroblast growth factor and human epidermal growth factor (20 ng/mL each) (Shenandoah), human platelet-derived growth factor (PDGF)-A and PDGF-B (20 ng/mL) (Shendandoah), heparin (10 ng/mL) (StemCell Technologies), and B27 without Vitamin A (Invitrogen).

## **Assay for transposase-accessible chromatin (ATAC-seq) library preparation**

ATAC-seq for cell lines was performed similarly to previously published protocols (Buenrostro et al., 2015; Corces et al., 2017) with some modifications. Cells were dissociated and 100,000 cells were washed twice with cold PBS at 4°C. Cells were resuspended in 50 uL of ATAC-Resuspension Buffer (10 mM Tris-HCl pH 7.4, 10 mM NaCl, 3 mM MgCl<sub>2</sub>, 0.1% Igepal, 0.1% Tween-20, and 0.01% Digitonin) and triturated until cells were lysed. Samples were incubated on ice for 3 minutes, washed with 1 mL of the buffer (excluding 0.1% Igepal), and centrifuged at 500 RCF for 10 minutes at 4°C. The pellet was resuspended in 50 uL of transposition mixture containing 25 uL of 2x TD Buffer (20 mM Tris-HCl pH 7.6, 10 mM MgCl<sub>2</sub>, 20% Dimethyl Formamide), 5 uL Transposase (Illumina Nextera Kit), 0.5 uL 0.1% digitonin, 0.5 uL 10% Tween-20, and PBS, and incubated at 37°C for 60 minutes, and DNA recovered using Zymo DNA Clean and Concentrator-5 Kit. Libraries were generated by PCR in 50 uL reaction (20 uL of samples, 25 uL 2x NEBNext Master Mix, and 2.5 uL of each custom primers made by Integrated DNA Technologies (IDT) (for sequences see (Buenrostro et al., 2013)). The PCR reaction was as

follows: 72°C for 5 minutes, 98°C for 30 sec, and 5 cycles of 98°C for 10 sec, 63°C for 30 sec, and 72°C for 1 minute. DNA was recovered using Zymo DNA Clean and Concentrator-5 Kit.

## **Bioinformatics**

ATAC-seq samples were sequenced in duplicate using HiSeq at Novogene with paired-end 150 bp sequencing. Adaptors were removed from raw paired-end sequencing files using bbdutk (BBMap version 38.70 BBDuk, [sourceforge.net/projects/bbmap](https://sourceforge.net/projects/bbmap)). Reads were aligned to the hg19 genome using Bowtie2 (version 1.1.2, (Langmead et al., 2009)). The resultant Sequence Alignment Map (SAM) files were compressed to the Binary Alignment Map (BAM) files on which mitochondrial reads were removed using samtools (samtools 1.4, (Li et al., 2009)). Peaks were called using HOMER (v4.11, (Heinz et al., 2010)). Unique peaks in each cell line were identified using the R package DiffBind (R version 3.6.3, DiffBind version 2.12.0, (Ross-Innes et al., 2012; Stark and Brown, n.d.)). Gene ontology analysis was performed using DAVID and GREAT (Huang et al., 2009a, 2009b; McLean et al., 2010). Motif analysis was performed using MEME-ChIP and FIMO (versions 5.4.1, (Grant et al., 2011; Machanick and Bailey, 2011) and HOMER (v4.11, (Heinz et al., 2010)). Modeling of DNA footprinting in ATAC-seq peaks was performed using HINT-ATAC (v0.13.2, (Li et al., 2019)).

## **Reverse transcription PCR**

RNA was extracted from cells using NucleoSpin RNA Kit (Macherey-Nagel) from which cDNA was made using the iScript cDNA Synthesis Kit (Bio-Rad). RT-qPCR was performed using the PowerUp SYBR Green Master Mix (Applied Biosystems; for human *COBL* and *OLIG2*, normalized to GAPDH) on a Stratagene Mx3005P. Primers are listed (5'-to-3') as follows:

COBL forward	TCGCAGCAGAACTTGGTTCCG
COBL reverse	GCATGGCTCCCATTGAGCA
OLIG2 forward	TGGCTTCAAGTCATCCTCGTC

OLIG2 reverse

ATGGCGATGTTGAGGTCGTG

GAPDH forward

GGAGCGAGATCCCTCCAAAAT

GAPDH reverse

GGCTGTTGTCATACTTCTCATGG

### **Statistical Analysis**

For statistics comparing global RNA of parental to wild-type lines by qPCR, Student's *t*-tests with a minimum of  $n=4$  biological replicates were performed using GraphPad *t*-test Calculator. Error bars represent s.e.m. ATAC-seq statistics were performed with the program DiffBind in R. The Benjamini adjusted *p*-value was used to determine significance for gene ontology analysis. Otherwise the standard *p*-value was used.

### **Acknowledgements**

We thank our previous postdoctoral scholar Dr. Kuang-Yui Chen for producing the CRISPR-Cas9 H3.3 wild-type cell lines that were a basis for this study. This work was supported by grants from the Alex Lemonade Stand Foundation and NINDS (1R01NS106878) to P.S.K.

# Figure Legends

## Figure 1.

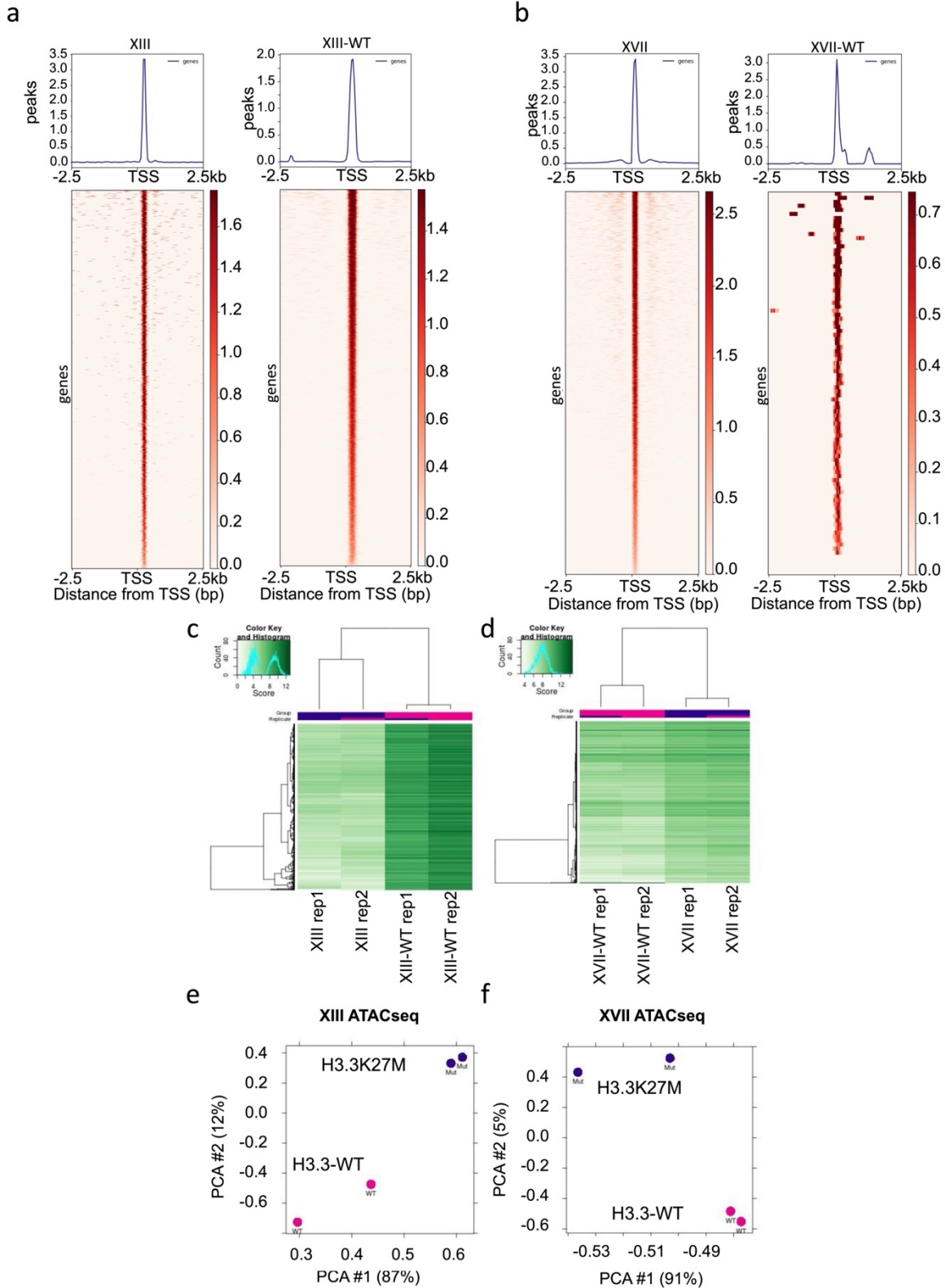


**Figure 1. Genome-wide profile of accessible chromatin regions in H3.3K27M and H3.3-WT DIPG tumor samples.** **a.** Read density heatmaps and average profiles of ATAC-seq peaks for XIII and XIII WT, **b** XVII and XVII WT. **c** Hierarchical clustering analysis of accessible chromatin regions via ATAC-seq comparing XIII and XIII WT, **d** XVII and XVII WT. **e** Principal component analysis (PCA) of significantly differential peaks between XIII and XIII WT, **f** XVII and XVII WT.

**Figure 2.**

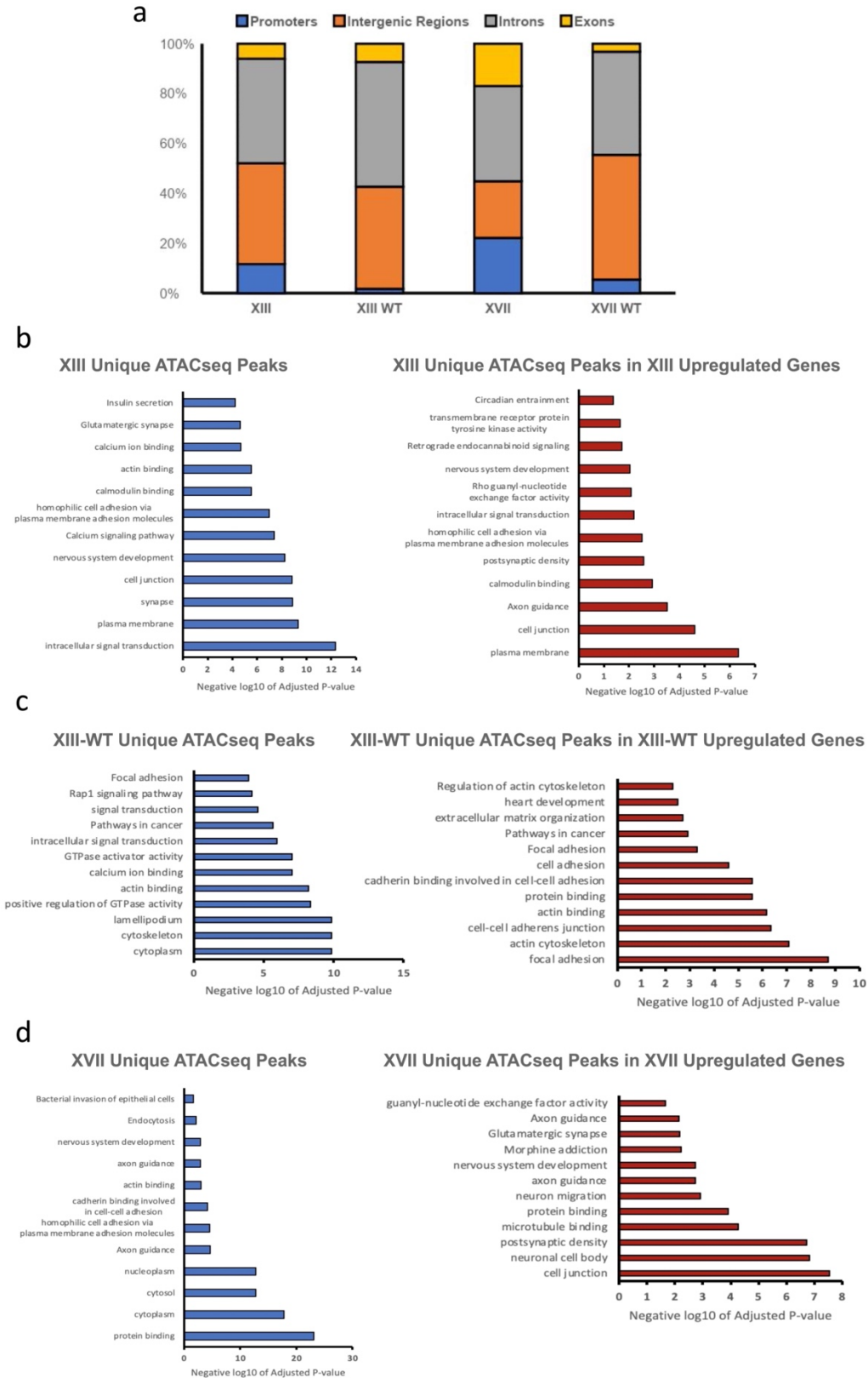


**Figure 2. H3.3K27M DIPG cells are enriched for open chromatin peaks in upregulated genes related to the nervous system compared to their isogenic gene-edited wild-type counterparts.** **a** Bar plot showing proportion of peaks in various genomic regions. Promoters were defined as 1 kb upstream of the TSS and 2kb downstream. 75% or more of the peaks for each line were found in Intergenic regions or Introns. **b.** Gene ontology analysis of differential open chromatin (blue, left side) and specifically open chromatin regions linked to increased gene expression (red, right side) in XIII, **c** XIII WT, and **d** XVII. For enriched GO terms p-values were obtained from the Benjamini-Hochberg method.



**Figure 3. H3.3K27M and H3.3-WT DIPG have differentially accessible enhancer regions. a** GREAT analysis of differentially open chromatin regions between parental (XIII and XVII) and CRISPR gene-edited isogenic wild-type lines (XIII-WT). **b.** Gene tracks with our ATAC-seq, H3K27ac peaks from Nagaraja et al., 2017 GEO: GSE94259, and enhancer regions defined by GREAT analysis for genes of interest.

**Figure 4.**

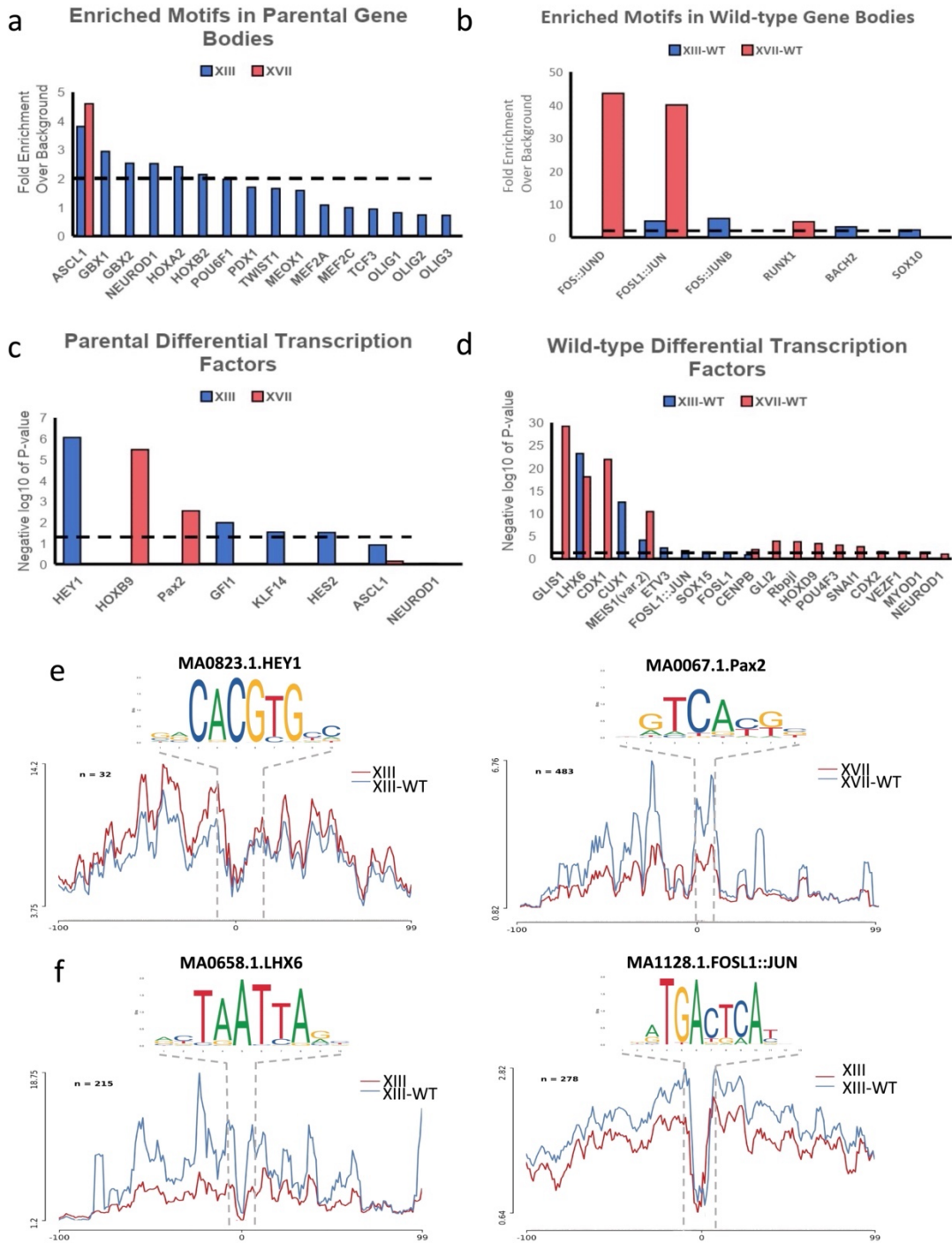


**Figure 4. Determination of physiologically relevant enriched transcription factors in H3.3K27M and H3.3 wild-type cells.** **a-b** Motifs identified using MEME-ChIP and number of times that motif occurred in the ATAC-seq peaks was determined using FIMO. Background was calculated by scrambling DNA sequence and inputting that sequence into FIMO. Threshold for significant fold enrichment was set to 2 (black dashed line). **c-d** HINT-ATAC identified DNA binding footprints in ATAC-seq data made by transcription factors. Those that were statistically significant ( $p$ -value $<0.05$ , black dashed line) and of interest from MEME-ChIP analysis are plotted for **c** parental and **d** wild-type. **e** HINT-ATAC line plots showing the differential footprints of transcription factors significantly differentially bound in XIII (HEY1) and XVII (Pax2), and **f** XIII-WT (LHX6 and FOSL1::JUN).

**Figure 5.**

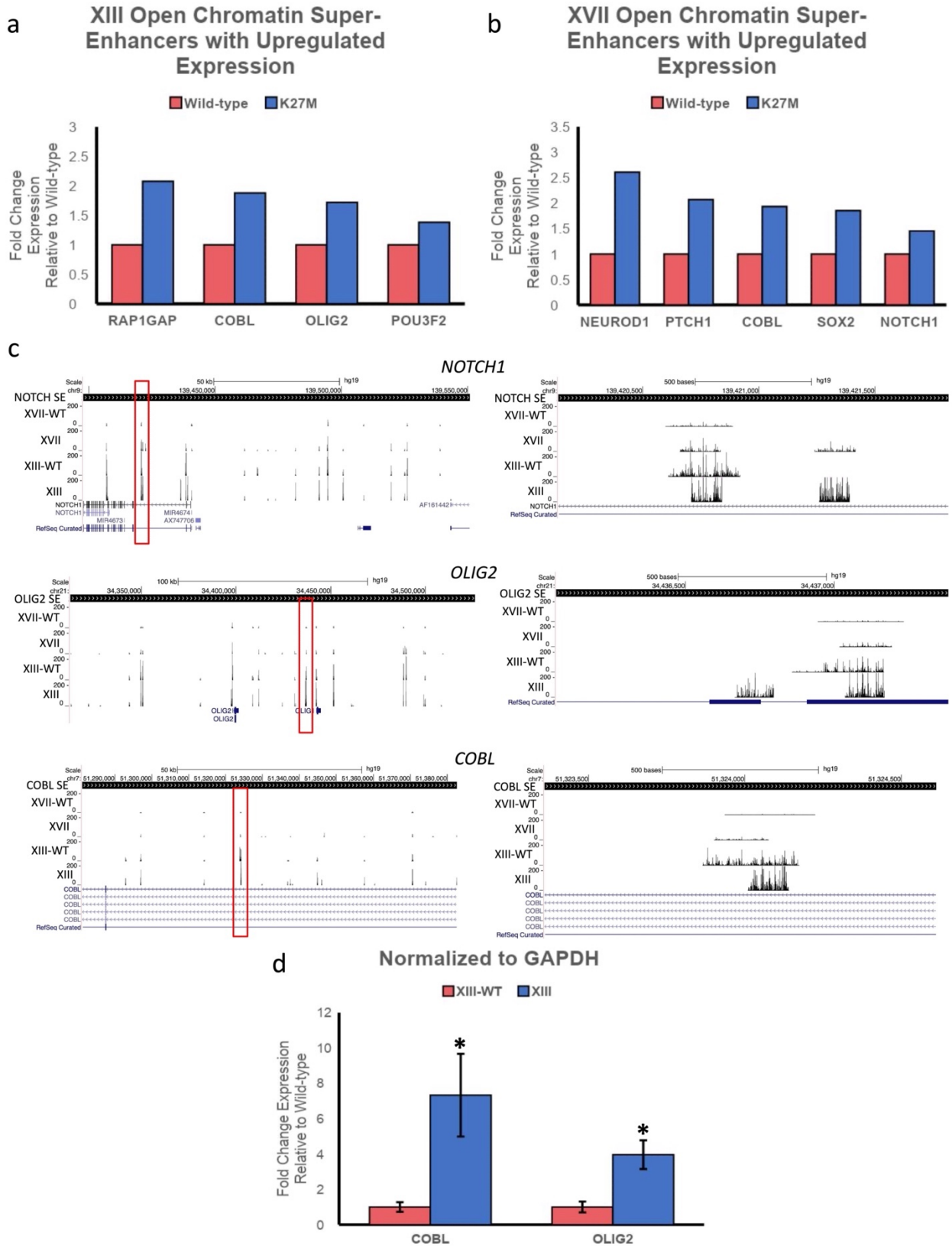


**Figure 5. H3.3K27M DIPG cells have accessible super-enhancers resulting in increased gene expression compared to H3.3-WT DIPG samples. a** Select super-enhancers of interest with open chromatin according to ATAC-seq data and increased gene expression via Tag-seq ranked according to fold change relative to H3.3-WT in **XIII** and **b XVII**. **c** Gene tracks with ATAC-seq peaks from UCSC Genome Browser of sample super-enhancer regions of interest. **d** COBL and OLIG2 were selected for validation using qPCR. Fold change expression in H3.3K27M DIPG were calculated relative to H3.3-WT. n=4, \*p-value<0.05, and error bars were calculated based on SEM.

Figure 6.

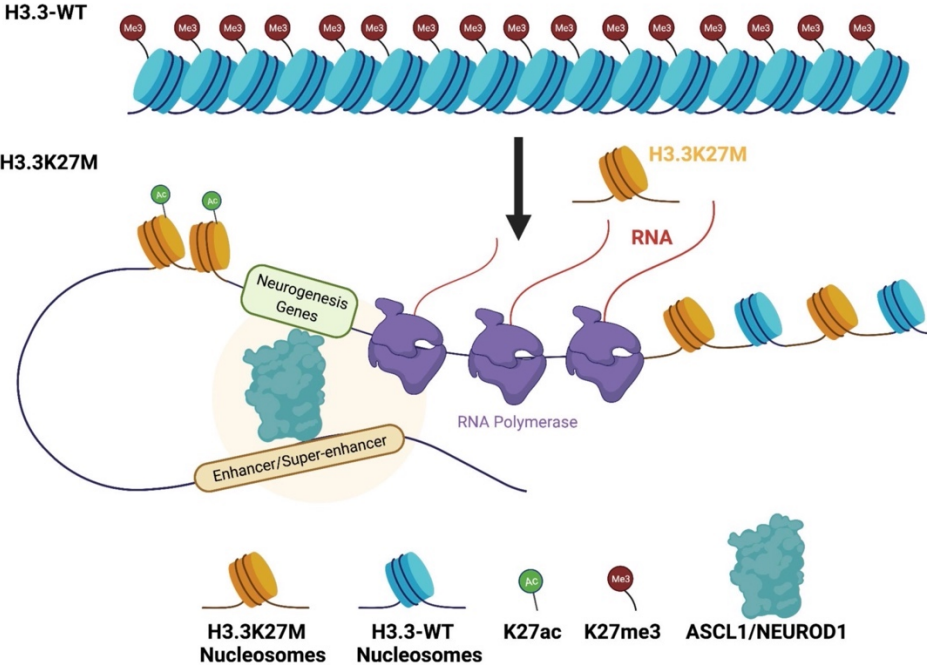


**Figure 6. Model of how H3.3K27M affects the chromatin landscape and subsequent gene expression.** Normal brain cells have H3K27me3 throughout the genome resulting in heterochromatin and decreased gene expression at neuronal, NOTCH signaling, and oncogenesis genes. After the introduction of point mutation to *H3F3A* resulting in the H3.3K27M mutation. H3K27me3 levels are decreased and H3K27ac levels increase. The chromatin begins to open upon deposition of H3.3K27M-H3K27ac nucleosomes at enhancer and super-enhancers responsible for regulating expression of neurogenesis genes. *ASCL1* and *NEUROD1* transcription factors bind to their respective motifs in these regions. We propose that *ASCL1* and *NEUROD1* binding facilitates enhancer and super-enhancer and further open the chromatin regions ultimately resulting in increased expression of neurogenesis, NOTCH, and oncogenesis genes. Adapted from “Regulation of Transcription in Eukaryotic Cells”, by BioRender.com (2021). Retrieved from <https://app.biorender.com/biorender-templates>

## References

- Ahuja, R., Pinyol, R., Reichenbach, N., Custer, L., Klingensmith, J., Kessels, M.M., Qualmann, B., 2007. Cordon-Bleu Is an Actin Nucleation Factor and Controls Neuronal Morphology. *Cell* 131, 337–350. <https://doi.org/10.1016/j.cell.2007.08.030>
- Bender, S., Tang, Y., Lindroth, A.M., Hovestadt, V., Jones, D.T.W., Kool, M., Zapatka, M., Northcott, P.A., Sturm, D., Wang, W., Radlwimmer, B., Højfeldt, J.W., Truffaux, N., Castel, D., Schubert, S., Ryzhova, M., Şeker-Cin, H., Gronych, J., Johann, P.D., Stark, S., Meyer, J., Milde, T., Schuhmann, M., Ebinger, M., Monoranu, C.-M., Ponnuswami, A., Chen, S., Jones, C., Witt, O., Collins, V.P., von Deimling, A., Jabado, N., Puget, S., Grill, J., Helin, K., Korshunov, A., Lichter, P., Monje, M., Plass, C., Cho, Y.-J., Pfister, S.M., 2013. Reduced H3K27me3 and DNA Hypomethylation Are Major Drivers of Gene Expression in K27M Mutant Pediatric High-Grade Gliomas. *Cancer Cell* 24, 660–672. <https://doi.org/10.1016/j.ccr.2013.10.006>
- Brown, Z.Z., Müller, M.M., Jain, S.U., Allis, C.D., Lewis, P.W., Muir, T.W., 2014. Strategy for “Detoxification” of a Cancer-Derived Histone Mutant Based on Mapping Its Interaction with the Methyltransferase PRC2. *J. Am. Chem. Soc.* 136, 13498–13501. <https://doi.org/10.1021/ja5060934>
- Buenrostro, J.D., Giresi, P.G., Zaba, L.C., Chang, H.Y., Greenleaf, W.J., 2013. Transposition of native chromatin for fast and sensitive epigenomic profiling of open chromatin, DNA-binding proteins and nucleosome position. *Nat Methods* 10, 1213–1218. <https://doi.org/10.1038/nmeth.2688>
- Buenrostro, J.D., Wu, B., Chang, H.Y., Greenleaf, W.J., 2015. ATAC-seq: A Method for Assaying Chromatin Accessibility Genome-Wide. *Current Protocols in Molecular Biology* 109. <https://doi.org/10.1002/0471142727.mb2129s109>
- Castel, D., Philippe, C., Calmon, R., Le Dret, L., Truffaux, N., Boddaert, N., Pagès, M., Taylor, K.R., Saulnier, P., Lacroix, L., Mackay, A., Jones, C., Sainte-Rose, C., Blauwblomme, T., Andreiuolo, F., Puget, S., Grill, J., Varlet, P., Debily, M.-A., 2015. Histone H3F3A and HIST1H3B K27M mutations define two subgroups of diffuse intrinsic pontine gliomas with different prognosis and phenotypes. *Acta Neuropathol* 130, 815–827. <https://doi.org/10.1007/s00401-015-1478-0>
- Castel, D., Philippe, C., Kergrohen, T., Sill, M., Merlevede, J., Barret, E., Puget, S., Sainte-Rose, C., Kramm, C.M., Jones, C., Varlet, P., Pfister, S.M., Grill, J., Jones, D.T.W., Debily, M.-A., 2018. Transcriptomic and epigenetic profiling of ‘diffuse midline gliomas, H3 K27M-mutant’ discriminate two subgroups based on the type of histone H3 mutated and not supratentorial or infratentorial location. *acta neuropathol commun* 6, 117. <https://doi.org/10.1186/s40478-018-0614-1>
- Chan, K.-M., Fang, D., Gan, H., Hashizume, R., Yu, C., Schroeder, M., Gupta, N., Mueller, S., James, C.D., Jenkins, R., Sarkaria, J., Zhang, Z., 2013. The histone H3.3K27M mutation in pediatric glioma reprograms H3K27 methylation and gene expression. *Genes & Development* 27, 985–990. <https://doi.org/10.1101/gad.217778.113>
- Chen, K.-Y., Bush, K., Klein, R.H., Cervantes, V., Lewis, N., Naqvi, A., Carcaboso, A.M., Lechpammer, M., Knoepfler, P.S., 2020. Reciprocal H3.3 gene editing identifies K27M and G34R mechanisms in pediatric glioma including NOTCH signaling. *Commun Biol* 3, 363.

<https://doi.org/10.1038/s42003-020-1076-0>

Cheng, Y., Liao, S., Xu, G., Hu, J., Guo, D., Du, F., Contreras, A., Cai, K.Q., Peri, S., Wang, Y., Corney, D.C., Noronha, A.M., Chau, L.Q., Zhou, G., Wiest, D.L., Bellacosa, A., Wechsler-Reya, R.J., Zhao, Y., Yang, Z., 2020. NeuroD1 Dictates Tumor Cell Differentiation in Medulloblastoma. *Cell Reports* 31, 107782. <https://doi.org/10.1016/j.celrep.2020.107782>

Corces, M.R., Trevino, A.E., Hamilton, E.G., Greenside, P.G., Sinnott-Armstrong, N.A., Vesuna, S., Satpathy, A.T., Rubin, A.J., Montine, K.S., Wu, B., Kathiria, A., Cho, S.W., Mumbach, M.R., Carter, A.C., Kasowski, M., Orloff, L.A., Risca, V.I., Kundaje, A., Khavari, P.A., Montine, T.J., Greenleaf, W.J., Chang, H.Y., 2017. An improved ATAC-seq protocol reduces background and enables interrogation of frozen tissues. *Nature Methods* 14, 959–962. <https://doi.org/10.1038/nmeth.4396>

Creyghton, M.P., Cheng, A.W., Welstead, G.G., Kooistra, T., Carey, B.W., Steine, E.J., Hanna, J., Lodato, M.A., Frampton, G.M., Sharp, P.A., Boyer, L.A., Young, R.A., Jaenisch, R., 2010. Histone H3K27ac separates active from poised enhancers and predicts developmental state. *Proceedings of the National Academy of Sciences* 107, 21931–21936. <https://doi.org/10.1073/pnas.1016071107>

Fang, D., Gan, H., Cheng, L., Lee, J.-H., Zhou, H., Sarkaria, J.N., Daniels, D.J., Zhang, Z., 2018. H3.3K27M mutant proteins reprogram epigenome by sequestering the PRC2 complex to poised enhancers. *eLife* 7, e36696. <https://doi.org/10.7554/eLife.36696>

Feng, J., Liu, T., Qin, B., Zhang, Y., Liu, X.S., 2012. Identifying ChIP-seq enrichment using MACS. *Nat Protoc* 7, 1728–1740. <https://doi.org/10.1038/nprot.2012.101>

Filbin, M.G., Tirosh, I., Hovestadt, V., Shaw, M.L., Escalante, L.E., Mathewson, N.D., Neftel, C., Frank, N., Pelton, K., Hebert, C.M., Haberler, C., Yizhak, K., Gojo, J., Egervari, K., Mount, C., van Galen, P., Bonal, D.M., Nguyen, Q.-D., Beck, A., Sinai, C., Czech, T., Dorfer, C., Goumnerova, L., Lavarino, C., Carcaboso, A.M., Mora, J., Mylvaganam, R., Luo, C.C., Peyrl, A., Popović, M., Azizi, A., Batchelor, T.T., Frosch, M.P., Martinez-Lage, M., Kieran, M.W., Bandopadhyay, P., Beroukhim, R., Fritsch, G., Getz, G., Rozenblatt-Rosen, O., Wucherpennig, K.W., Louis, D.N., Monje, M., Slavc, I., Ligon, K.L., Golub, T.R., Regev, A., Bernstein, B.E., Suvà, M.L., 2018. Developmental and oncogenic programs in H3K27M gliomas dissected by single-cell RNA-seq. *Science* 360, 331–335. <https://doi.org/10.1126/science.aao4750>

Funato, K., Major, T., Lewis, P.W., Allis, C.D., Tabar, V., 2014. Use of human embryonic stem cells to model pediatric gliomas with H3.3K27M histone mutation. *Science* 346, 1529–1533. <https://doi.org/10.1126/science.1253799>

Gao, Z., Ure, K., Ables, J.L., Lagace, D.C., Nave, K.-A., Goebbels, S., Eisch, A.J., Hsieh, J., 2009. Neurod1 is essential for the survival and maturation of adult-born neurons. *Nature Neuroscience* 12, 1090–1092. <https://doi.org/10.1038/nn.2385>

Grant, C.E., Bailey, T.L., Noble, W.S., 2011. FIMO: scanning for occurrences of a given motif. *Bioinformatics* 27, 1017–1018. <https://doi.org/10.1093/bioinformatics/btr064>

Grasso, C.S., Tang, Y., Truffaux, N., Berlow, N.E., Liu, L., Debily, M.-A., Quist, M.J., Davis, L.E., Huang, E.C., Woo, P.J., Ponnuswami, A., Chen, S., Johung, T.B., Sun, W., Kogiso, M., Du, Y.,

Qi, L., Huang, Y., Hütt-Cabezas, M., Warren, K.E., Le Dret, L., Meltzer, P.S., Mao, H., Quezado, M., van Vuurden, D.G., Abraham, J., Fouladi, M., Svalina, M.N., Wang, N., Hawkins, C., Nazarian, J., Alonso, M.M., Raabe, E.H., Hulleman, E., Spellman, P.T., Li, X.-N., Keller, C., Pal, R., Grill, J., Monje, M., 2015. Functionally defined therapeutic targets in diffuse intrinsic pontine glioma. *Nat Med* 21, 555–559. <https://doi.org/10.1038/nm.3855>

Guichet, P.-O., Bieche, I., Teigell, M., Serguera, C., Rothhut, B., Rigau, V., Scamps, F., Ripoll, C., Vacher, S., Taviaux, S., Chevassus, H., Duffau, H., Mallet, J., Susini, A., Joubert, D., Bauchet, L., Hugnot, J.-P., 2013. Cell death and neuronal differentiation of glioblastoma stem-like cells induced by neurogenic transcription factors. *Glia* 61, 225–239. <https://doi.org/10.1002/glia.22429>

Haag, D., Mack, N., Benites Goncalves da Silva, P., Statz, B., Clark, J., Tanabe, K., Sharma, T., Jäger, N., Jones, D.T.W., Kawauchi, D., Wernig, M., Pfister, S.M., 2021. H3.3-K27M drives neural stem cell-specific gliomagenesis in a human iPSC-derived model. *Cancer Cell* 39, 407-422.e13. <https://doi.org/10.1016/j.ccell.2021.01.005>

Haag, N., Schwintzer, L., Ahuja, R., Koch, N., Grimm, J., Heuer, H., Qualmann, B., Kessels, M.M., 2012. The Actin Nucleator Cobl Is Crucial for Purkinje Cell Development and Works in Close Conjunction with the F-Actin Binding Protein Abp1. *J. Neurosci.* 32, 17842–17856. <https://doi.org/10.1523/JNEUROSCI.0843-12.2012>

Harutyunyan, A.S., Krug, B., Chen, H., Papillon-Cavanagh, S., Zeinieh, M., De Jay, N., Deshmukh, S., Chen, C.C.L., Belle, J., Mikael, L.G., Marchione, D.M., Li, R., Nikbakht, H., Hu, B., Cagnone, G., Cheung, W.A., Mohammadnia, A., Bechet, D., Faury, D., McConechy, M.K., Pathania, M., Jain, S.U., Ellezam, B., Weil, A.G., Montpetit, A., Salomoni, P., Pastinen, T., Lu, C., Lewis, P.W., Garcia, B.A., Kleinman, C.L., Jabado, N., Majewski, J., 2019. H3K27M induces defective chromatin spread of PRC2-mediated repressive H3K27me2/me3 and is essential for glioma tumorigenesis. *Nat Commun* 10, 1262. <https://doi.org/10.1038/s41467-019-09140-x>

Heinz, S., Benner, C., Spann, N., Bertolino, E., Lin, Y.C., Laslo, P., Cheng, J.X., Murre, C., Singh, H., Glass, C.K., 2010. Simple Combinations of Lineage-Determining Transcription Factors Prime cis-Regulatory Elements Required for Macrophage and B Cell Identities. *Molecular Cell* 38, 576–589. <https://doi.org/10.1016/j.molcel.2010.05.004>

Hennika, T., Hu, G., Olaciregui, N.G., Barton, K.L., Ehteda, A., Chitranjan, A., Chang, C., Gifford, A.J., Tsoli, M., Ziegler, D.S., Carcaboso, A.M., Becher, O.J., 2017. Pre-Clinical Study of Panobinostat in Xenograft and Genetically Engineered Murine Diffuse Intrinsic Pontine Glioma Models. *PLOS ONE* 12, e0169485. <https://doi.org/10.1371/journal.pone.0169485>

Herz, H.-M., Morgan, M., Gao, X., Jackson, J., Rickels, R., Swanson, S.K., Florens, L., Washburn, M.P., Eissenberg, J.C., Shilatifard, A., 2014. Histone H3 lysine-to-methionine mutants as a paradigm to study chromatin signaling. *Science* 345, 1065–1070. <https://doi.org/10.1126/science.1255104>

Hou, W., Izadi, M., Nemitz, S., Haag, N., Kessels, M.M., Qualmann, B., 2015. The Actin Nucleator Cobl Is Controlled by Calcium and Calmodulin. *PLOS Biology* 13, e1002233. <https://doi.org/10.1371/journal.pbio.1002233>

Huang, D.W., Sherman, B.T., Lempicki, R.A., 2009a. Systematic and integrative analysis of large gene lists using DAVID bioinformatics resources. *Nat Protoc* 4, 44–57.

<https://doi.org/10.1038/nprot.2008.211>

Huang, D.W., Sherman, B.T., Lempicki, R.A., 2009b. Bioinformatics enrichment tools: paths toward the comprehensive functional analysis of large gene lists. *Nucleic Acids Research* 37, 1–13. <https://doi.org/10.1093/nar/gkn923>

Hurtado, C., Safarova, A., Smith, M., Chung, R., Bruyneel, A.A.N., Gomez-Galeno, J., Oswald, F., Larson, C.J., Cashman, J.R., Ruiz-Lozano, P., Janiak, P., Suzuki, T., Mercola, M., 2019. Disruption of NOTCH signaling by a small molecule inhibitor of the transcription factor RBPJ. *Sci Rep* 9, 10811. <https://doi.org/10.1038/s41598-019-46948-5>

Justin, N., Zhang, Y., Tarricone, C., Martin, S.R., Chen, S., Underwood, E., De Marco, V., Haire, L.F., Walker, P.A., Reinberg, D., Wilson, J.R., Gambelin, S.J., 2016. Structural basis of oncogenic histone H3K27M inhibition of human polycomb repressive complex 2. *Nature Communications* 7, 11316. <https://doi.org/10.1038/ncomms11316>

Khuong-Quang, D.-A., Buczkowicz, P., Rakopoulos, P., Liu, X.-Y., Fontebasso, A.M., Bouffet, E., Bartels, U., Albrecht, S., Schwartzentruber, J., Letourneau, L., Bourgey, M., Bourque, G., Montpetit, A., Bourret, G., Lepage, P., Fleming, A., Lichter, P., Kool, M., von Deimling, A., Sturm, D., Korshunov, A., Faury, D., Jones, D.T., Majewski, J., Pfister, S.M., Jabado, N., Hawkins, C., 2012. K27M mutation in histone H3.3 defines clinically and biologically distinct subgroups of pediatric diffuse intrinsic pontine gliomas. *Acta Neuropathol* 124, 439–447. <https://doi.org/10.1007/s00401-012-0998-0>

Krug, B., De Jay, N., Harutyunyan, A.S., Deshmukh, S., Marchione, D.M., Guilhamon, P., Bertrand, K.C., Mikael, L.G., McConechy, M.K., Chen, C.C.L., Khazaei, S., Koncar, R.F., Agnihotri, S., Faury, D., Ellezam, B., Weil, A.G., Ursini-Siegel, J., De Carvalho, D.D., Dirks, P.B., Lewis, P.W., Salomoni, P., Lupien, M., Arrowsmith, C., Lasko, P.F., Garcia, B.A., Kleinman, C.L., Jabado, N., Mack, S.C., 2019. Pervasive H3K27 Acetylation Leads to ERV Expression and a Therapeutic Vulnerability in H3K27M Gliomas. *Cancer Cell* 35, 782-797.e8. <https://doi.org/10.1016/j.ccell.2019.04.004>

Langmead, B., Trapnell, C., Pop, M., Salzberg, S.L., 2009. Ultrafast and memory-efficient alignment of short DNA sequences to the human genome. *Genome Biology* 10, R25. <https://doi.org/10.1186/gb-2009-10-3-r25>

Larson, J.D., Kasper, L.H., Paugh, B.S., Jin, H., Wu, G., Kwon, C.-H., Fan, Y., Shaw, T.I., Silveira, A.B., Qu, C., Xu, R., Zhu, X., Zhang, Junyuan, Russell, H.R., Peters, J.L., Finkelstein, D., Xu, B., Lin, T., Tinkle, C.L., Patay, Z., Onar-Thomas, A., Pounds, S.B., McKinnon, P.J., Ellison, D.W., Zhang, Jinghui, Baker, S.J., 2019. Histone H3.3 K27M Accelerates Spontaneous Brainstem Glioma and Drives Restricted Changes in Bivalent Gene Expression. *Cancer Cell* 35, 140-155.e7. <https://doi.org/10.1016/j.ccell.2018.11.015>

Lee, C.-H., Yu, J.-R., Granat, J., Saldaña-Meyer, R., Andrade, J., LeRoy, G., Jin, Y., Lund, P., Stafford, J.M., Garcia, B.A., Ueberheide, B., Reinberg, D., 2019. Automethylation of PRC2 promotes H3K27 methylation and is impaired in H3K27M pediatric glioma. *Genes Dev.* 33, 1428–1440. <https://doi.org/10.1101/gad.328773.119>

Lewis, P.W., Muller, M.M., Koletsky, M.S., Cordero, F., Lin, S., Banaszynski, L.A., Garcia, B.A., Muir, T.W., Becher, O.J., Allis, C.D., 2013. Inhibition of PRC2 Activity by a Gain-of-Function H3 Mutation Found in Pediatric Glioblastoma. *Science* 340, 857–861.

<https://doi.org/10.1126/science.1232245>

Li, H., Handsaker, B., Wysoker, A., Fennell, T., Ruan, J., Homer, N., Marth, G., Abecasis, G., Durbin, R., 1000 Genome Project Data Processing Subgroup, 2009. The Sequence Alignment/Map format and SAMtools. *Bioinformatics* 25, 2078–2079. <https://doi.org/10.1093/bioinformatics/btp352>

Li, Z., Schulz, M.H., Look, T., Begemann, M., Zenke, M., Costa, I.G., 2019. Identification of transcription factor binding sites using ATAC-seq. *Genome Biol* 20, 45. <https://doi.org/10.1186/s13059-019-1642-2>

Lin, G.L., Wilson, K.M., Ceribelli, M., Stanton, B.Z., Woo, P.J., Kreimer, S., Qin, E.Y., Zhang, X., Lennon, J., Nagaraja, S., Morris, P.J., Quezada, M., Gillespie, S.M., Duveau, D.Y., Michalowski, A.M., Shinn, P., Guha, R., Ferrer, M., Klumpp-Thomas, C., Michael, S., McKnight, C., Minhas, P., Itkin, Z., Raabe, E.H., Chen, L., Ghanem, R., Geraghty, A.C., Ni, L., Andreasson, K.I., Vitanza, N.A., Warren, K.E., Thomas, C.J., Monje, M., 2019. Therapeutic strategies for diffuse midline glioma from high-throughput combination drug screening. *Sci. Transl. Med.* 11, eaaw0064. <https://doi.org/10.1126/scitranslmed.aaw0064>

Lovén, J., Hoke, H.A., Lin, C.Y., Lau, A., Orlando, D.A., Vakoc, C.R., Bradner, J.E., Lee, T.I., Young, R.A., 2013. Selective Inhibition of Tumor Oncogenes by Disruption of Super-Enhancers. *Cell* 153, 320–334. <https://doi.org/10.1016/j.cell.2013.03.036>

Machanick, P., Bailey, T.L., 2011. MEME-ChIP: motif analysis of large DNA datasets. *Bioinformatics* 27, 1696–1697. <https://doi.org/10.1093/bioinformatics/btr189>

Mackay, A., Burford, A., Carvalho, D., Izquierdo, E., Fazal-Salom, J., Taylor, K.R., Bjerke, L., Clarke, M., Vinci, M., Nandhabalan, M., Temelso, S., Popov, S., Molinari, V., Raman, P., Waanders, A.J., Han, H.J., Gupta, S., Marshall, L., Zacharoulis, S., Vaidya, S., Mandeville, H.C., Bridges, L.R., Martin, A.J., Al-Sarraj, S., Chandler, C., Ng, H.-K., Li, X., Mu, K., Trabelsi, S., Brahim, D.H.-B., Kisliakov, A.N., Konovalov, D.M., Moore, A.S., Carcaboso, A.M., Sunol, M., de Torres, C., Cruz, O., Mora, J., Shats, L.I., Stavale, J.N., Bidinotto, L.T., Reis, R.M., Entz-Werle, N., Farrell, M., Cryan, J., Crimmins, D., Caird, J., Pears, J., Monje, M., Debily, M.-A., Castel, D., Grill, J., Hawkins, C., Nikbakht, H., Jabado, N., Baker, S.J., Pfister, S.M., Jones, D.T.W., Fouladi, M., von Bueren, A.O., Baudis, M., Resnick, A., Jones, C., 2017. Integrated Molecular Meta-Analysis of 1,000 Pediatric High-Grade and Diffuse Intrinsic Pontine Glioma. *Cancer Cell* 32, 520-537.e5. <https://doi.org/10.1016/j.ccell.2017.08.017>

McLean, C.Y., Bristor, D., Hiller, M., Clarke, S.L., Schaar, B.T., Lowe, C.B., Wenger, A.M., Bejerano, G., 2010. GREAT improves functional interpretation of cis-regulatory regions. *Nat Biotechnol* 28, 495–501. <https://doi.org/10.1038/nbt.1630>

Meel, M.H., Gooijer, M.C. de, Metselaar, D.S., Sewing, A.C.P., Zwaan, K., Waranecki, P., Breur, M., Buil, L.C.M., Lagerweij, T., Wedekind, L.E., Twisk, J.W.R., Koster, J., Hashizume, R., Raabe, E.H., Carcaboso, A.M., Bugiani, M., Phoenix, T.N., Tellingén, O. van, Vuurden, D.G. van, Kaspers, G.J.L., Hulleman, E., 2020. Combined Therapy of AXL and HDAC Inhibition Reverses Mesenchymal Transition in Diffuse Intrinsic Pontine Glioma. *Clin Cancer Res* 26, 3319–3332. <https://doi.org/10.1158/1078-0432.CCR-19-3538>

Mohammad, F., Weissmann, S., Leblanc, B., Pandey, D.P., Højfeldt, J.W., Comet, I., Zheng, C., Johansen, J.V., Rapin, N., Porse, B.T., Tvardovskiy, A., Jensen, O.N., Olaciregui, N.G.,

Lavarino, C., Suñol, M., de Torres, C., Mora, J., Carcaboso, A.M., Helin, K., 2017. EZH2 is a potential therapeutic target for H3K27M-mutant pediatric gliomas. *Nat Med* 23, 483–492. <https://doi.org/10.1038/nm.4293>

Monje, M., Mitra, S.S., Freret, M.E., Raveh, T.B., Kim, J., Masek, M., Attema, J.L., Li, G., Haddix, T., Edwards, M.S.B., Fisher, P.G., Weissman, I.L., Rowitch, D.H., Vogel, H., Wong, A.J., Beachy, P.A., 2011. Hedgehog-responsive candidate cell of origin for diffuse intrinsic pontine glioma. *Proceedings of the National Academy of Sciences* 108, 4453–4458. <https://doi.org/10.1073/pnas.1101657108>

Nagaraja, S., Quezada, M.A., Gillespie, S.M., Arzt, M., Lennon, J.J., Woo, P.J., Hovestadt, V., Kambhampati, M., Filbin, M.G., Suva, M.L., Nazarian, J., Monje, M., 2019. Histone Variant and Cell Context Determine H3K27M Reprogramming of the Enhancer Landscape and Oncogenic State. *Molecular Cell* 76, 965–980.e12. <https://doi.org/10.1016/j.molcel.2019.08.030>

Nagaraja, S., Vitanza, N.A., Woo, P.J., Taylor, K.R., Liu, F., Zhang, L., Li, M., Meng, W., Ponnuswami, A., Sun, W., Ma, J., Hulleman, E., Swigut, T., Wysocka, J., Tang, Y., Monje, M., 2017. Transcriptional Dependencies in Diffuse Intrinsic Pontine Glioma. *Cancer Cell* 31, 635–652.e6. <https://doi.org/10.1016/j.ccell.2017.03.011>

Nikbakht, H., Panditharatna, E., Mikael, L.G., Li, R., Gayden, T., Osmond, M., Ho, C.-Y., Kambhampati, M., Hwang, E.I., Faury, D., Siu, A., Papillon-Cavanagh, S., Bechet, D., Ligon, K.L., Ellezam, B., Ingram, W.J., Stinson, C., Moore, A.S., Warren, K.E., Karamchandani, J., Packer, R.J., Jabado, N., Majewski, J., Nazarian, J., 2016. Spatial and temporal homogeneity of driver mutations in diffuse intrinsic pontine glioma. *Nat Commun* 7, 11185. <https://doi.org/10.1038/ncomms11185>

Park, N.I., Guilhamon, P., Desai, K., McAdam, R.F., Langille, E., O'Connor, M., Lan, X., Whetstone, H., Coutinho, F.J., Vanner, R.J., Ling, E., Prinos, P., Lee, L., Selvadurai, H., Atwal, G., Kushida, M., Clarke, I.D., Voisin, V., Cusimano, M.D., Bernstein, M., Das, S., Bader, G., Arrowsmith, C.H., Angers, S., Huang, X., Lupien, M., Dirks, P.B., 2017. ASCL1 Reorganizes Chromatin to Direct Neuronal Fate and Suppress Tumorigenicity of Glioblastoma Stem Cells. *Cell Stem Cell* 21, 209–224.e7. <https://doi.org/10.1016/j.stem.2017.06.004>

Pataskar, A., Jung, J., Smialowski, P., Noack, F., Calegari, F., Straub, T., Tiwari, V.K., 2016. NeuroD1 reprograms chromatin and transcription factor landscapes to induce the neuronal program. *EMBO J* 35, 24–45. <https://doi.org/10.15252/embj.201591206>

Pathania, M., De Jay, N., Maestro, N., Harutyunyan, A.S., Nitarska, J., Pahlavan, P., Henderson, S., Mikael, L.G., Richard-Londt, A., Zhang, Y., Costa, J.R., Hébert, S., Khazaei, S., Ibrahim, N.S., Herrero, J., Riccio, A., Albrecht, S., Ketteler, R., Brandner, S., Kleinman, C.L., Jabado, N., Salomoni, P., 2017. H3.3K27M Cooperates with Trp53 Loss and PDGFRA Gain in Mouse Embryonic Neural Progenitor Cells to Induce Invasive High-Grade Gliomas. *Cancer Cell* 32, 684–700.e9. <https://doi.org/10.1016/j.ccell.2017.09.014>

Piunti, A., Hashizume, R., Morgan, M.A., Bartom, E.T., Horbinski, C.M., Marshall, S.A., Rendleman, E.J., Ma, Q., Takahashi, Y., Woodfin, A.R., Misharin, A.V., Abshiru, N.A., Lulla, R.R., Saratsis, A.M., Kelleher, N.L., James, C.D., Shilatifard, A., 2017. Therapeutic targeting of polycomb and BET bromodomain proteins in diffuse intrinsic pontine gliomas. *Nat Med* 23, 493–500. <https://doi.org/10.1038/nm.4296>

Puget, S., Philippe, C., Bax, D.A., Job, B., Varlet, P., Junier, M.-P., Andreiuolo, F., Carvalho, D., Reis, R., Guerrini-Rousseau, L., Roujeau, T., Dessen, P., Richon, C., Lazar, V., Teuff, G.L., Sainte-Rose, C., Georger, B., Vassal, G., Jones, C., Grill, J., 2012. Mesenchymal Transition and PDGFRA Amplification/Mutation Are Key Distinct Oncogenic Events in Pediatric Diffuse Intrinsic Pontine Gliomas. *PLOS ONE* 7, e30313. <https://doi.org/10.1371/journal.pone.0030313>

Rajakulendran, N., Rowland, K.J., Selvadurai, H.J., Ahmadi, M., Park, N.I., Naumenko, S., Dolma, S., Ward, R.J., So, M., Lee, L., MacLeod, G., Pasilliao, C., Brandon, C., Clarke, I.D., Cusimano, M.D., Bernstein, M., Batada, N., Angers, S., Dirks, P.B., 2019. Wnt and Notch signaling govern self-renewal and differentiation in a subset of human glioblastoma stem cells. *Genes Dev.* 33, 498–510. <https://doi.org/10.1101/gad.321968.118>

Ross-Innes, C.S., Stark, R., Teschendorff, A.E., Holmes, K.A., Ali, H.R., Dunning, M.J., Brown, G.D., Gojis, O., Ellis, I.O., Green, A.R., Ali, S., Chin, S.-F., Palmieri, C., Caldas, C., Carroll, J.S., 2012. Differential oestrogen receptor binding is associated with clinical outcome in breast cancer. *Nature* 481, 389–393. <https://doi.org/10.1038/nature10730>

Saratsis, A.M., Kambhampati, M., Snyder, K., Yadavilli, S., Devaney, J.M., Harmon, B., Hall, J., Raabe, E.H., An, P., Weingart, M., Rood, B.R., Magge, S.N., MacDonald, T.J., Packer, R.J., Nazarian, J., 2014. Comparative multidimensional molecular analyses of pediatric diffuse intrinsic pontine glioma reveals distinct molecular subtypes. *Acta Neuropathol* 127, 881–895. <https://doi.org/10.1007/s00401-013-1218-2>

Sarthy, J.F., Meers, M.P., Janssens, D.H., Henikoff, J.G., Feldman, H., Paddison, P.J., Lockwood, C.M., Vitanza, N.A., Olson, J.M., Ahmad, K., Henikoff, S., 2020. Histone deposition pathways determine the chromatin landscapes of H3.1 and H3.3 K27M oncohistones. *eLife* 9, e61090. <https://doi.org/10.7554/eLife.61090>

Schwartzentruber, J., Korshunov, A., Liu, X.-Y., Jones, D.T.W., Pfaff, E., Jacob, K., Sturm, D., Fontebasso, A.M., Quang, D.-A.K., Tönjes, M., Hovestadt, V., Albrecht, S., Kool, M., Nantel, A., Konermann, C., Lindroth, A., Jäger, N., Rausch, T., Ryzhova, M., Korbel, J.O., Hielscher, T., Hauser, P., Garami, M., Klekner, A., Bogner, L., Ebinger, M., Schuhmann, M.U., Scheurlen, W., Pekrun, A., Frühwald, M.C., Roggendorf, W., Kramm, C., Dürken, M., Atkinson, J., Lepage, P., Montpetit, A., Zakrzewska, M., Zakrzewski, K., Liberski, P.P., Dong, Z., Siegel, P., Kulozik, A.E., Zapatka, M., Guha, A., Malkin, D., Felsberg, J., Reifenberger, G., von Deimling, A., Ichimura, K., Collins, V.P., Witt, H., Milde, T., Witt, O., Zhang, C., Castelo-Branco, P., Lichter, P., Faury, D., Tabori, U., Plass, C., Majewski, J., Pfister, S.M., Jabado, N., 2012. Driver mutations in histone H3.3 and chromatin remodelling genes in paediatric glioblastoma. *Nature* 482, 226–231. <https://doi.org/10.1038/nature10833>

Stafford, J.M., Lee, C.-H., Voigt, P., Descostes, N., Saldaña-Meyer, R., Yu, J.-R., Leroy, G., Oksuz, O., Chapman, J.R., Suarez, F., Modrek, A.S., Bayin, N.S., Placantonakis, D.G., Karajannis, M.A., Snuderl, M., Ueberheide, B., Reinberg, D., 2018. Multiple modes of PRC2 inhibition elicit global chromatin alterations in H3K27M pediatric glioma. *Science Advances* 4, eaau5935. <https://doi.org/10.1126/sciadv.aau5935>

Stark, R., Brown, G., n.d. DiffBind: Differential binding analysis of ChIP-Seq peak data 75.

Sturm, D., Witt, H., Hovestadt, V., Khuong-Quang, D.-A., Jones, D.T.W., Konermann, C., Pfaff, E., Tönjes, M., Sill, M., Bender, S., Kool, M., Zapatka, M., Becker, N., Zucknick, M., Hielscher, T., Liu, X.-Y., Fontebasso, A.M., Ryzhova, M., Albrecht, S., Jacob, K., Wolter, M., Ebinger, M.,

Schuhmann, M.U., van Meter, T., Frühwald, M.C., Hauch, H., Pekrun, A., Radlwimmer, B., Niehues, T., von Komorowski, G., Dürken, M., Kulozik, A.E., Madden, J., Donson, A., Foreman, N.K., Drissi, R., Fouladi, M., Scheurlen, W., von Deimling, A., Monoranu, C., Roggendorf, W., Herold-Mende, C., Unterberg, A., Kramm, C.M., Felsberg, J., Hartmann, C., Wiestler, B., Wick, W., Milde, T., Witt, O., Lindroth, A.M., Schwartzentruber, J., Faury, D., Fleming, A., Zakrzewska, M., Liberski, P.P., Zakrzewski, K., Hauser, P., Garami, M., Klekner, A., Bognar, L., Morrissy, S., Cavalli, F., Taylor, M.D., van Sluis, P., Koster, J., Versteeg, R., Volckmann, R., Mikkelsen, T., Aldape, K., Reifenberger, G., Collins, V.P., Majewski, J., Korshunov, A., Lichter, P., Plass, C., Jabado, N., Pfister, S.M., 2012. Hotspot Mutations in H3F3A and IDH1 Define Distinct Epigenetic and Biological Subgroups of Glioblastoma. *Cancer Cell* 22, 425–437. <https://doi.org/10.1016/j.ccr.2012.08.024>

Tate, M.C., Lindquist, R.A., Nguyen, T., Sanai, N., Barkovich, A.J., Huang, E.J., Rowitch, D.H., Alvarez-Buylla, A., 2015. Postnatal growth of the human pons: A morphometric and immunohistochemical analysis. *Journal of Comparative Neurology* 523, 449–462. <https://doi.org/10.1002/cne.23690>

Taylor, I.C., Hütt-Cabezas, M., Brandt, W.D., Kambhampati, M., Nazarian, J., Chang, H.T., Warren, K.E., Eberhart, C.G., Raabe, E.H., 2015. Disrupting NOTCH Slows Diffuse Intrinsic Pontine Glioma Growth, Enhances Radiation Sensitivity, and Shows Combinatorial Efficacy With Bromodomain Inhibition. *Journal of Neuropathology & Experimental Neurology* 74, 778–790. <https://doi.org/10.1097/NEN.0000000000000216>

Vierbuchen, T., Ostermeier, A., Pang, Z.P., Kokubu, Y., Südhof, T.C., Wernig, M., 2010. Direct conversion of fibroblasts to functional neurons by defined factors. *Nature* 463, 1035–1041. <https://doi.org/10.1038/nature08797>

Vue, T.Y., Kollipara, R.K., Borromeo, M.D., Smith, T., Mashimo, T., Burns, D.K., Bachoo, R.M., Johnson, J.E., 2020. ASCL1 regulates neurodevelopmental transcription factors and cell cycle genes in brain tumors of glioma mouse models. *Glia* 68, 2613–2630. <https://doi.org/10.1002/glia.23873>

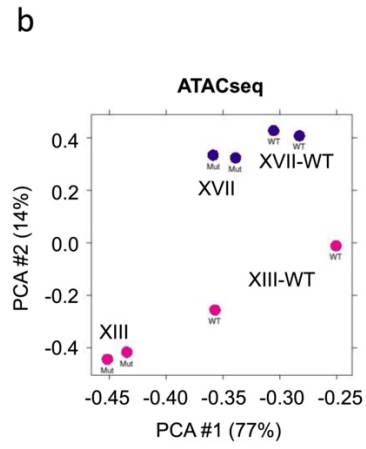
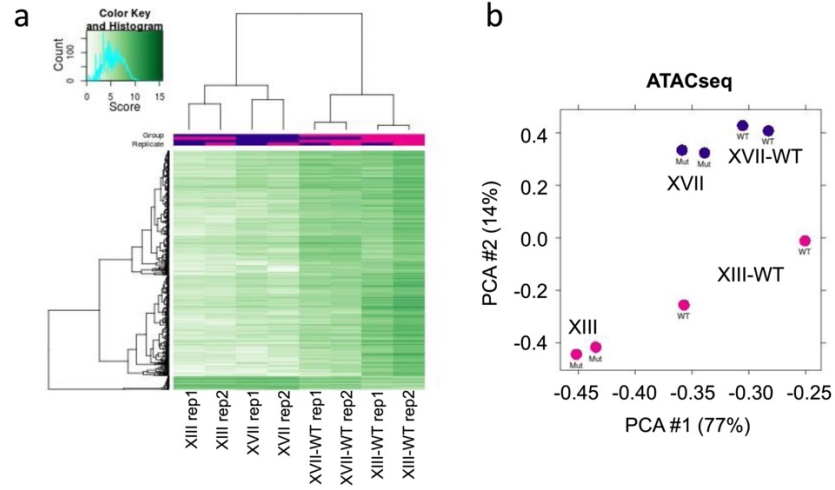
Wang, J., Huang, T.Y.-T., Hou, Y., Bartom, E., Lu, X., Shilatfard, A., Yue, F., Saratsis, A., 2021. Epigenomic landscape and 3D genome structure in pediatric high-grade glioma. *Science Advances* 7, eabg4126. <https://doi.org/10.1126/sciadv.abg4126>

Yuen, B.T.K., Knoepfler, P.S., 2013. Histone H3.3 Mutations: A Variant Path to Cancer. *Cancer Cell* 24, 567–574. <https://doi.org/10.1016/j.ccr.2013.09.015>

Zhang, Y., Liu, T., Meyer, C.A., Eeckhoute, J., Johnson, D.S., Bernstein, B.E., Nusbaum, C., Myers, R.M., Brown, M., Li, W., Liu, X.S., 2008. Model-based Analysis of ChIP-Seq (MACS). *Genome Biology* 9, R137. <https://doi.org/10.1186/gb-2008-9-9-r137>

## Supplemental Figure Legends

### Supplemental Figure S1.

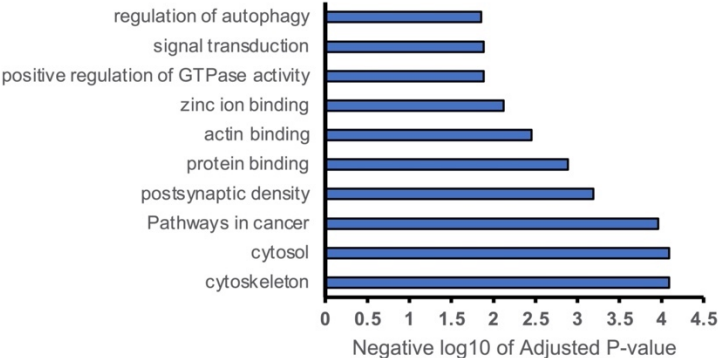


**Supplemental Figure S1. Genome-wide profile of accessible chromatin regions in H3.3K27M and H3.3-WT DIPG tumor samples.** **a** Hierarchical clustering analysis of accessible chromatin regions via ATAC-seq comparing XIII XVII. **b** Principal component analysis (PCA) of significantly differential peaks between all glioma lines.

Supplemental Figure S2.

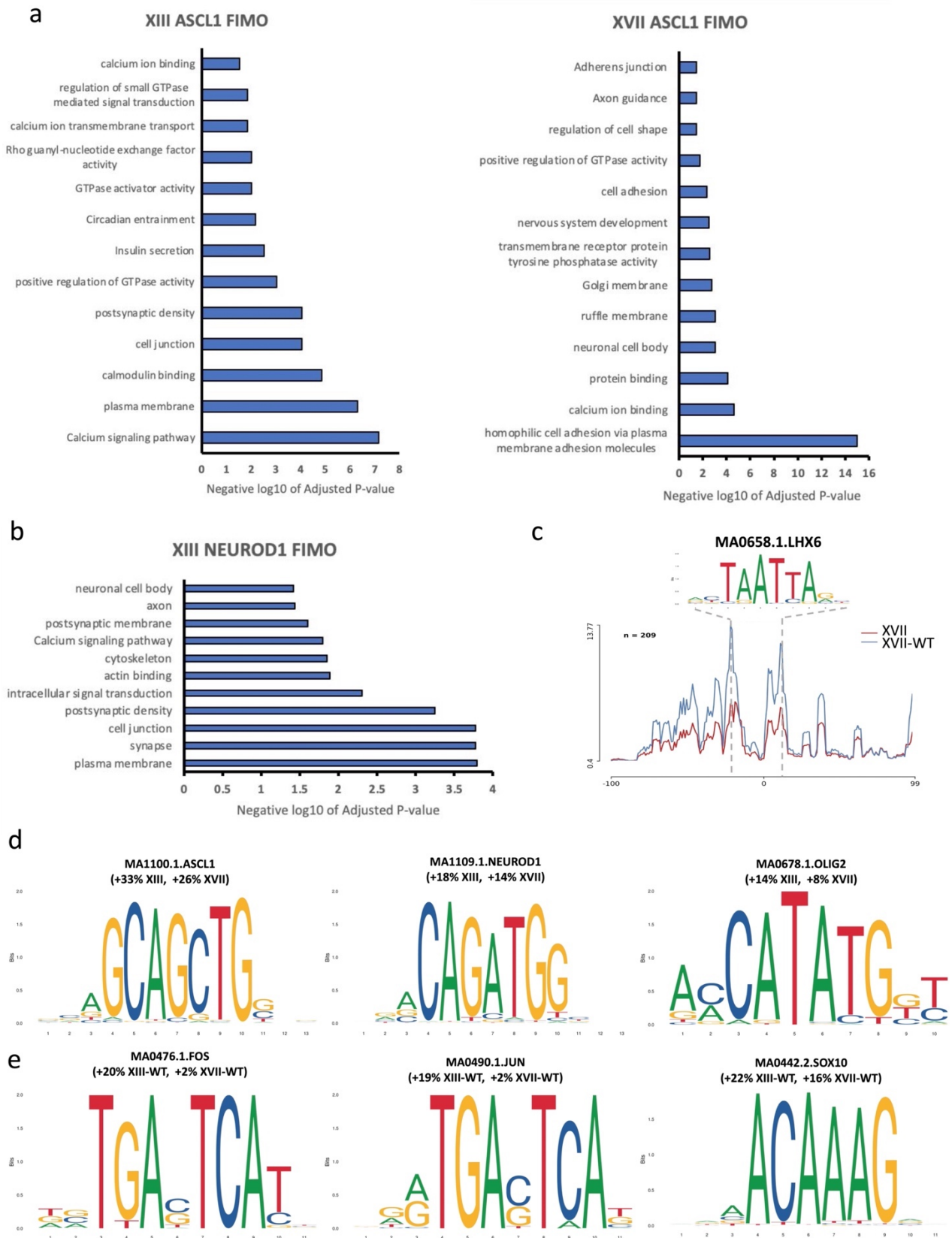
a

Wild-type H3.3 Unique ATACseq Peaks Across All Samples



**Supplemental Figure S2. H3.3K27M DIPG cells are enriched for open chromatin peaks genes related to the nervous system and GTPase activity compared to their isogenic gene-edited wild-type counterparts. a.** Gene ontology analysis of differential open chromatin regions in both isogenic gene-edited wild-type cell lines. For enriched GO terms p-values were obtained from the Benjamini-Hochberg method.

### Supplemental Figure S3.



**Supplemental Figure S3. H3.3K27M DIPGs specific transcription factor binding sites are enriched in nervous system and neuronal development genes.** **a.** Gene ontology analysis of differential open chromatin regions with ASCL1 and, **b** NEUROD1 transcription factor binding motifs. For enriched GO terms p-values were obtained from the Benjamini-Hochberg method. **c.** HINT-ATAC line plots showing the differential footprints of transcription factors significantly differentially bound in XVII-WT (LHX6) **d.** Transcription factor motifs identified as enriched via MEME-ChIP/FIMO and Homer. Percentage indicates increase of motifs in XIII and XVII, and **e** XIII-WT and XVII-WT cell lines over background.

## Supplemental Tables

**Supplementary Table 1. Summary of HOMER and DiffBind results for ATAC-seq samples.**

### DIPG Cell Line ATAC-seq Analysis

Sample	Peaks Counts
XIII rep 1	64,889
XIII rep 2	59,906
XIII WT rep 1	68,076
XIII WT rep 2	91,934
XVII rep 1	51,520
XVII rep 2	82,559
XVII WT rep 1	70,331
XVII WT rep 2	42,148

### DiffBind Analysis

Sample	Unique Peaks
XIII	4,522
XIII WT	12,860
XVII	13,136
XVII WT	211

### Gene Region Peak Analysis

Samples	Unique Peaks	Promoters	Gene Bodies	Intergenic Regions	Gene Bodies Excluding Promoter	Introns	Exons
XIII	4,522	625	2,347	2,156	1,722	2,235	323
XIII WT	12,860	238	7,158	5,652	6,920	6,900	1,001
XVII	13,136	3,858	8,366	3,960	4,508	6,641	2,949
XVII WT	211	12	95	110	83	91	7

### DiffBind Analysis

Sample	Unique Peaks
XIII + XVII	463
XIII-WT + XVII-WT	3,401

**Supplementary Table 2. Overlap of gene expression changes and ATAC-seq peak changes between WT and K27M cells.**

Line XIII	K27M up genes	K27M down genes
XIII only ATAC-seq peaks	1,881	1,215
XIII-WT only ATAC-seq peaks	1,814	4,874

Line XVII	K27M up genes	K27M down genes
XVII only ATAC-seq peaks	5,627	1,758
XVII-WT only ATAC-seq peaks	41	119

**Supplementary Table 3. Overlap of enhancer and super-enhancer regions with ATAC-seq peaks in XIII and XVII cell lines.**

<b>Samples</b>	<b>Unique Peaks</b>	<b>Overlap with H3K27ac</b>	<b>Overlap with Enhancers</b>
XIII	4,522	2,046	1,920
XIII WT	12,860	1,489	1,368
XVII	13,136	7,422	4,145
XVII WT	211	20	19

<b>Samples</b>	<b>Unique Peaks</b>	<b>Overlap with Super-Enhancers</b>
XIII	4,522	306
XIII WT	12,860	292
XVII	13,136	309
XVII WT	211	2

**Supplementary Table 4. Super-enhancers with open chromatin and increased gene-expression in parental DIPG lines**

XII			XVII			Common Super-Enhancers and Upregulated Genes			XIII			XVI		
Super-Enhancers and Upregulated Genes	FC	P-value	Super-Enhancers and Upregulated Genes	FC	P-value	Super-Enhancers and Upregulated Genes	FC	P-value	Super-Enhancers and Upregulated Genes	FC	P-value	Super-Enhancers and Upregulated Genes	FC	P-value
LINGO1	1.9932354	7.8164E-09	ADGRG1	2.046863	2.5332E-12	CFI2	1.56380782	1.2103E-05	CR1	1.379678	0.03540256			
TIAM1	1.87795616	9.5973E-09	FGF3BP3	2.3922636	3.0898E-11	COBL	1.87952161	1.1689E-05	1.93367696	1.4767E-05				
SORCS2	2.13885942	6.5372E-08	SOX4	1.88888473	2.2223E-10	DAB2IP	1.52067244	0.0247361	1.39931474	0.03672152				
ADCY1	1.85139265	1.5007E-07	LSAMP	2.05182921	2.8292E-10	FAM222A	1.84481051	8.5273E-05	2.23414063	1.8527E-07				
PPP7R2C	1.82768304	1.9448E-07	SOX2	1.85301402	4.7245E-10	GAB2	1.83271797	4.3403E-07	1.92656759	5.3269E-08				
ZNF521	1.94430668	3.846E-07	TSN21	1.99880883	8.8862E-10	LINC01158	1.98030178	1.1547E-06	1.43626461	0.03846277				
GAB2	1.83271797	4.3403E-07	PROX1	2.12832578	1.546E-09	SAS1B	1.35640593	0.00666657	1.71515005	2.3017E-06				
NXN2	1.85276592	5.3131E-07	PTN21	1.96315259	4.3024E-09	ST32B	1.93951186	1.1657E-05	1.94638897	1.2783E-06				
NXN1	1.97155109	8.889E-07	MAGEF1	1.86552794	4.9594E-09	TSN21	1.64883882	3.0271E-06	1.99882883	8.8862E-10				
LINC001158	1.98030178	1.1547E-06	ETV1	1.96282112	5.8116E-09									
ANGPT12	1.88472195	1.376E-06	NRRA2	2.11227987	2.3468E-08									
GAS7	1.97905667	1.5391E-06	PTC1A	2.07059168	3.1084E-08									
NAV1	1.80757451	1.5998E-06	CAHM	2.27209431	3.6696E-08									
TSN21	1.64883882	3.0271E-06	PMP2	2.03715111	3.7879E-08									
USP3	1.64988801	3.7323E-06	GAB2	1.92656759	5.3269E-08									
FLRT1	2.63800811	4.1019E-06	FZD9	2.17737864	8.2431E-08									
PTN	1.61651192	4.1891E-06	FAM222A	2.23414063	1.8527E-07									
FAM59C	1.91722014	5.8423E-06	SNRP7	2.25792881	2.5298E-07									
ATOH8	1.93865577	6.5193E-06	ADGRL1	1.77330378	2.5639E-07									
VSTM4	1.88422454	7.8964E-06	PIA2	1.70141986	2.9484E-07									
ACT1	1.85478787	8.6662E-06	PRK3	1.75212245	3.8024E-07									
GRM4	2.13457818	9.6463E-06	PHLDA1	1.61646414	4.5437E-07									
MTSS1	1.74467704	1.1554E-05	L0C100908844	1.87643032	4.8986E-07									
STK32B	1.93801196	1.1657E-05	PCN47	1.75549149	5.5286E-07									
COBL	1.87952161	1.1689E-05	STK32B	1.94658077	1.2783E-06									
CELF2	1.668300782	2.1010E-05	DJIS1P6	1.89636469	1.2797E-06									
PDFA	1.74175463	1.4463E-05	SIC5	1.788126	1.4286E-06									
SEZ6L	1.9419581	1.6919E-05	SASH1	1.71515005	2.5017E-06									
TNFRSF1B	2.12711053	1.7702E-05	FAM134B	1.67617283	2.6467E-06									
DAPICAP	2.07624859	1.8397E-05	PTN192	2.03551159	3.148E-06									
OLG2	1.71854997	2.6386E-05	NEUROD1	2.6065836	3.5272E-06									
MYL9	2.00979451	3.1303E-05	EPHA3	1.98715857	4.0361E-06									
GRK1	1.76234805	4.8556E-05	TRIR2	1.65006303	6.0819E-06									
STK32AS	2.1400873	8.748E-05	ADG1	1.75319663	6.7016E-06									
FAM222A	1.84841051	8.5273E-05	SC2D	1.95778276	1.0213E-05									
AGAP1	1.52455004	9.3141E-05	SCG2	1.80115483	1.248E-05									
EFNA2	1.89693573	0.00010139	COBL	1.93367696	1.4767E-05									
PLEKHA6	1.83044332	0.00010577	TUBB2B	1.52941029	1.9266E-05									
PRKX2	1.92921127	0.0001245	GM2NC	1.81700829	2.6556E-05									
MEF2A	1.52396098	0.00014689	TOX	1.55560254	3.2173E-05									
BC7A	1.55269095	0.00015088	FAM102A	1.48193236	9.0732E-05									
SEMSA5	2.37129475	0.00015823	HR23	1.64953921	0.00012065									
UPPE	1.53956566	0.00016043	KCNJ10	2.24141221	0.00012134									
AP3A2	1.56307711	0.00016615	LINC00461	1.49646549	0.00013335									
SEMA4D	1.67222074	0.00017608	FVA1	2.03521511	0.00015014									
RGS3	1.57135733	0.00019713	FAT3	1.63817411	0.00018951									
DNM13A	1.68570408	0.00024446	FAM105A	2.73799156	0.00021181									
PRKX1	1.61640784	0.00024545	PCD4P3	1.5184296	0.00023929									
FAM48A	1.51598618	0.00027652	HDACS	1.70969064	0.00045537									
GPR153	1.7204888	0.00031497	ARHGAP2	1.49918196	0.00061903									
TRIM67	1.80207968	0.00033998	ATP1B2	1.82252973	0.00066486									
IFP411	1.61488484	0.00035034	PCN47	1.75549149	0.00067946									
GRK1	1.74862508	0.0004266	ITPK3	1.87257273	0.00069262									
KCNJ12	1.67705221	0.00063982	LINC00673	1.4439377	0.00071547									
MGIL1	1.78201181	0.00068817	MTRN	1.6676252	0.00072621									
DC11B	1.63734669	0.00070377	CS	1.9988489	0.00083381									
PFEL2	1.52075548	0.00095669	NOTCH1	1.45178116	0.00117553									
SULF2	1.48322004	0.00103615	SOX1	1.59214713	0.00121824									
GSF1	1.45565624	0.00116304	NDF1	1.55886317	0.00135485									
ARC	2.25385859	0.00128933	CGRP62	1.39968673	0.00156788									
NKAPKAP2	1.87329234	0.00146605	HLCS2A	1.79880101	0.0018145									
RTN4RL1	1.92841078	0.00156791	TFAP4	1.76159546	0.00206686									
SMAAD2	1.40138436	0.00183301	RUNX1T1	1.45149309	0.0024898									
CDN3	1.72569607	0.00185167	ACVR2A	1.41838884	0.00277657									
CAF	1.43056372	0.00185493	ZNF219	1.41554334	0.00280316									
KCN4	1.76779159	0.00197706	POU3F2	1.38345498	0.00298261									
LRRN2	1.75056739	0.00200803	EPHA4	1.49591821	0.00315287									
ZBTB7C	1.7863765	0.00209178	LDLRAD3	1.36568144	0.0032302									
WIN2	1.7537252	0.00215221	TMEM38B	1.56112342	0.00369758									
SRECF	1.458182302	0.00234267	KNOP1	1.39460963	0.00402388									
OPCM	1.99954964	0.0027399	MARKS11	1.3870254	0.00533283									
KLH25	1.5380888	0.00280299	CELF2	1.379678	0.00540256									
SNRPB2	1.32954555	0.00305554	REBE	1.35176934	0.00593212									
RE3	1.59422187	0.00386267	RNF38	1.49103663	0.0062332									
MEGF11	1.65519822	0.00462331	DAB2IP	1.39931474	0.00671232									
SH3BP4	1.36146878	0.00469543	MAN1L2	1.35942287	0.00747869									
NCK2	1.49846495	0.00505707	ATG101	1.33713993	0.00793328									
CS-S2	1.44800772	0.0052699	LINC01158	1.58623661	0.00846277									
TMEM132E	1.78609795	0.00628111	PRK3	1.32508844	0.00966643									
LINC00634	2.15270257	0.00633387	PUF60	1.34467367	0.00991173									
SASH1	1.35640593	0.00666657	STK40	1.377899	0.01165429									
NFATC1	1.44640533	0.00668457	FOXO2	1.35510571	0.0119935									
LRRTM2	1.7936051	0.00777794	CHK15	1.33921577	0.01239711									
CLIP2	1.5055774	0.00796664	CHRM3	1.62450841	0.01299037									
TCF7L2	1.30092447	0.01007034	NUDT2	1.32446957	0.01311093									
CDH13	1.4609266	0.01287364	SOX13	1.46049466	0.0128248									
NFPA3	1.27346226	0.01297112	TTLL4</											

**Supplementary Table 5. Super-enhancers with open chromatin and increased gene-expression in isogenic wild-type lines**

XIII WT			XVII WT		
Super-Enhancers and Downregulated Genes	FC	P-value	Super-Enhancers and Downregulated Genes	FC	P-value
ACTN4	0.3611	5.07E-19	KLF9	0.20120945	7.3872E-29
ADAM12	0.1398	1.26E-56			
AES	0.6581	2.27E-05			
B4GALT5	0.5932	2.01E-06			
CBR1	0.1034	1.23E-40			
CCND3	0.6388	5.97E-05			
CDH5	0.0711	4.19E-14			
CLU	0.4702	2.41E-10			
CTBP2	0.6152	1.86E-06			
CUEDC1	0.3234	1.87E-22			
DIRAS3	0.1912	1.59E-17			
DLGAP1-AS2	0.1160	1.68E-03			
ECE1	0.3625	1.98E-22			
GNA12	0.6613	8.36E-05			
KIRREL	0.4543	4.66E-03			
LAMC1	0.6607	1.88E-03			
LDLRAD3	0.6303	1.11E-05			
LIMD1	0.6149	1.00E-02			
LINC00511	0.3967	2.84E-02			
LOC101926964	0.3237	6.03E-03			
LOC101929705	0.1265	2.54E-04			
LRIG1	0.4311	1.94E-10			
MACF1	0.5689	2.50E-08			
MAGEF1	0.7514	6.46E-03			
MBP	0.1587	2.33E-32			
ME3	0.0966	6.56E-08			
MSI2	0.5304	1.46E-03			
MYH9	0.4855	4.84E-12			
NACC2	0.7617	1.91E-02			
NCOR2	0.5770	3.53E-07			
NDRG1	0.3562	7.35E-21			
PCDH10	0.3018	1.38E-27			
PHLDA1	0.5252	1.41E-11			
PPF1BP1	0.6475	2.68E-05			
PSD3	0.5482	4.05E-08			
RAB31	0.5340	3.71E-09			
RCAN1	0.1387	1.88E-72			
RNF144B	0.2318	5.27E-08			
SH3PXD2B	0.4928	7.15E-12			
SLC6A6	0.2631	7.05E-16			
SOCS3	0.3358	4.08E-06			
SOD3	0.3092	4.15E-04			
SOX2	0.6227	1.58E-06			
ST3GAL1	0.2203	1.07E-38			
TMEM189	0.4051	2.76E-13			
TNK2	0.7578	2.26E-02			
TRDMT1	0.4290	2.24E-03			
TRIM2	0.5468	6.56E-08			
VAMP3	0.6181	1.21E-03			
VAPA	0.6883	2.71E-04			
VGLL4	0.7754	2.84E-02			
ZNF217	0.6832	2.86E-03			

## **CHAPTER 3**

### **Conclusions and Future Directions**

The K27M and G34R/V mutations in histone H3.3 are key defining features of DIPG and GBM tumors. This is thought to be largely due to the epigenetic disruptions these histone mutations cause, which then result in dysregulation of gene expression. H3.3G34R/V is much less understood compared to H3.3K27M. The main known consequence of H3.3G34R/V being fluctuations in H3K36 methylation status, the direction and mechanism of which is currently debated, and resulting changes in gene expression (Bjerke et al., 2013; Chen et al., 2020; Fontebasso et al., 2014; Funato et al., 2014; Jain et al., 2020; Lewis et al., 2013; Schwartzentruber et al., 2012; Voon et al., 2018). H3K27M results in global reduction of H3K27me<sub>3</sub> and those sites that retain H3K27me<sub>3</sub>, and therefore remain suppressed, correspond to tumor suppressors and neuronal development genes (Bender et al., 2013; Chan et al., 2013; Lewis et al., 2013). Further, H3.3K27M cells also display an increase in H3K27ac at enhancers and super-enhancers resulting in increased expression of genes related to several pathways important to development and tumor formation including Hedgehog and NOTCH signaling as well as neurogenesis (Nagaraja et al., 2019, 2017). Importantly, NOTCH and neurogenesis pathway perturbation is one of the few known shared characteristics between H3.3K27M and G34R/V pediatric brain tumors (Chen et al., 2020). This highlights the importance of these pathways in pediatric brain tumors and points to at least one common mechanism for drug treatments when sequencing of a patient tumor is unavailable. However, there is still much left to be understood about both tumor types regarding the impact histone mutations have on epigenetic marks, chromatin structure dynamics, downstream effector pathway, and future effective drug treatments that can be used in the clinic.

The H3.3K27M mutation is proposed to be one of the first mutations to occur during tumorigenesis and is necessary for tumor maintenance and progression (Chen et al., 2020; Funato et al., 2014; Harutyunyan et al., 2019; Larson et al., 2019; Nikbakht et al., 2016; Pathania et al., 2017). However, DIPGs and GBMs with H3.1K27M (a canonical H3 variant) and wild-type H3 exist making determining which epigenetic and transcriptomic alterations are specific to

H3.3K27M DIPG an important area of study. Here I investigated the role of H3.3 and H3.3K27M in chromatin dynamics in two isogenic CRISPR gene-edited DIPG patient cell lines using ATAC-seq. I found that H3.3K27M and wild-type H3.3 had distinct regions of open chromatin and these regions corresponded to several of the previously established upregulated genes in the respective cell lines with H3.3K27M being enriched for nervous system genes, while wild-type H3.3 was enriched for genes related to adhesion and morphology (Chen et al., 2020). Given our previous study and others have proposed that ASCL1 plays an important role in DIPG and GBM, particularly in relation to NOTCH and WNT signaling (Chen et al., 2020; Nagaraja et al., 2017; Park et al., 2017; Rajakulendran et al., 2019; Vue et al., 2020), we hypothesized that transcription factors such as ASCL1 would be enriched in open chromatin regions unique to K27M cells. To test this, I used motif analysis programs to determine if the binding motif for ASCL1 or any other important transcription factors were enriched in H3.3K27M unique open chromatin regions. Indeed, H3.3K27M DIPG are enriched for several developmentally linked transcription factor binding sites including ASCL1 and NEUROD1. I propose that both of these transcription factors, in addition to H3K27ac, promote an open chromatin configuration at neural development and oncogenesis genes contributing to tumor formation and maintenance. We have previously conducted ChIP-seq for H3K27me3 and H3.3 in our isogenic lines (Chen et al., 2020) and important next steps would be to conduct ChIP-seq in these same lines for other histone marks such as H3K27ac, H3K4me3, and H3K36me3. To date, H3K27ac ChIP-seq has been conducted in H3.3K27M and has been compared to H3K27ac ChIP-seq of isogenic H3.3K27M knockout DIPGs, H3.1K27M, and H3.3 wild-type lines to determine which sites are H3.3K27M specific (Krug et al., 2019; Nagaraja et al., 2019, 2017; Wang et al., 2021) all of which can have different physiological effects. Additionally, in order to validate our motif modeling, future work may include ChIP-seq for ASCL1, NEUROD1, or other downstream transcription factors that I identified to determine where these factors are physically binding in the genome and how these binding sites change based on *H3F3A* status.

H3.3K27M DIPG cells had unique euchromatin regions at enhancers and super-enhancers related to neurogenesis and neuronal development including NOTCH, neuronal stem cell maintenance, and oligodendrocyte differentiation. The cell of origin of DIPGs is still an open question with some groups arguing that the H3.3K27M mutation arises in NPCs/NSCs and additional mutations necessary for tumor formation first occur later in development in OPCs (Filbin et al., 2018; Haag et al., 2021; Nagaraja et al., 2019; Tate et al., 2015). The presence of enhancer regions related to both the NSC and OPC lineage supports this model. We also observed increased open chromatin in both gene bodies and enhancers related to several signaling pathways in addition to NOTCH, which is in agreement with previous work indicating that H3.3K27M is enriched for enhancers and super-enhancers related to several signaling pathways (Nagaraja et al., 2017). This provides insight into other possible targetable pathways that are unique to H3.3K27M and therefore highly targeted drugs that are less likely to negatively affect surrounding healthy tissue. Altogether our study indicates that H3.3K27M specific euchromatic regions map to nervous system development and signaling pathway genes which provides support for a possible cell of origin mechanism and further insights into other drug targets to be explored.

Many of the possible treatment approaches discussed here hold a high degree of future promise pending further studies and clinical trials. However, there are processes that have only recently been revealed to be important to DIPG biology and disease progression, which could be additional candidate targets for drug treatment. It has been established that glioblastoma stem cells (GSCs) with high levels of ASCL1 are sensitive to both NOTCH and WNT/ $\beta$ catenin inhibition (Park et al., 2017; Rajakulendran et al., 2019) and more recently it has been found that H3.3K27M DIPGs have increased levels of ASCL1, therefore, making Wnt inhibitory drugs together with the previously discussed NOTCH inhibitors (GSI and RIN1) a possible type of therapy for DIPG that has not yet been explored (Chen et al., 2020; Hurtado et al., 2019; Pathania et al., 2017; Taylor et al., 2015; Vue et al., 2020) Knockdown studies in H3.3K27M cells and knock-out studies in

GBM mouse models have shown that decreased *ASCL1* results in decreased cell viability both *in vivo* and *in vitro* (Chen et al., 2020; Vue et al., 2020). Furthermore, over-expression of *ASCL1* in H3.3 wild-type cells is sufficient to increase viability through the activation of NOTCH signaling, indicating that *ASCL1* is an important junction in DIPG maintenance and that drugs that can target processes up or downstream of *ASCL1* or *ASCL1* itself are worth investigating further (Chen et al., 2020). Further supporting the idea that inhibition of Wnt signaling could be a future therapy for DIPG, the WNT planar cell polarity (WNT/PCP) pathway is active in H3.3K27M DIPG and results in the activation of Rho family member A (RhoA), which is known to play an important role in glioma invasion (Nagaraja et al., 2019; Pathania et al., 2017). Therefore, WNT inhibiting therapies could be doubly effective because WNT signaling contributes to tumor invasion via Rho and maintenance as a downstream effector of *ASCL1* and NOTCH signaling (Vue et al., 2020). Additionally, the majority of treatment options have been explored only in H3.3K27M cells and much less is known about the potential effectiveness of specific drugs in H3.3G34R/V GBMs. Future drug studies including specifically on H3.3G34R/V cells will be crucial in further understanding the unique biology of GBMs with these histone mutations and developing potential therapies. The progress that has been made to find effective therapies for this disease is encouraging and the vulnerabilities that have recently been discovered provide even more treatment possibilities for future patients. However, the H3.3 mutant glioma remains a challenging target given their aggressiveness and ability to evolve resistance.

## References

- Bender, S., Tang, Y., Lindroth, A.M., Hovestadt, V., Jones, D.T.W., Kool, M., Zapatka, M., Northcott, P.A., Sturm, D., Wang, W., Radlwimmer, B., Højfeldt, J.W., Truffaux, N., Castel, D., Schubert, S., Ryzhova, M., Şeker-Cin, H., Gronych, J., Johann, P.D., Stark, S., Meyer, J., Milde, T., Schuhmann, M., Ebinger, M., Monoranu, C.-M., Ponnuswami, A., Chen, S., Jones, C., Witt, O., Collins, V.P., von Deimling, A., Jabado, N., Puget, S., Grill, J., Helin, K., Korshunov, A., Lichter, P., Monje, M., Plass, C., Cho, Y.-J., Pfister, S.M., 2013. Reduced H3K27me3 and DNA Hypomethylation Are Major Drivers of Gene Expression in K27M Mutant Pediatric High-Grade Gliomas. *Cancer Cell* 24, 660–672. <https://doi.org/10.1016/j.ccr.2013.10.006>
- Bjerke, L., Mackay, A., Nandhabalan, M., Burford, A., Jury, A., Popov, S., Bax, D.A., Carvalho, D., Taylor, K.R., Vinci, M., Bajrami, I., McGonnell, I.M., Lord, C.J., Reis, R.M., Hargrave, D., Ashworth, A., Workman, P., Jones, C., 2013. Histone H3.3 Mutations Drive Pediatric Glioblastoma through Upregulation of MYCN. *Cancer Discovery* 3, 512–519. <https://doi.org/10.1158/2159-8290.CD-12-0426>
- Chan, K.-M., Fang, D., Gan, H., Hashizume, R., Yu, C., Schroeder, M., Gupta, N., Mueller, S., James, C.D., Jenkins, R., Sarkaria, J., Zhang, Z., 2013. The histone H3.3K27M mutation in pediatric glioma reprograms H3K27 methylation and gene expression. *Genes & Development* 27, 985–990. <https://doi.org/10.1101/gad.217778.113>
- Chen, K.-Y., Bush, K., Klein, R.H., Cervantes, V., Lewis, N., Naqvi, A., Carcaboso, A.M., Lechpammer, M., Knoepfler, P.S., 2020. Reciprocal H3.3 gene editing identifies K27M and G34R mechanisms in pediatric glioma including NOTCH signaling. *Commun Biol* 3, 363. <https://doi.org/10.1038/s42003-020-1076-0>
- Filbin, M.G., Tirosh, I., Hovestadt, V., Shaw, M.L., Escalante, L.E., Mathewson, N.D., Neftel, C., Frank, N., Pelton, K., Hebert, C.M., Haberler, C., Yizhak, K., Gojo, J., Egervari, K., Mount, C., van Galen, P., Bonal, D.M., Nguyen, Q.-D., Beck, A., Sinai, C., Czech, T., Dorfer, C., Goumnerova, L., Lavarino, C., Carcaboso, A.M., Mora, J., Mylvaganam, R., Luo, C.C., Peyrl, A., Popović, M., Azizi, A., Batchelor, T.T., Frosch, M.P., Martinez-Lage, M., Kieran, M.W., Bandopadhyay, P., Beroukhi, R., Fritsch, G., Getz, G., Rozenblatt-Rosen, O., Wucherpennig, K.W., Louis, D.N., Monje, M., Slavc, I., Ligon, K.L., Golub, T.R., Regev, A., Bernstein, B.E., Suvà, M.L., 2018. Developmental and oncogenic programs in H3K27M gliomas dissected by single-cell RNA-seq. *Science* 360, 331–335. <https://doi.org/10.1126/science.aao4750>
- Fontebasso, A.M., Gayden, T., Nikbakht, H., Neirinck, M., Papillon-Cavanagh, S., Majewski, J., Jabado, N., 2014. Epigenetic dysregulation: a novel pathway of oncogenesis in pediatric brain tumors. *Acta Neuropathol* 13.
- Funato, K., Major, T., Lewis, P.W., Allis, C.D., Tabar, V., 2014. Use of human embryonic stem cells to model pediatric gliomas with H3.3K27M histone mutation. *Science* 346, 1529–1533. <https://doi.org/10.1126/science.1253799>
- Haag, D., Mack, N., Benites Goncalves da Silva, P., Statz, B., Clark, J., Tanabe, K., Sharma, T., Jäger, N., Jones, D.T.W., Kawachi, D., Wernig, M., Pfister, S.M., 2021. H3.3-K27M drives neural stem cell-specific gliomagenesis in a human iPSC-derived model. *Cancer Cell* 39, 407–422.e13. <https://doi.org/10.1016/j.ccell.2021.01.005>

Harutyunyan, A.S., Krug, B., Chen, H., Papillon-Cavanagh, S., Zeinieh, M., De Jay, N., Deshmukh, S., Chen, C.C.L., Belle, J., Mikael, L.G., Marchione, D.M., Li, R., Nikbakht, H., Hu, B., Cagnone, G., Cheung, W.A., Mohammadnia, A., Bechet, D., Faury, D., McConechy, M.K., Pathania, M., Jain, S.U., Ellezam, B., Weil, A.G., Montpetit, A., Salomoni, P., Pastinen, T., Lu, C., Lewis, P.W., Garcia, B.A., Kleinman, C.L., Jabado, N., Majewski, J., 2019. H3K27M induces defective chromatin spread of PRC2-mediated repressive H3K27me2/me3 and is essential for glioma tumorigenesis. *Nat Commun* 10, 1262. <https://doi.org/10.1038/s41467-019-09140-x>

Hurtado, C., Safarova, A., Smith, M., Chung, R., Bruyneel, A.A.N., Gomez-Galeno, J., Oswald, F., Larson, C.J., Cashman, J.R., Ruiz-Lozano, P., Janiak, P., Suzuki, T., Mercola, M., 2019. Disruption of NOTCH signaling by a small molecule inhibitor of the transcription factor RBPJ. *Sci Rep* 9, 10811. <https://doi.org/10.1038/s41598-019-46948-5>

Jain, S.U., Khazaei, S., Marchione, D.M., Lundgren, S.M., Wang, X., Weinberg, D.N., Deshmukh, S., Juretic, N., Lu, C., Allis, C.D., Garcia, B.A., Jabado, N., Lewis, P.W., 2020. Histone H3.3 G34 mutations promote aberrant PRC2 activity and drive tumor progression. *PNAS*. <https://doi.org/10.1073/pnas.2006076117>

Krug, B., De Jay, N., Harutyunyan, A.S., Deshmukh, S., Marchione, D.M., Guilhamon, P., Bertrand, K.C., Mikael, L.G., McConechy, M.K., Chen, C.C.L., Khazaei, S., Koncar, R.F., Agnihotri, S., Faury, D., Ellezam, B., Weil, A.G., Ursini-Siegel, J., De Carvalho, D.D., Dirks, P.B., Lewis, P.W., Salomoni, P., Lupien, M., Arrowsmith, C., Lasko, P.F., Garcia, B.A., Kleinman, C.L., Jabado, N., Mack, S.C., 2019. Pervasive H3K27 Acetylation Leads to ERV Expression and a Therapeutic Vulnerability in H3K27M Gliomas. *Cancer Cell* 35, 782-797.e8. <https://doi.org/10.1016/j.ccell.2019.04.004>

Larson, J.D., Kasper, L.H., Paugh, B.S., Jin, H., Wu, G., Kwon, C.-H., Fan, Y., Shaw, T.I., Silveira, A.B., Qu, C., Xu, R., Zhu, X., Zhang, Junyuan, Russell, H.R., Peters, J.L., Finkelstein, D., Xu, B., Lin, T., Tinkle, C.L., Patay, Z., Onar-Thomas, A., Pounds, S.B., McKinnon, P.J., Ellison, D.W., Zhang, Jinghui, Baker, S.J., 2019. Histone H3.3 K27M Accelerates Spontaneous Brainstem Glioma and Drives Restricted Changes in Bivalent Gene Expression. *Cancer Cell* 35, 140-155.e7. <https://doi.org/10.1016/j.ccell.2018.11.015>

Lewis, P.W., Muller, M.M., Koletsky, M.S., Cordero, F., Lin, S., Banaszynski, L.A., Garcia, B.A., Muir, T.W., Becher, O.J., Allis, C.D., 2013. Inhibition of PRC2 Activity by a Gain-of-Function H3 Mutation Found in Pediatric Glioblastoma. *Science* 340, 857–861. <https://doi.org/10.1126/science.1232245>

Nagaraja, S., Quezada, M.A., Gillespie, S.M., Arzt, M., Lennon, J.J., Woo, P.J., Hovestadt, V., Kambhampati, M., Filbin, M.G., Suva, M.L., Nazarian, J., Monje, M., 2019. Histone Variant and Cell Context Determine H3K27M Reprogramming of the Enhancer Landscape and Oncogenic State. *Molecular Cell* 76, 965-980.e12. <https://doi.org/10.1016/j.molcel.2019.08.030>

Nagaraja, S., Vitanza, N.A., Woo, P.J., Taylor, K.R., Liu, F., Zhang, L., Li, M., Meng, W., Ponnuswami, A., Sun, W., Ma, J., Hulleman, E., Swigut, T., Wysocka, J., Tang, Y., Monje, M., 2017. Transcriptional Dependencies in Diffuse Intrinsic Pontine Glioma. *Cancer Cell* 31, 635-652.e6. <https://doi.org/10.1016/j.ccell.2017.03.011>

Nikbakht, H., Panditharatna, E., Mikael, L.G., Li, R., Gayden, T., Osmond, M., Ho, C.-Y., Kambhampati, M., Hwang, E.I., Faury, D., Siu, A., Papillon-Cavanagh, S., Bechet, D., Ligon, K.L., Ellezam, B., Ingram, W.J., Stinson, C., Moore, A.S., Warren, K.E., Karamchandani, J.,

Packer, R.J., Jabado, N., Majewski, J., Nazarian, J., 2016. Spatial and temporal homogeneity of driver mutations in diffuse intrinsic pontine glioma. *Nat Commun* 7, 11185. <https://doi.org/10.1038/ncomms11185>

Park, N.I., Guilhamon, P., Desai, K., McAdam, R.F., Langille, E., O'Connor, M., Lan, X., Whetstone, H., Coutinho, F.J., Vanner, R.J., Ling, E., Prinos, P., Lee, L., Selvadurai, H., Atwal, G., Kushida, M., Clarke, I.D., Voisin, V., Cusimano, M.D., Bernstein, M., Das, S., Bader, G., Arrowsmith, C.H., Angers, S., Huang, X., Lupien, M., Dirks, P.B., 2017. ASCL1 Reorganizes Chromatin to Direct Neuronal Fate and Suppress Tumorigenicity of Glioblastoma Stem Cells. *Cell Stem Cell* 21, 209-224.e7. <https://doi.org/10.1016/j.stem.2017.06.004>

Pathania, M., De Jay, N., Maestro, N., Harutyunyan, A.S., Nitarska, J., Pahlavan, P., Henderson, S., Mikael, L.G., Richard-Londt, A., Zhang, Y., Costa, J.R., Hébert, S., Khazaei, S., Ibrahim, N.S., Herrero, J., Riccio, A., Albrecht, S., Ketteler, R., Brandner, S., Kleinman, C.L., Jabado, N., Salomoni, P., 2017. H3.3K27M Cooperates with Trp53 Loss and PDGFRA Gain in Mouse Embryonic Neural Progenitor Cells to Induce Invasive High-Grade Gliomas. *Cancer Cell* 32, 684-700.e9. <https://doi.org/10.1016/j.ccell.2017.09.014>

Rajakulendran, N., Rowland, K.J., Selvadurai, H.J., Ahmadi, M., Park, N.I., Naumenko, S., Dolma, S., Ward, R.J., So, M., Lee, L., MacLeod, G., Pasilliao, C., Brandon, C., Clarke, I.D., Cusimano, M.D., Bernstein, M., Batada, N., Angers, S., Dirks, P.B., 2019. Wnt and Notch signaling govern self-renewal and differentiation in a subset of human glioblastoma stem cells. *Genes Dev.* 33, 498–510. <https://doi.org/10.1101/gad.321968.118>

Schwartzentruber, J., Korshunov, A., Liu, X.-Y., Jones, D.T.W., Pfaff, E., Jacob, K., Sturm, D., Fontebasso, A.M., Quang, D.-A.K., Tönjes, M., Hovestadt, V., Albrecht, S., Kool, M., Nantel, A., Konermann, C., Lindroth, A., Jäger, N., Rausch, T., Ryzhova, M., Korbel, J.O., Hielscher, T., Hauser, P., Garami, M., Klekner, A., Bogner, L., Ebinger, M., Schuhmann, M.U., Scheurlen, W., Pekrun, A., Frühwald, M.C., Roggendorf, W., Kramm, C., Dürken, M., Atkinson, J., Lepage, P., Montpetit, A., Zakrzewska, M., Zakrzewski, K., Liberski, P.P., Dong, Z., Siegel, P., Kulozik, A.E., Zapatka, M., Guha, A., Malkin, D., Felsberg, J., Reifenberger, G., von Deimling, A., Ichimura, K., Collins, V.P., Witt, H., Milde, T., Witt, O., Zhang, C., Castelo-Branco, P., Lichter, P., Faury, D., Tabori, U., Plass, C., Majewski, J., Pfister, S.M., Jabado, N., 2012. Driver mutations in histone H3.3 and chromatin remodelling genes in paediatric glioblastoma. *Nature* 482, 226–231. <https://doi.org/10.1038/nature10833>

Tate, M.C., Lindquist, R.A., Nguyen, T., Sanai, N., Barkovich, A.J., Huang, E.J., Rowitch, D.H., Alvarez-Buylla, A., 2015. Postnatal growth of the human pons: A morphometric and immunohistochemical analysis. *Journal of Comparative Neurology* 523, 449–462. <https://doi.org/10.1002/cne.23690>

Taylor, I.C., Hütt-Cabezas, M., Brandt, W.D., Kambhampati, M., Nazarian, J., Chang, H.T., Warren, K.E., Eberhart, C.G., Raabe, E.H., 2015. Disrupting NOTCH Slows Diffuse Intrinsic Pontine Glioma Growth, Enhances Radiation Sensitivity, and Shows Combinatorial Efficacy With Bromodomain Inhibition. *Journal of Neuropathology & Experimental Neurology* 74, 778–790. <https://doi.org/10.1097/NEN.0000000000000216>

Voon, H.P.J., Udugama, M., Lin, W., Hii, L., Law, R.H.P., Steer, D.L., Das, P.P., Mann, J.R., Wong, L.H., 2018. Inhibition of a K9/K36 demethylase by an H3.3 point mutation found in paediatric glioblastoma. *Nat Commun* 9, 3142. <https://doi.org/10.1038/s41467-018-05607-5>

Vue, T.Y., Kollipara, R.K., Borromeo, M.D., Smith, T., Mashimo, T., Burns, D.K., Bachoo, R.M., Johnson, J.E., 2020. ASCL1 regulates neurodevelopmental transcription factors and cell cycle genes in brain tumors of glioma mouse models. *Glia* 68, 2613–2630. <https://doi.org/10.1002/glia.23873>

Wang, J., Huang, T.Y.-T., Hou, Y., Bartom, E., Lu, X., Shilatifard, A., Yue, F., Saratsis, A., 2021. Epigenomic landscape and 3D genome structure in pediatric high-grade glioma. *Science Advances* 7, eabg4126. <https://doi.org/10.1126/sciadv.abg4126>